FREE VIBRATIONAL ANALYSIS OF SOME STRUCTURAL COMPONENTS WITH TIMOSHENKO EFFECTS USING FINITE ELEMENT METHOD

by

KULTAR SINGH

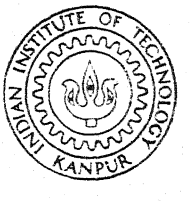

DEPARTMENT OF MECHANICAL ENGINEERING

INDIAN INSTITUTE OF TECHNOLOGY KANPUR

AUGUST, 1982

FREE VIBRATIONAL ANALYSIS OF SOME STRUCTURAL COMPONENTS WITH TIMOSHENKO EFFECTS USING FINITE ELEMENT METHOD

A Thesis Submitted
in Partial Fulfilment of the Requirements
for the Degree of

DOCTOR OF PHILOSOPHY

by

KULTAR SINGH

to the

DEPARTMENT OF MECHANICAL ENGINEERING
INDIAN INSTITUTE OF TECHNOLOGY KANPUR

AUGUST, 1982

Dedicated to

Dearest Sister

GUDDI

CERTIFICATE

This is to certify that work entitled 'FREE VIBRATIONAL ANALYSIS OF SOME STRUCTURAL COMPONENTS WITH TIMOSHENKO EFFECTS USING FINITE ELEMENT METHOD' has been carried out under my supervision by Shri Kultar Singh and has not been submitted elsewhere for a degree.

Bhupinder Pal Singh.
BHUPINDER PAL SINGH
Assistant Professor
Department of Mech.Engg.
I.I.T. Kanpur.

ACKNOWLEDGEMENTS

I take this opportunity to express my deep sense of gratitude towards my supervisor Dr. Bhupinder Pal Singh for suggesting me these very basic and challenging problems, for his untiring guidance, encouragement, enthusiasm, valuable discussions and criticism. I have no words to thank him for his concern about the early completion of the work. It was the brotherly treatment and homely atmosphere created by him and his family members which enabled me to complete the work in such a short span.

I am thankful to Drs. Vishv Mohan and Prakash Porey for their cooperation and help in creating the atmosphere conducive for working and providing the appropriate change of atmosphere whenever needed.

I thank all my friends and the staff members of IIT Kanpur who helped me in many ways.

My thanks are due to Mr. N.S. Srivastava for excellent tracings and Mr. C.M. Abraham for a careful and excellent typing of the manuscript.

KULTAR SINGH

TABLE OF CONTENTS

		Page
LIST OF FIGURES		viii
LIST OF TABLES		ix
NOMENCLATURE		xii
SYNOPSIS		xvi
CHAPTER I	: INTRODUCTION	1
1.1	: LITERATURE SURVEY	2
1.2	: PRESENT STUDY	9
CHAPTER II	: THE FINITE ELEMENT METHOD	13
2.1	: METHODS FOR SOLVING THE PROBLEM	13
2.1.1	: Exact Solutions	13
2.1.2	: Approximate Solutions	14
2.2	: THE FINITE ELEMENT METHOD	15
2.2.1	: General Procedure	16
2.2.2	: The Weighted Residuals Approach	18
2.2.3	: Requirements for Interpolation Functions	20
CHAPTER III	: BEAMS: FORMULATION AND SHAPE FUNCTIONS	21
3.1	: FORMULATION	22
3.1.1	: Approach A : One Governing Differential Equation	22
3.1.2	: Approach B : Two Simultaneous Governing Differential Equations	25
3.2	: SHAPE FUNCTIONS	29
3.2.1	: Shape Functions for Approach A	31
3.2.2	: Shape Functions for Approach B	32

Page

CHAPTER IV	: RINGS AND SECTORS : FORMULATION AND SHAPE FUNCTIONS	34
4.1	: EQUATION OF MOTION	34
4.2	: FORMULATION	37
4.2.1	: A Thin Ring or Sector	39
4.2.2	: A Thick Ring or Sector	41
4.3	: SHAPE FUNCTIONS	45
CHAPTER V	: DISCS : FORMULATION AND SHAPE FUNCTION	49
5.1	: FORMULATION	50
5.2	: SHAPE FUNCTIONS	55
CHAPTER VI	: RESULTS AND DISCUSSION	57
6.1	: SOLUTION PROCEDURE	57
6.1.1	: Classical Equations	57
6.1.2	: Equations with Timoshenko Effects	57
6.1.3	: Solution Algorithm	58
6.2	: NUMERICAL RESULTS AND DISCUSSION	59
6.2.1	: Beams : Approach A	60
6.2.2	: Beams : Approach B	68
6.2.3	: Thin Rings	78
6.2.4	: Thick Rings	91
6.2.5	: Thin Discs	97
6.2.6	: Thick Discs	121
6.3	: SUMMARY	127
CHAPTER VII	: CONCLUSIONS	128
REFERENCES		130
APPENDIX A	: BOUNDARY CONDITIONS AND ELEMENT MATRICES FOR BEAMS	136
A.1	: BOUNDARY CONDITIONS	136
A.2	: ELEMENT MATRICES	136
A.2.1	: Approach A	137
A.2.2	: Approach B	138

Page

APPENDIX B	:	BOUNDARY CONDITIONS AND ELEMENT MATRICES FOR RINGS	140
B.1	:	BOUNDARY CONDITIONS	140
B.2	:	ELEMENT MATRICES	141
APPENDIX C	:	BOUNDARY CONDITIONS AND ELEMENT MATRICES FOR DISCS	144
C.1	:	BOUNDARY CONDITIONS	144
C.2	:	ELEMENT MATRICES	145

LIST OF FIGURES

Figure No.		Page
3.1	: Typical finite element of a beam	23
4.1	: Free body diagram of an element of a ring or sector	35
4.2	: Typical finite element of a ring or sector	38
5.1	: Typical annular finite element of a disc	51
6.1	: Variation of frequency with linear spring, k_s	69
6.2	: Variation of frequency with linear spring, k_s	70
6.3	: Variation of frequency with re, for given k_s = 0.0, --- Δ ---; k_s = 5.0, ——o——	71
6.4	: Variation of frequency with re, for given k_s = 5.0 and k_t = 5.0	72
6.5	: A tapered beam	77
6.6	: Sectors on various end conditions	80
6.7	: Rings on different number of equi-spaced radial supports	86
6.8	: Rotating ring on two radial supports	87
6.9	: 180°-sector on three radial supports with unequal bays	90
6.10	: Variation of frequency with nodal diameters, n, for various rotational speeds, $\bar{\Omega}$	114
6.11	: Variation of frequency with nodal diameters, n, for various rotational speeds, $\bar{\Omega}$	115
6.12	: Variation of frequency with nodal diameters, n, for various rotational speeds, $\bar{\Omega}$	116
6.13	: Constant thickness idealization of a tapered disc, 2-element ——.——, 4 element ----- .	117

LIST OF TABLES

Table No.		Page
1.1	: Summary of different Timoshenko beam elements [4]	3
1.2	: Summary of various thick disc/plate elements	10
6.1	: Natural frequencies, $\bar{\omega}_n$, for cantilever beam 1 of Thomas et al. [4]	61
6.2	: Comparison of % error in results of Thomas et al. [4] and present work	61
6.3	: Natural frequencies, $\bar{\omega}_n$, of cantilever beam 2 of Thomas et al. [4]	62
6.4	: Comparison of % error in results of Thomas et al. [4] and present work	63
6.5	: Comparison of % error in Kapur's results [14] and the present work for 2 elements	64
6.6	: Comparison of % error in results of Davis et al. [10] and the present work	65
6.7	: Natural frequencies, $\bar{\omega}_n$, of simply-supported and clamped-clamped beams, re = 0.02 and se = 0.02	66
6.8	: Natural frequencies, $\bar{\omega}_n$ of simply-supported and clamped-clamped beams, re = 0.10 and se = 0.10	67
6.9	: Natural frequencies, $\bar{\omega}_n$ of the uniform cantilever and simply-supported beams, re = 0.02 and se = 0.02	74
6.10	: Natural frequencies, $\bar{\omega}_n$, of the uniform cantilever and simply-supported beams, re = 0.10 and se = 0.15	75
6.11	: Natural frequencies, $\bar{\omega}_n$ of a tapered cantilever beam, re = 0.10 and se = 0.15	76
6.12	: Natural frequencies, $\bar{\omega}_n$, of a free-ring	79

Table No.		Page
6.13	: Natural frequencies, $\bar{\omega}_n$, of different sectors with free-, hinged-, and fixed-ends	81
6.14	: Natural frequencies, $\bar{\omega}_n$, of a ring on different number of equi-spaced radial supports	84
6.15	: Natural frequencies, $\bar{\omega}_n$, of a rotating ring for different rotational speeds, $\bar{\Omega}$	88
6.16	: Natural frequencies, $\bar{\omega}_n$, of an 180^o-sector on 3-supports with unequal bays	91
6.17	: Natural frequencies, $\bar{\omega}_n$, of a free-ring, re = 0.10 and se = 0.1704	92
6.18	: Natural frequencies, $\bar{\omega}_n$, of a free-ring, re = 0.1378 and se = 0.2425	93
6.19	: Natural frequencies, $\bar{\omega}_n$, of a ring on radial supports, re = 0.05 and se = 0.0866	94
6.20	: Natural frequencies, $\bar{\omega}_n$, of various sectors on hinged ends, re=0.05 and se = 0.0866	95
6.21	: Natural frequencies, $\bar{\omega}_n$, of various fixed-fixed sectors, re = 0.05 and se = 0.0866	97
6.22	: Natural frequencies, $\bar{\omega}_n$, of rotating rings on radial supports, re = 0.05 and se = 0.0866	98
6.23	: Natural frequencies, $\bar{\omega}_n$, of a centrally clamped disc, Ratio = 0.276	101
6.24	: Natural frequencies, $\bar{\omega}_n$, of a centrally clamped disc vibrating in zero-nodal circle mode for various values of Ratio	103
6.25	: Natural frequencies, $\bar{\omega}_n$, of a centrally clamped disc, Ratio = 0.300	104
6.26	: Natural frequencies, $\bar{\omega}_n$, of a centrally clamped disc vibrating in zero-nodal circle modes, for various values of Ratio	106

Table No.		Page
6.27	: Natural frequencies, $\bar{\omega}_n$, of a centrally clamped rotating disc, Ratio = 0.276	110
6.28	: Natural frequencies, $\bar{\omega}_n$, of a centrally clamped tapered disc, Ratio = 0.276	118
6.29	: Natural frequencies, $\bar{\omega}_n$, of a centrally clamped disc, Ratio = 0.276, re = 0.02 and se = 0.02	122
6.30	: Natural frequencies, $\bar{\omega}_n$, of a centrally clamped disc, Ratio = 0.276, re = 0.08 se = 0.08	123
6.31	: Natural frequencies, $\bar{\omega}_n$, of a centrally clamped rotating disc, Ratio = 0.276, re = 0.02 and se = 0.02	125

NOMENCLATURE

a,b	inner and outer radii of disc
$a,b,c,d,e,f,$ $a_i,b_i,i=1,2,..$	constants in the assumed deflection functions
A	area of cross-section
$[A_i],i=1,2,\ldots$	elemental constitutive matrices
$\{B\},\{B_i\},i=1,2,..$	boundary condition vectors
C	non-dimensionalization factor, $=\frac{\rho AR^4}{EI_1}$
$C_i,i=1,2,\ldots$	constants in rotational stress functions
D	flexural rigidity, $=EI/(1-\nu^2)$
$[D],[D_i],i=1,2,$	dynamical matrices
Dm	domain
e	element number
EI,EI_1	flexural rigidity
f	known scalar function of independent variables
F	shear force
$F_i,Z_i,i=1,2,..$	functions as defined in appendices
G	modulus of rigidity
h	element length
j,k	node numbers
k_s,k_t,K_s,K_t	spring stiffnesses
$[K],[K_i],i=1,2,$	stiffness matrices
l,m	number of unknowns or nodal parameters
L	length of component
$\mathcal{L}$	linear or nonlinear differential operator

M	bending moment
$[M],[M_i],i=1,2,..$	mass matrices
n	mode number
$N_i,i=1,2,..$	interpolating functions
ND	number of nodal parameters
q	load acting on the component
r	local variable in radial direction
re	non-dimensional rotatory inertia
R	radius
Ratio	ratio of inner to outer radii, = a/b
$Res^{(e)},Res_i^{(e)}$, $i=1,2$	residues
se	non-dimensional shear factor
t	time variable
T	tension in ring or thickness of disc
u	radial displacement
w,w_b,w_s,W	transverse or tangential displacement
$\{w\}$	vector of unknowns
x	local variable for X
X	beam longitudinal variable
$\{X_i\}$	vector at ith iteration
y	circumferential distance, = $R\theta$
$\{Y_i\},i=1,2,..$	boundary conditions constitutive vectors
α	numerical shape factor for cross-section
β	elemental angle of a sector finite element
γ	shear deformation

∇	differential operator
ε	a small number
θ	variable in the tangential direction
ν	Poisson's ratio
$\xi_i, i=1,2,$	natural coordinates
ρ	mass density
$\sigma_{rr}, \sigma_{\theta\theta}$	radial and tangential stresses
Σ	surface enclosing domain Dm
ϕ	unknown scalar function
ψ	bending slope
$\omega_o, \omega^*, \omega_n, \bar{\omega}_n, \omega_{nc},$	natural frequencies of vibration
$\Omega, \bar{\Omega}$	rotational speeds
$\{\ \}$	column vector
$\lfloor\ \rfloor$	row vector
$[\ ]$	square matrix

Subscripts

o	Timoshenko effects are zero
b	bending for beams, or evaluation at radius b for discs
i	ith component
j,k	evaluation at jth and kth nodes
n	nth mode
nC	nth mode, classical value
R	evaluation at radius R
θ	evaluation at angle θ

Superscripts

e	eth element
n	nodal parameters
w	displacement
ψ	bending slope
$(')$	derivative w.r.to space coordinate
$(\dot{})$	derivative w.r. to time
$(\bar{})$	non-dimensional quantity
$(^*)$	spring stiffness is zero

SYNOPSIS

FREE VIBRATIONAL ANALYSIS OF SOME STRUCTURAL COMPONENTS WITH TIMOSHENKO EFFECTS USING FINITE ELEMENT METHOD

A Thesis Submitted
In Partial Fulfilment of the Requirements
for the Degree of
DOCTOR OF PHILOSOPHY
by
KULTAR SINGH
to the
Department of Mechanical Engineering
Indian Institute of Technology, Kanpur
July, 1982

The Timoshenko effects play an important role in the analysis of structural components frequently appearing in the design problems. Keeping this in view, economically efficient analysis techniques are essential. With this aim, the elemental matrices for the finite element formulation of various structural components, viz., beams, rings, sectors and discs, have been deduced logically from the governing differential equations using the Galerkin method.

The Timoshenko beam has been analysed using two approaches. The first approach applies to a uniform beam characterized by a single governing differential equation. The second approach uses two simultaneous governing differential equations and is applicable to any beam. Though the

elemental matrices for second approach are given for a linear variation of the cross-sectional parameters, the evaluation of matrices for any other variation is straightforward.

The equations of motion of a ring or sector, with and without Timoshenko effects, are improved to include the rotational speed effects. The finite element equations are systematically derived from these governing differential equations. A quintic polynomial, satisfying the compatibility of derivatives upto second order, has been used for the ring finite element. It is shown logically that the order of the interpolating function remains same, in case of the analysis of rings and sectors, with and without Timoshenko effects.

In a similar logical fashion the finite element equations have been derived for a uniform disc, with and without Timoshenko effects. The results for a tapered disc are obtained by idealizing it with the constant thickness elements.

It is very easy and straight-forward to satisfy all the natural boundary conditions in the analysis of structural components, when the finite element equations are deduced using the Galerkin method. This is illustrated by the results for the various problems discussed in the thesis.

The critical ratio of the inner to outer diameter is evaluated for a centrally clamped disc. The lowest frequency for ratios above the critical value occurs for the one nodal diameter and zero nodal circle mode instead of the zero nodal diameter and zero nodal circle mode. The change of critical frequency, with rotational speed, has been studied for a centrally clamped disc.

It is illustrated that the order of interpolating function does not change when the Timoshenko effects are included in the analysis of structural components. The rotational stresses pose no additional complexity and cause no change in the interpolating function when considered in the analysis of rings and discs.

CHAPTER I

INTRODUCTION

The advancement of technology and high speed machines and vehicles has necessitated the need for a more accurate analysis of the structural and machine components. The classical solutions of vibrational problem of various structural components, like beams, sectors, rings, discs etc., have long been obtained. These are adequately applicable to lower modes of vibration. The higher speeds, generally, result in excitation of vibration modes of higher order where the Timoshenko effects, namely, the rotatory inertia and the shear effect, play an important role. The governing equations, with the Timoshenko effects included, become complicated and the analytical solutions become difficult or impossible. Even for the simplest component, the Timoshenko beam, the analytical solutions are not possible for all sorts of boundary conditions and for all variations of thickness of beam. Simple geometric shapes and boundary conditions can only be analysed analytically. For other components it becomes virtually impossible to obtain analytical solutions. Keeping these problems in view, various attempts have been made to obtain numerical solutions to various structural problems. In the present study the finite element method

has been used to solve various vibrational problems of the structural components.

1.1 LITERATURE SURVEY

The most important and basic structural component is the beam. The error introduced by neglecting the Timoshenko effects is small for lower modes of thin and long beams, but turns out to be significant for higher modes of all beam. Archer [1] has given a finite element formulation based on classical theory. For a general beam, it is essential to develop a convenient analysis technique based on Timoshenko beam theory [2] i.e., including the effects of rotatory inertia and the shear.

Huang [3] has derived the exact frequency equations, for simple end conditions, of uniform beams based on Timoshenko beam theory. The equations are not conveniently usable for design purposes and cannot take-care-of the variations in the cross-section. Moreover, it is quite cumbersome to derive the frequency equations for more involved boundary conditions and for beams on multiple-supports. Thus, the requirement for a numerical technique to analyse the Timoshenko beam.

A number of Timoshenko beam finite elements have been proposed in literature [4-15]. Thomas et al [4] have very comprehensively discussed the earlier elements and have proposed a new element with six nodal parameters. The

elements have been classified into two groups, simple elements and complex elements. An element with two nodes and four nodal parameters is termed as simple element and the one with more nodes and/or nodel parameters is classified as complex. Table 1.1 gives the summary of different elements and is reproduced from Thomas et al. [4]. None of these shape functions have been deduced logically, instead the interpolation functions for the transverse displacement and the shear have been selected arbitrarily. In some cases, it becomes difficult to satisfy the natural boundary conditions. A detailed review of these functions is given in Chapter III.

Table 1.1

Summary of different Timoshenko beam elements[4]

Element	Reference	No.of Nodes	No.of parameters	Parameters
A	[5-11]	2	4	w, ψ
B	[12,13]	2	4	$w, \frac{dw}{dx}$
C	[14]	2	8	$w_b, \frac{dw_b}{dx}, w_s, \frac{dw_s}{dx}$
D	[13]	3	7	$w, \frac{dw}{dx}, \psi$ at each end; ψ at middle node
E	[15]	4	8	w, ψ
F	[4]	2	6	w, ψ, γ

The sector or the ring is equally important structural component. The understanding of vibrational characteristics of complicated structures, such as gears, aircraft fuselags, missiles, etc., is facilitated by understanding the dynamic characteristics of rings on radial supports. Dynamic characteristics of free-thin rings have long been investigated by several authors [16-19]. Different methods have been proposed by several researchers [20-34] for the vibrational analysis of thin rings with and without radial supports. Rao and Sundararajan [22] have determined natural frequencies and mode shapes of free and radially supported thin and thick rings by constructing the frequency determinant using the differential equation approach. The method proposed is not suitable for large number of supports because the order of the frequency determinant increases six-folds with increase in number of supports. Moreover, even for small number of supports, their results are inaccurate [23,24]. For a thin ring with large number of equi-spaced radial supports, Sahay and Sundararajan [25] presented another method, which is not suitable for small number of supports. Also, the violation of inextensibility condition of the centre-line, assumed in their formulation, results in erroneous values[24]. McDaniel [26] used the complementary transfer matrix method for dynamic analysis of the thin ring on elastic supports. Murthy and Nigam [23] used the transfer matrix approach to investigate the problem of the thin ring on equi-spaced

radial supports. It appears that the adhoc assumption, that the vibration mode of the complete ring can be obtained by repeating the mode of one bay, has resulted in missing certain frequencies for the ring with more than two supports. Mallik and Mead [24] applied a wave approach to solve the problem of the thin ring on equi-spaced, radial supports. The pre-condition of the method is that the structure must be repetitive. This leaves the method to be of limited use.

In most of the earlier works, the shape functions for rings have been deduced from those for cylindrical shells [27-29] by specializing them to two-dimensions. Sabir et al. [30-33] deduced the shape functions for the analysis of static arches from the shape functions for cylindrical shells [27-29] and made a comparison of these. Sabir and Ashwell [34] extended their work to dynamic analysis of thin arches/sectors and thin rings. The shape functions suggested are not general enough to take-care-of all types of geometrically different rings and sectors. Also the number of elements required for convergence of results is considerably large, varying from 15 to 20.

The classical solution, given by Hoppe [16], neglecting the effects of shear deformation and rotatory inertia, is applicable to low nodal diameter modes of thin rings. Carefully carried-out experimental studies [18,35] have revealed

that, even for thin rings, considerable error is introduced when the number of nodal diameters become large. Kirkhope [36] has reported that Federhofer [37] has derived an exact solution in terms of Bessel's functions for free rings including the effects of shear deformation, rotatory inertia and extension. The results are not readily applicable to design problems [36]. Seidel and Erdelyi [38] have used an energy approach to derive an approximate solution, with assumptions regarding nonlinear normal strain through the cross-section, and an average shear angle. The cubic frequency equation obtained is further reduced to quadratic expression by showing the effects of mid-surface extension to be negligible. Rao and Sundararajan [22] solved the differential equation of inextensible motion for the natural frequencies and mode shapes of the thick rings. The assumption of inextensibility results in a quadratic frequency equation. For large T/R ratio, the results of references [22,38] deviate considerably from experimental values. Using the energy approach and making certain simplifying assumptions, Kirkhope [36] derived a frequency expression for in-plane vibrations of a free in-extensible thick ring as

$$\omega_n^2 = \omega_{nc}^2 \left[\frac{1}{(1+n^2 \frac{EI}{\alpha AGR^2})+(I/AR^2)\{(n^2-1)/(n^2+1)\}\{1/(1+n^2 \frac{EI}{\alpha AGR^2})\}}\right] \qquad (1.1)$$

In the design of turbines, nuclear reactors, machine structures, etc., discs are an important component. The analytical solution for vibrations of an unconstrained, uniform, thin disc was carried-out by Kirchhoff [39]. The work was further extended to include the effect of rotational in-plane stresses in free and centrally clamped discs by Lamb and Southwell [40] and Southewell [41]. Mote [42] has proposed an approximate solution procedure, based on Rayleigh-Ritz technique, for the analysis of initially stressed circular discs. The analytical solutions are almost impossible to obtain for discs of variable thickness and for discs including Timoshenko effects. For such problems, numerical techniques, like finite element method, have to be used.

The dynamic behaviour of the discs can be predicted by annular and sector elements. For symmetric vibrations of discs, the annular elements are more convenient to use. The variation of displacement in the angular direction is exactly represented by trigonometric functions, therefore, the annular elements can be termed as semi-analytical. Polynomial approximation is used in the radial direction. Thus, the problem reduces from two-dimensions to one-dimension with a considerable saving in nodal parameters and increase in accuracy.

Several annular finite element formulations based on thin plate theory have been reported in literature [43-49]. Kirkhope and Wilson [43] have proposed an annular finite element using different cosine functions for each vibration mode to represent displacement function in angular direction. A cubic polynomial is used for representing displacement function in radial direction. The element has 2 nodes, 4 nodal parameters and linear or parabolic variation in thickness. The element was further developed by Kirkhope and Wilson [44] to include the effects of rotation and pre-stress. Kennedy and Gorman [45] used the original element to study the effects of centrifugal and thermal stresses on dynamic characteristics of variable thickness discs. There are many other formulations proposed for thin discs [46-49] in literature.

A number of elements have been proposed for dynamic analysis of thick discs [49-53]. Wilson and Kirkhope [50] have developed a 2 node, 8 nodal parameters element with linear variation of thickness. The nodal parameters being the displacement, radial slope, and the radial and tangential shear rotations. A 3 node, 6 nodal parameters and parabolic profile annular element has been developed by Hinton [51] for axisymmetric vibrations of thick arbitrary plates. The nodal parameters being the displacement and slope at each node. Mota Soares et al [49] have developed a 3 node, 9 nodal parameters annular thick element with parabolic

profile. The parameters are the displacement, and the radial and tangential slopes at each node. An annular element for the axisymmetric vibrations of circular uniform plates has been proposed by Raju and Venkateswara Rao [52]. The element has 2 nodes, 8 nodal parameters, the displacement and its derivative, and the shear rotation and its derivative are the parameters at each node. The element is also used for nonlinear dynamic analysis of circular plates. Mota Soares and Petyt [53] have developed an annular finite element, for dynamic analysis of arbitrary discs, based on Mindlin plate theory. The element has 2 nodes and 12 nodal parameters. The parameters per node are the displacement, radial and angular slopes, and the radial derivatives of displacement, and the radial and tangential slopes.

A summary of various finite elements for analysis of thick discs/plates is given in Table 1.2.

1.2 PRESENT STUDY

It was observed through the literature review that even though considerable amount of work has been reported on the finite element formulations of various structural components, most of them appear to be lacking the logic of the finite element method. Almost in all cases the interpolating functions are selected without considering the compatibility and completeness requirements. The functions selected are,

Table 1.2

Summary of various thick disc/plate elements

Author(s)	Reference	No.of nodes	No.of parameters	Parameters at each node
Mota Soares, Petyt and Salama	[49]	3	9	displacement, and the radial and tangential slopes
Wilson and Kirkhope	[50]	2	8	displacement, radial slope, radial and tangential shear rotations
Hinton	[51]	3	6	displacement and slope
Raju and Venkateswara Rao	[52]	2	8	displacement and its derivative, the shear rotation and its derivative
Mota Soares and Petyt	[53]	2	12	displacement, radial and angular slopes, and their derivatives

in general, of unnecessarily higher order, thereby increasing the number of variables. Keeping in view, the importance of the analysis of these components and frequency of their occurrence in the design problems, it is desirable that the analysis techniques used must be economically efficient. With this in mind, the elemental matrices for finite element formulation of various structural components have been deduced

logically from the governing differential equations using the Galerkin method.

In case of the Timoshenko beam formulation two approaches are used. Approach A, using a single governing differential equation for a uniform beam. Approach B,using two simultaneous governing differential equations for a general beam. Though the elemental matrices for Approach B are given for a linear variation of cross-sectional parameters, the evaluation of the matrices for any variation of taper is straight-forward. Both of the new elements fall in the category of simple elements as classified by Thomas et al [4]. The derivations are given in Chapter III.

The derivation of the elemental equations for the rings and sectors, with and without Timoshenko effects, is given in Chapter IV. It is shown logically that the order of the interpolating function is same in both the cases. The interpolating function for a line element using compatibility upto second order derivatives has been used for the analysis of rings and sectors.

Chapter V deals with the derivation of finite element equations for the discs, with and without Timoshenko effects. The derivation is given for uniform discs only, because the results for rotational stresses for a tapered disc are not available in closed form. Hence, the

matrices have to be obtained by numerical integration in case of a tapered disc.

The efficiency and accuracy of the formulations have been illustrated by comparing the results for various problems with the available results wherever possible. Results for many of the unsolved problems are also presented. The ease with which the natural boundary conditions can be satisfied is illustrated by the results for a Timoshenko beam with linear and torsional springs attached at the ends. It is also illustrated that the inclusion of Timoshenko effects does not change the order of the interpolating function, which has been done in almost all the earlier formulations. The rotational stresses pose no additional complexity when included in rings or discs.

Finally, the conclusions are given in Chapter VII.

CHAPTER II

THE FINITE ELEMENT METHOD

The general kind of the eigen-value problem, that is to be solved, can be formulated as follows. Consider some domain Dm bounded by the surface Σ. Let φ be a scalar function defined in the interior of Dm such that the behaviour of φ in Dm is given by

$$\mathcal{L}(\varphi) - f = 0 \qquad (2.1)$$

where f is a known scalar function of independent variables, and $\mathcal{L}$ is a linear or nonlinear differential operator, with physical parameters as known constants or known functions.

2.1 METHODS FOR SOLVING THE PROBLEM

The general problem is to find the unknown function φ which satisfies equation (2.1) and the associated boundary conditions specified on the surface Σ.

The various method available can be classified into the following broad categories :

i) Exact solutions

ii) Approximate solutions.

2.1.1 Exact Solutions

Some of the techniques used for finding the exact solutions are :

a) Separation of variables

b) Similarity solutions

c) Fourier and Laplace transformations.

The exact solutions are possible for a small number of relatively simple problems. Most of these have already been solved. They are the classical problems.

2.1.2 Approximate Solutions

The majority of the engineering problems are solved by the approximate solution procedures. Some of these procedures are :

a) Perturbation methods

b) Power series

c) Probability schemes

d) Method of weighted residuals

e) Finite difference techniques

f) Rayleigh-Ritz method

g) Finite element method.

The regular and singular perturbation methods are applicable only when the nonlinear terms are small compared to linear terms. The power series method is powerful, but the generation of coefficient for each term is a tedious work. Also, at times it is difficult to show the convergence of the series. Hence, the usefulness of these methods is limited. The probability schemes are useful only when the quantity desired is a statistical parameter.

With the use of high-speed digital computers the four currently outstanding method for obtaining approximate solutions of high accuracy are the method of weighted residuals, the finite difference method, the Rayleigh-Ritz method, and the finite element method. The approximating functions, to be used in the method of weighted residuals, and the Rayleigh-Ritz method, must satisfy the boundary conditions on Σ . The pre-satisfaction of the boundary conditions makes the selection of the approximating function awkward for complicated/stringent boundary conditions. Hence, the use of these methods is again limited to the problems with simple boundary conditions.

In the finite difference and the finite element methods, the selection of the function is not governed by the boundary conditions to be satisfied. Instead, the conditions are applied later to the problem. The approximation of the complicated geometries by the finite difference method is more crude as compared to the finite element method, because in finite difference method the domain is sub-divided with the help of parallel straight lines only. Thus, the finite element method appears to be the most suitable approximate method out of the available lot.

2.2 THE FINITE ELEMENT METHOD

In the finite element method there are four ways in

which the elemental properties can be formulated.

i) The direct approach, based on the direct stiffness method of structural analysis. The use of this approach is very limited because it can be applied only to relatively simple problems.

ii) The variational approach is a more versatile and more advanced approach. It is based on the calculus of variations and involves extremizing a functional. The functional, in solid mechanics problems, is generally, the energy formulation in one form or the other.

iii) A third and even more versatile approach to deriving the elemental properties is known as the weighted residuals approach. This approach begins with the governing differential equations of the problem and proceeds without relying on a functional of the variational statement. This approach is used for the solution of all the problems in the present work and is discussed in detail in Section 2.2.2.

iv) The energy balance approach, based on the balance of thermal and/or mechanical energy of a system, requires no variational statements.

2.2.1 General Procedure

Irrespective of the approach used to find the elemental properties, the finite element method always follows an

orderly step-by-step process. The various steps are :

i) DISCRETIZE THE CONTINUUM : The first step is to divide the continuum or the solution region into the sub-regions, i.e., the finite elements.

ii) SELECT INTERPOLATION FUNCTIONS : The next step is to assign nodes to each element and then choose the interpolation function to represent the field variable over the element. Quite often, the polynomials are selected as the interpolation functions because of the ease of differentiation and integration. The number of the nodes assigned to the element, the nature and number of the unknowns at each node, determined by the requirements listed in Section 2.2.3, govern the degree of the polynomials.

iii) FIND THE ELEMENT PROPERTIES : Once the finite element model has been established, the matrix equation expressing the properties of the individual elements can be determined by the use of one of the four approaches discussed above, depending upon the nature of the problem.

iv) ASSEMBLE THE ELEMENT PROPERTIES TO OBTAIN THE SYSTEM EQUATIONS : The next step is to combine the matrix equations expressing the behaviour of the elements and form the matrix equations expressing the behaviour of

the entire solution region or the system. The nature and form of the system equations is same as that of individual element equations except that they contain many more terms because all the nodes are included.

Before the system equations are ready for solution, they must be modified to account for the boundary conditions.

v) SOLVE THE SYSTEM EQUATIONS : The assembly process of step (iv) gives a set of simultaneous equations, to be solved to obtain the unknown nodal values of the field variable. A number of standard techniques exist for solving linear as well as nonlinear simultaneous equations.

vi) MAKE ADDITIONAL COMPUTATIONS IF DESIRED : Sometimes, the variables dependent on field variable are required. Now these calculations can be done with the values of field variables obtained at the nodes.

2.2.2 The Weighted Residuals Approach

Because of the broad choice of the weighting functions for error distribution principles, there is a variety of weighted residual techniques. The error distribution principle most often used to derive finite element equations is the Galerkin method.

According to the Galerkin method the weighting functions are chosen to be the same as the approximating functions used to represent φ.

Since equation (2.1) is valid over the entire solution domain, so it is valid over the domain of any element, e, also. Approximating the dependent variable, φ, over the element as

$$\varphi \simeq \varphi^{(e)} = \sum_{i=1}^{m} N_i^{(e)} \varphi_i^{(e)} = \lfloor N^{(e)} \rfloor \{\varphi\}^{(e)} \qquad (2.2)$$

where $N_i^{(e)}$ are the assumed interpolation functions defined over the element and $\varphi_i^{(e)}$ are the m-unknown nodal parameters. Substitution of equation (2.2) in equation (2.1) gives the residue as

$$\text{Res}^{(e)} = \mathcal{L}(\varphi^{(e)}) - f^{(e)} \qquad (2.3)$$

Then, from the Galerkin method, we have, the equations governing the behaviour of an element as

$$\int_{Dm^{(e)}} [\mathcal{L}(\varphi^{(e)}) - f^{(e)}] N_i^{(e)} \, d\, Dm^{(e)} = 0 \quad i=1,2,\ldots,m \qquad (2.4)$$

Since the operator $\mathcal{L}$ contains higher order derivatives, the order of the interpolation polynomials required will be higher. To reduce the order of the polynomials we carry out the integration by parts in equation (2.4) till there is an overall reduction in the order of derivative. When integration by parts is possible, it offers a convenient way to introduce the natural boundary conditions that must be satisfied on some portion of the boundary.

2.2.3 Requirements for Interpolation Functions

To guarantee the monotonic convergence, the interpolation functions $\lfloor N^{(e)} \rfloor$ in equation (2.2) be chosen so that the following general requirements are met, Huebner [54] :

i) At element interface (boundaries) the field variable φ and any of its partial derivatives upto one order less than the highest-order derivative appearing under the integral sign in the modified form of equation (2.4), i.e., after integration by parts, must be continuous.

ii) All uniform states of φ and its partial derivatives upto the highest order appearing in the modified form of equation (2.4) should have representation in $\varphi^{(e)}$ when, in the limit, the element size shrinks to zero.

The first one is known as the compatibility requirement, and the second as the completeness requirement .

CHAPTER III

BEAMS : FORMULATION AND SHAPE FUNCTIONS

The beam is one of the basic components which exists in almost all structures. The effects of rotatory inertia and the shear were first studied in this component.

Consider a beam of flexural rigidity EI, modulus of rigidity G, cross-sectional area A, mass density ρ, and numerical shape factor for cross-section α. The coupled equations of motion for the deflection, w, and the bending slope, ψ, are [2,55]

$$\frac{\partial}{\partial X}\left(EI\,\frac{\partial \psi}{\partial X}\right) + \alpha AG\left(\frac{\partial w}{\partial X} - \psi\right) - \rho I\,\frac{\partial^2 \psi}{\partial t^2} = 0 \qquad (3.1)$$

$$\rho A\,\frac{\partial^2 w}{\partial t^2} - \frac{\partial}{\partial X}\left(\alpha AG\left(\frac{\partial w}{\partial X} - \psi\right)\right) = 0 \qquad (3.2)$$

In case of a uniform beam these can be combined to give a single equation in deflection, w, as

$$EI\,\frac{\partial^4 w}{\partial X^4} + \rho A\,\frac{\partial^2 w}{\partial t^2} - \left(\rho I + EI\,\frac{\rho}{\alpha G}\right)\frac{\partial^4 w}{\partial X^2\,\partial t^2} + \rho I\,\frac{\rho}{\alpha G}\,\frac{\partial^4 w}{\partial t^4} = 0 \qquad (3.3)$$

Using these equations, the finite element equations are derived and then the shape functions are deduced.

3.1 FORMULATION

Uniform beam is considered first in Approach A and then the general beam in Approach B.

3.1.1 Approach A : One Governing Differential Equation

Assuming a polynomial function for the deflection as

$$w^{(e)} = [\,N\,]\{w\}^{(ne)} \tag{3.4}$$

over an element 'e', Figure 3.1, and substituting in equation (3.3), we get the residue as

$$Res^{(e)} = EI\,\frac{\partial^4 w^{(e)}}{\partial x^4} + \rho A\,\frac{\partial^2 w^{(e)}}{\partial t^2} - \left(\rho I + EI\,\frac{\rho}{\alpha G}\right)\frac{\partial^4 w^{(e)}}{\partial x^2\,\partial t^2} + \rho I\,\frac{\rho}{\alpha G}\,\frac{\partial^4 w^{(e)}}{\partial t^4} \tag{3.5}$$

Applying the Galerkin method to minimize the residue over the domain of the element, e, we get

$$\int_0^h N_i\, Res^{(e)}\, dx = 0 \qquad i = 1,2, \ldots, m \tag{3.6}$$

or

$$EI \int_0^h N_i\,\frac{\partial^4 w^{(e)}}{\partial x^4}\,dx + \rho A \int_0^h N_i\,\frac{\partial^2 w^{(e)}}{\partial t^2}\,dx - \left(\rho I + EI\,\frac{\rho}{\alpha G}\right)\int_0^h N_i\,\frac{\partial^4 w^{(e)}}{\partial x^2\partial t^2}\,dx + \rho I\,\frac{\rho}{\alpha G}\int_0^h N_i\,\frac{\partial^4 w^{(e)}}{\partial t^4}\,dx = 0$$

$$i = 1,2, \ldots, m \tag{3.7}$$

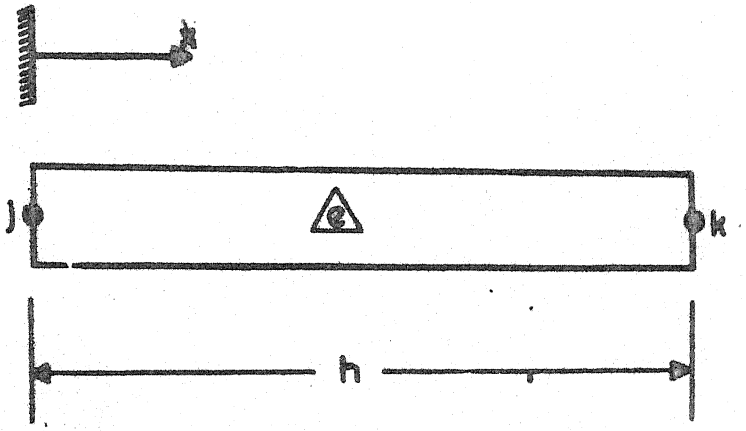

Figure 3.1. Typical finite element of a beam.

Integration by parts results in

$$(N_i\ EI\ \frac{\partial^3 w^{(e)}}{\partial x^3})\Big|_0^h - (N_i'\ EI\ \frac{\partial^2 w^{(e)}}{\partial x^2})\Big|_0^h + EI \int_0^h N_i''\ \frac{\partial^2 w^{(e)}}{\partial x^2}\ dx +$$

$$\rho A \int_0^h N_i\ \ddot{w}^{(e)}\ dx - (N_i(\rho I + EI\ \frac{\rho}{\alpha G})\ \frac{\partial^3 w^{(e)}}{\partial x\, \partial t^2})\Big|_0^h +$$

$$(\rho I + EI\ \frac{\rho}{\alpha G}) \int_0^h N_i'\ \frac{\partial \ddot{w}^{(e)}}{\partial x} dx + \rho I\ \frac{\rho}{\alpha G} \int_0^h N_i\ \dddot{w}^{(e)}\ dx = 0;$$

$$i = 1, 2, \ldots, m \qquad (3.8)$$

where (') prime denotes a derivative w.r.to x and (•) dot denotes a derivative w.r. to time, t.

Expressing equation (3.8) in vector notation and using equation (3.4), the elemental equations of motion are obtained as

$$(\{N\}\ EI\ \frac{\partial^3 w^{(e)}}{\partial x^3})\Big|_0^h - (\{N'\}\ EI\ \frac{\partial^2 w^{(e)}}{\partial x^2})\Big|_0^h - (\{N\}(\rho I +$$

$$EI\ \frac{\rho}{\alpha G})\frac{\partial^3 w^{(e)}}{\partial x\, \partial t^2})\Big|_0^h + EI \int_0^h \{N''\}\,[N'']\ dx\ \{w\}^{(ne)} +$$

$$(\rho A \int_0^h \{N\}\,[N]\ dx + (\rho I + EI\ \frac{\rho}{\alpha G}) \int_0^h \{N'\}\,[N']dx)\{\ddot{w}\}^{(ne)} +$$

$$\rho I \frac{\rho}{\alpha G} \int_0^h \{N\}\,[N]\ dx\ \{\dddot{w}\}^{(ne)} = 0 \qquad (3.9)$$

$$\text{or } [M_2]^{(e)}\{\dddot{w}\}^{(ne)} + [M_1]^{(e)}\{\ddot{w}\}^{(ne)} + [K]^{(e)}\{w\}^{(ne)} = \{B_1\}^{(ne)} \qquad (3.10)$$

where

$$[K]^{(e)} = EI[A_1]$$

$$[M_1]^{(e)} = \rho A[A_3] + \left(\rho I + EI\,\frac{\rho}{\alpha G}\right)[A_2]$$

$$[M_2]^{(e)} = \rho I\,\frac{\rho}{\alpha G}\,[A_3]$$

$$[A_1] = \int_o^h \{N''\}[N'']\,dx$$

$$[A_2] = \int_o^h [\{N'\}\,[N']\,dx$$

$$[A_3] = \int_o^h \{N\}[N]\,dx$$

and $$\{B_1\}^{(ne)} = -\left(\{N\}\,EI\,\frac{\partial^3 w(e)}{\partial x^3}\right)\Bigg|_o^h + \left(\{N\}\left(\rho I + EI\,\frac{\rho}{\alpha G}\right)\frac{\partial^3 w(e)}{\partial x\,\partial t^2}\right)\Bigg|_o^h +$$

$$+\left(\{N'\}\,EI\,\frac{\partial^2 w(e)}{\partial x^2}\right)\Bigg|_o^h = \{Y_1\} + \{Y_2\}$$

3.1.2 Approach B : Two Simultaneous Governing Differential Equations

In case of a non-uniform beam, the coupled equations of motion (3.1) and (3.2) could not be combined into one equation. An alternative approach to solve these equations simultaneously is used.

Assuming a polynomial interpolating function for the deflection, w, as

$$w^{(e)} = \lfloor N^{w} \rfloor \{ w \}^{(ne)} \tag{3.11}$$

and another polynomial interpolating function for the bending slope, ψ, as

$$\psi^{(e)} = \lfloor N^{\psi} \rfloor \{ \psi \}^{(ne)} \tag{3.12}$$

where the superscripts w and ψ denote the interpolating functions for $w^{(e)}$ and $\psi^{(e)}$, respectively, over the domain of the element 'e'. Substituting equations (3.11) and (3.12) in equations (3.1) and (3.2), the two residues are obtained as

$$Res_1^{(e)} = \frac{\partial}{\partial x}\left(EI \frac{\partial \psi^{(e)}}{\partial x}\right) + \alpha AG\left(\frac{\partial w^{(e)}}{\partial x} - \psi^{(e)}\right) - \rho I \frac{\partial^2 \psi^{(e)}}{\partial t^2} \tag{3.13}$$

$$Res_2^{(e)} = \rho A \frac{\partial^2 w^{(e)}}{\partial t^2} - \frac{\partial}{\partial x}\left(\alpha AG\left(\frac{\partial w^{(e)}}{\partial x} - \psi^{(e)}\right)\right) \tag{3.14}$$

The residue $Res_1^{(e)}$, equation (3.13), is from the equation of motion of rotation, therefore, it has to be minimized with respect to the interpolating functions of the bending slope. The residue, $Res_2^{(e)}$, of equation of translatory motion, equation (3.14), has to be minimized with respect to the interpolating functions of the deflection.

Hence, applying the Galerkin method, we get

$$\int_0^h N_i^{\psi} \, Res_1^{(e)} \, dx = 0 \qquad i = 1,2, \ldots, l \tag{3.15}$$

$$\int_0^h N_i^{w} \, Res_2^{(e)} \, dx = 0 \qquad i = 1,2, \ldots, m \tag{3.16}$$

where l and m are the number of nodal parameters for bending slope and deflection respectively.

Substituting equation (3.13) in equation (3.15) and integrating by parts, we get

$$(N_i \, EI \, \frac{\partial \psi^{(e)}}{\partial x})\Big|_0^h - \int_0^h N_i' \, EI \, \frac{\partial \psi^{(e)}}{\partial x} \, dx + \int_0^h N_i \, \alpha AG(\frac{\partial w^{(e)}}{\partial x} - \psi^{(e)}) - \int_0^h N_i \, \rho I \, \ddot{\psi}^{(e)} \, dx = 0 \; ; \; i = 1,2, \ldots, m \tag{3.17}$$

Expressing in vector notation and using equations (3.11) and (3.12), the above equation (3.17) reduces to

$$(\{N\} \; EI \, \frac{\partial \psi^{(e)}}{\partial x})\Big|_0^h - \int_0^h EI \{N'\} \, [N'] \, dx \, \{\psi\}^{(ne)} - \int_0^h \alpha AG \{N\} [N] \, dx \, \{\psi\}^{(ne)} + \int_0^h \alpha AG \{N\} [N] \, dx \, \{w\}^{(ne)} - \int_0^h \rho I \{N\} [N] \, dx \, \{\ddot{\psi}\}^{(ne)} = 0 \tag{3.18}$$

Similarly, equation (3.16) yields

$$-(\{N^w\}\,\alpha AG(\frac{\partial w^{(e)}}{\partial x} - \psi^{(e)}))\Big|_o^h + \int_o^h \alpha AG\{N'^w\}[N'^w]dx\,\{w\}^{(ne)} -$$

$$\int_o^h \alpha AG\,\{N'^w\}[N\,]\,dx\,\{\psi\}^{(ne)} + \int_o^h \rho A\,\{N^w\}[N^w]dx\,\{\ddot{w}\}^{(ne)} = 0 \qquad (3.19)$$

Equations (3.18) and (3.19) can be combined as

$$\begin{bmatrix} [M_1] & [O] \\ [O] & [M_2] \end{bmatrix}^{(e)} \begin{Bmatrix} \ddot{w} \\ \ddot{\psi} \end{Bmatrix}^{(ne)} + \begin{bmatrix} [K_1] & [K_2] \\ [K_2]^T & [K_3] \end{bmatrix}^{(ne)} \begin{Bmatrix} w \\ \psi \end{Bmatrix}^{(ne)} =$$

$$\{B_2\}^{(ne)} \qquad (3.20)$$

where

$$[K_1] = \int_o^h \alpha AG\,\{N'^w\}\,[N'^w]\,dx$$

$$[K_2] = -\int_o^h \alpha AG\,\{N'^w\}\,[N^\psi]\,dx$$

$$[K_3] = \int_o^h (EI\,\{N'^\psi\}[N'^\psi] + \alpha AG\,\{N^\psi\}[N^\psi])\,dx$$

$$[M_1] = \int_o^h \rho A\,\{N^w\}[N^w]\,dx$$

$$[M_2] = \int_o^h \rho I\,\{N^\psi\}[N^\psi]\,dx$$

and

$$\{B_2\}^{(ne)} = \left\{ \begin{array}{l} (\{N^w\}\ \alpha AG(\frac{\partial w^{(e)}}{\partial x} - \psi^{(e)}))\Big|_o^h \\ (\{N^\psi\} EI \frac{\partial \psi^{(e)}}{\partial x})\Big|_o^h \end{array} \right\}$$

3.2 SHAPE FUNCTIONS

A review of the various shape functions reported in literature, as classified in Table 1.1, gives a better appraisal of the shape functions proposed in the present work.

i) Element A [5-11] : As reported by Thomas et al [4] that the element A formulations [5-11] are equivalent and can be reduced to anyone of them, so as a representative, the derivation given by Przemieniecki [11] is taken. The mass matrix has been derived using the kinetic energy formulation. The equations of static equilibrium have been used to derive the stiffness matrix by what is known as the direct method. This results in an inconsistent stiffness matrix, however, the error introduced is small enough to effect the accuracy of the results significantly.

ii) Element B [12,13] : Though the nodal parameters used, in this case, are w and $\frac{dw}{dx}$ but the elemental matrices transform to those given by element A, with the help of suitable coordinate transformation.

iii) Element C [14] : This element has two nodes with eight nodal parameters. It has a limitation that the abrupt changes in cross-section cannot be taken into account. There is a discontinuity of shear at such sections, but the element enforces continuity. Moreover, a higher order of interpolating function for shear has, unnecessarily, been employed.

iv) Element D [13] : In this case three nodes with seven nodal parameters are used. A quadratic interpolation for shear is used. This element has the same drawbacks as those of element C.

v) Element E [15] : The cubic interpolation functions for both w and ψ have been used. There are four nodes and eight parameters. Since the continuity of shear is not enforced, this element avoids the difficulty encountered by elements C and D.

vi) Element F [4] : It has two nodes with w, ψ and the shear deformation, γ, as the parameters. Using the relation [2,55]

$$\frac{dw}{dx} = \psi + \gamma \qquad (3.21)$$

with the help of suitable transformations, it can be shown that the parameters reduce to w, $\frac{dw}{dx}$ and γ, i.e., a cubic interpolation for the deflection and a linear for shear. This element also has the same difficulty as the elements

C and D, namely, this also enforces the continuity of shear at the abrupt changes of the cross-section.

A careful study of the above elements reveals that excepting elements A and B, which have inconsistent matrices, all others have been derived using interpolating functions of higher order than that required by the problem. Moreover, no reason has been given for selecting the particular functions. Each element has one or the other limitation, hence, none of them is general enough to solve the problem in its entity.

In the present analysis the shape functions are selected by considering the compatibility and completeness requirements, Huebner [54].

3.2.1 Shape Function for Approach A

The highest order of derivative under the integral sign in equation (3.9), is two, hence, the compatibility of the variable w and its first derivative is required. The completeness of all derivatives upto the third order, the highest order appearing in equation (3.9), is required. These are same as the requirements for standard interpolating function for the Bernoulli-Euler beam. Thus the function is, Desai and Abel [56],

$$w^{(e)} = \lfloor \xi_1^2(3-2\xi_1) \quad \xi_1^2\xi_2 h \quad \xi_2^2(3-2\xi_2) \quad -\xi_1\xi_2^2 h \rfloor \begin{Bmatrix} w_j \\ w_j' \\ w_k \\ w_k' \end{Bmatrix} \tag{3.22}$$

where

$$\xi_1 = 1-x/h \qquad \text{and} \qquad \xi_2 = x/h \tag{3.23}$$

The matrices $[A_1]$, $[A_2]$, $[A_3]$ and the vectors $\{Y_1\}$, $\{Y_2\}$, required in equation (3.10) using this function, equation (3.22), are given in Appendix A.

3.2.2 Shape Functions for Approach B

The highest order of derivative of w and ψ under the integral sign in equations (3.18) and (3.19) is one, so compatibility of w and ψ is required. The completeness of w, ψ and their first order derivatives, the highest order in equation (3.18) and (3.19), is required. The functions satisfying these are

$$w^{(e)} = \lfloor \xi_1 \quad \xi_2 \rfloor \begin{Bmatrix} w_j \\ w_k \end{Bmatrix} \tag{3.24}$$

$$\psi^{(e)} = \lfloor \xi_1 \quad \xi_2 \rfloor \begin{Bmatrix} \psi_j \\ \psi_k \end{Bmatrix} \tag{3.25}$$

Therefore,

$$\lfloor N^{\psi} \rfloor = \lfloor N^{w} \rfloor = \lfloor N \rfloor = \lfloor \xi_1 \quad \xi_2 \rfloor \tag{3.26}$$

The matrices $[K_1]$, $[K_2]$, $[K_3]$, $[M_1]$, $[M_2]$, and the vector $\{B_2\}^{(ne)}$, using these interpolating functions and for a linear variation of cross-sectional properties, are given in Appendix A.

With the present formulation any variation of cross-sectional properties can be handled, without any approximation, at the time of integration of the elemental matrices. This is a clear-cut advantage over the earlier formulations where assumptions have been made to incorporate the cross-sectional property changes.

CHAPTER IV

RINGS AND SECTORS : FORMULATION AND SHAPE FUNCTIONS

4.1 EQUATIONS OF MOTION

The equation of motion of a thin ring, without rotational speed, has been given by various authors [22,57]. To include the effects of rotational speed, Ω, in the equation of motion, consider an element m m_1 n_1 n of a rotating ring or sector, as shown in Figure 4.1, of radius R, flexural rigidity about first axis EI_1, cross-sectional area A, and mass density ρ. If T is the tension, F is the shear force, M is the bending moment, q is the uniform load acting on the element, u is the radial displacement and w is the tangential displacement then the equations of motion in tangential and normal directions are

$$\frac{\partial T}{\partial \theta} - F = \rho AR \frac{\partial^2 w}{\partial t^2} \tag{4.1}$$

$$(F+ \frac{\partial F}{\partial \theta} d\theta)\cos \frac{d\theta}{2} - F \cos \frac{d\theta}{2} + (T+ \frac{\partial T}{\partial \theta} d\theta) \sin \frac{d\theta}{2} + T \sin \frac{d\theta}{2} -$$

$$q(R\, d\theta) = \rho AR[\frac{\partial^2 u}{\partial t^2} + (R+u)\, \Omega^2]\, d\theta \tag{4.2}$$

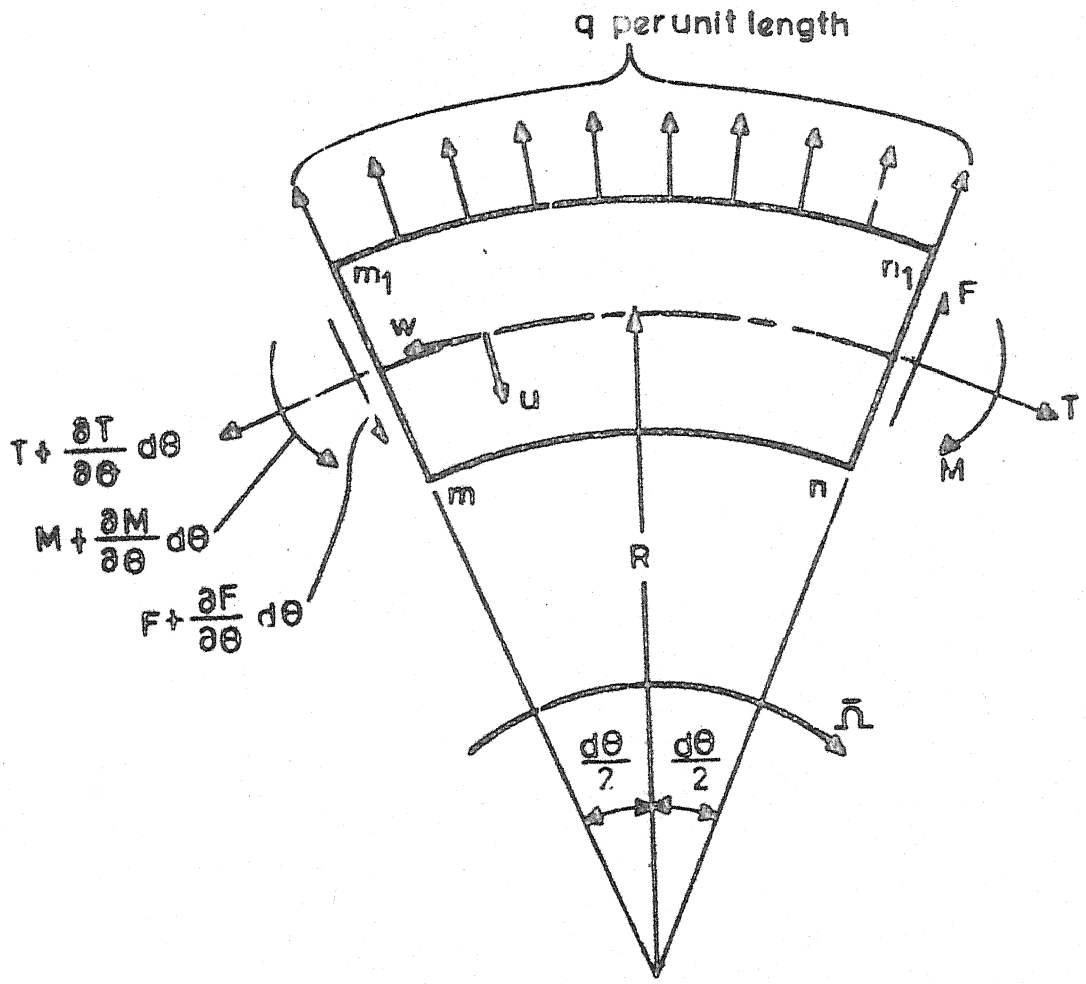

Figure 4.1. Free body diagram of an element of a ring or sector.

and, the moment about mass centre gives

$$\frac{\partial M}{\partial \theta} + FR = 0 \tag{4.3}$$

Simplification and taking limit as $d\theta \to 0$, reduces equation (4.2) to

$$\frac{\partial F}{\partial \theta} + T - qR = \rho AR\left[\frac{\partial^2 u}{\partial t^2} + (R+u)\,\Omega^2\right] \tag{4.4}$$

From theory of elasticity, Prescott [58], we have

$$M = \frac{EI_1}{R^2}\left(\frac{\partial^2 u}{\partial \theta^2} + \frac{\partial w}{\partial \theta}\right) \tag{4.5}$$

and condition of inextensibility of centre-line gives [22]

$$u = \frac{\partial w}{\partial \theta} \tag{4.6}$$

Using equations (4.5) and (4.6), equations (4.1), (4.3) and (4.4) can be combined as

$$\frac{\partial^6 w}{\partial \theta^6} + 2\frac{\partial^4 w}{\partial \theta^4} + \frac{\partial^2 w}{\partial \theta^2} = -\frac{\rho AR^4}{EI_1}\frac{\partial^2}{\partial t^2}\left(\frac{\partial^2 w}{\partial \theta^2} - w\right) - \frac{R^4}{EI_1}\frac{\partial q}{\partial \theta} - \frac{\rho AR^4}{EI_1}\Omega^2\frac{\partial^2 w}{\partial \theta^2} \tag{4.7}$$

For free in-plane vibrations of an inextensible, rotating thin ring or sector equation (3.7) reduces to

$$\frac{\partial^6 w}{\partial \theta^6} + 2\frac{\partial^4 w}{\partial \theta^4} + \left(1 + \frac{\rho A R^4}{EI_1}\Omega^2\right)\frac{\partial^2 w}{\partial \theta^2} = -\frac{\rho A R^4}{EI_1}\frac{\partial^2}{\partial t^2}\left(\frac{\partial^2 w}{\partial \theta^2} - w\right) \tag{4.8}$$

which is the governing differential equation of motion.

In the governing differential equation of motion for a non-rotating ring or sector including the Timoshenko effects [22], the rotational speed effects can be included in a similar fashion as

$$\frac{\partial^6 w}{\partial \theta^6} + 2\frac{\partial^4 w}{\partial \theta^4} + \left(1 + \frac{\rho A R^4}{EI_1}\Omega^2\right)\frac{\partial^2 w}{\partial \theta^2} = -\frac{\rho A R^4}{EI_1}\left(\frac{E}{\alpha G}\left(\frac{I_1}{AR^2}\right)^2 \cdot \right.$$

$$\frac{\rho A R^4}{EI_1}\frac{\partial^4}{\partial t^4}\left(\frac{\partial^2 w}{\partial \theta^2} - w\right) + \frac{\partial^2}{\partial t^2}\left(-\frac{I_1}{AR^2}\left(1 + \frac{E}{\alpha G}\right)\frac{\partial^4 w}{\partial \theta^4} + \right.$$

$$\left.\left.\left(1 - \frac{I_1}{AR^2}\left(2 - \frac{E}{\alpha G}\right)\right)\frac{\partial^2 w}{\partial \theta^2} - \left(1 + \frac{I_1}{AR^2}\right)w\right)\right) \tag{4.9}$$

4.2 FORMULATION

A typical finite element of a ring or sector subtending an angle β at the centre, is shown in Figure 4.2. The coordinate system is as shown and, hereafter, θ will refer to local coordinate unless otherwise stated.

Assume a polynomial function for the tangential displacement as

$$w^{(e)} = [N]\{w\}^{(ne)} \tag{4.10}$$

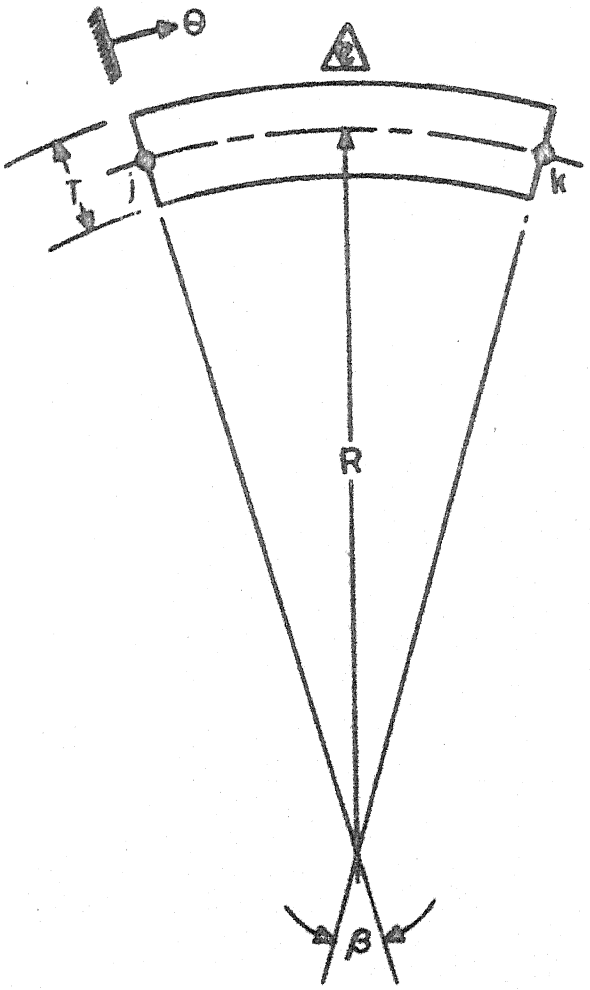

Figure 4.2. Typical finite element of a ring or sector.

4.2.1 A Thin Ring or Sector

Substituting equation (4.10) in equation (4.8), we get the residue as

$$Res^{(e)} = \frac{\partial^6 w(e)}{\partial \theta^6} + 2\frac{\partial^4 w(e)}{\partial \theta^4} + X\frac{\partial^2 w(e)}{\partial \theta^2} + C\left(\frac{\partial^4 w(e)}{\partial \theta^2 \partial t^2} - \frac{\partial^2 w(e)}{\partial t^2}\right) \tag{4.11}$$

where

$$X = 1 + \frac{\rho A R^4}{EI_1}\Omega^2$$

and

$$C = \frac{\rho A R^4}{EI_1}$$

Applying the Galerkin-method to minimize the residue of equation (4.11) over the domain of the element, we get

$$\int_0^\beta N_i \, Res^{(e)} \, d\theta = 0 \qquad i = 1,2, \ldots, m \tag{4.12}$$

or

$$\int_0^\beta N_i\left(\frac{\partial^6 w(e)}{\partial \theta^6} + 2\frac{\partial^4 w(e)}{\partial \theta^4} + X\frac{\partial^2 w(e)}{\partial \theta^2} + C\left(\frac{\partial^4 w(e)}{\partial \theta^2 \partial t^2} - \frac{\partial^2 w(e)}{\partial t^2}\right)\right) d\theta = 0 , \quad i = 1,2, \ldots, m$$

Integration by parts results in

$$\left(N_i\left(\frac{\partial^5 w^{(e)}}{\partial\theta^5} + 2\frac{\partial^3 w^{(e)}}{\partial\theta^3} + X\frac{\partial w^{(e)}}{\partial\theta} + C\frac{\partial^3 w^{(e)}}{\partial\theta\,\partial t^2}\right)\right)\Big|_0^\beta -$$

$$\left(N_i'\left(\frac{\partial^4 w^{(e)}}{\partial\theta^4} + 2\frac{\partial^2 w^{(e)}}{\partial\theta^2}\right)\right)\Big|_0^\beta + \left(N_i''\frac{\partial^3 w^{(e)}}{\partial\theta^3}\right)\Big|_0^\beta -$$

$$\int_0^\beta \left[N_i''\frac{\partial^3 w^{(e)}}{\partial\theta^3} - 2N_i''\frac{\partial^2 w^{(e)}}{\partial\theta^2} + XN_i'\frac{\partial w^{(e)}}{\partial\theta}\right]d\theta - C\int_0^\beta \left[N_i'\frac{\partial \ddot{w}^{(e)}}{\partial\theta} + N_i\ddot{w}^{(e)}\right]d\theta = 0, \quad i = 1,2,\ldots,m \tag{4.13}$$

where (') prime denotes a derivative w.r. to θ

and ($\cdot$) dot denotes a derivative w.r. to time, t.

Substituting equation (4.10) and using vector notation in equation (4.13) we get

$$\left(\{N\}\left(\frac{\partial^5 w^{(e)}}{\partial\theta^5} + 2\frac{\partial^3 w^{(e)}}{\partial\theta^3} + X\frac{\partial w^{(e)}}{\partial\theta} + C\frac{\partial^3 w^{(e)}}{\partial\theta\,\partial t^2}\right)\right)\Big|_0^\beta -$$

$$\left(\{N'\}\left(\frac{\partial^4 w}{\partial\theta^4} + 2\frac{\partial^2 w^{(e)}}{\partial\theta^2}\right)\right)\Big|_0^\beta + \left(\{N''\}\frac{\partial^3 w^{(e)}}{\partial\theta^3}\right)\Big|_0^\beta -$$

$$\int_0^\beta \left(\{N'''\}\lfloor N'''\rfloor - 2\{N''\}\lfloor N''\rfloor + X\{N'\}\lfloor N'\rfloor\right)d\theta\ \{w\}^{(ne)} -$$

$$C\int_0^\beta \left(\{N'\}\lfloor N'\rfloor + \{N\}\lfloor N\rfloor\right)d\theta\ \{\ddot{w}\}^{(ne)} = 0 \tag{4.14}$$

or

$$[M]^{(e)}\{\ddot{w}\}^{(ne)} + [K]^{(e)}\{w\}^{(ne)} = \{B_1\}^{(ne)} \tag{4.15}$$

where

$$[M]^{(e)} = C([A_3] + [A_4])$$

$$[K]^{(e)} = [A_1] - 2[A_2] + X[A_3]$$

such that

$$[A_1] = \int_0^\beta \{N'''\}[N'''] \, d\theta$$

$$[A_2] = \int_0^\beta \{N''\}[N''] \, d\theta$$

$$[A_3] = \int_0^\beta \{N'\}[N'] \, d\theta$$

$$[A_4] = \int_0^\beta \{N\}[N] \, d\theta$$

and

$$\{B_1\}^{(ne)} = \left(\{N\}\left(\frac{\partial^5 w(e)}{\partial\theta^5} + 2\frac{\partial^3 w(e)}{\partial\theta^3} + X\frac{\partial w(e)}{\partial\theta} + C\frac{\partial \ddot{w}(e)}{\partial\theta}\right)\right)\Big|_0^\beta -$$

$$\left(\{N'\}\left(\frac{\partial^4 w(e)}{\partial\theta^4} + 2\frac{\partial^2 w(e)}{\partial\theta^2}\right)\right)\Big|_0^\beta + \left(\{N''\}\left(\frac{\partial^3 w(e)}{\partial\theta^3}\right)\right)\Big|_0^\beta$$

$$= \{Y_1\} - \{Y_2\} + \{Y_3\}$$

4.2.2 A Thick Ring or Sector

Substituting equation (4.10) in equation (4.9) we get the residue as

$$Res^{(e)} = \frac{\partial^6 w^{(e)}}{\partial \theta^6} + 2\frac{\partial^4 w^{(e)}}{\partial \theta^4} + X\frac{\partial^2 w^{(e)}}{\partial \theta^2} + C\left(\frac{E}{\alpha G}\left(\frac{I_1}{AR^2}\right)^2 \cdot C\frac{\partial^4}{\partial t^4}\left(\frac{\partial^2 w^{(e)}}{\partial \theta^2} - w^{(e)}\right) + \frac{\partial^2}{\partial t^2}\left(-\frac{I_1}{AR^2}\left(1+\frac{E}{\alpha G}\right)\frac{\partial^4 w^{(e)}}{\partial \theta^4} + \left(1-\frac{I_1}{AR^2}\left(2-\frac{E}{\alpha G}\right)\right)\frac{\partial^2 w^{(e)}}{\partial \theta^2} - \left(1+\frac{I_1}{AR^2}\right)w^{(e)}\right)\right) \qquad (4.16)$$

Applying the Galerkin method to minimize the residue of equation (4.16) over the domain of the element 'e', we get

$$\int_0^\beta N_i \, Res^{(e)} \, d\theta = 0 \qquad i = 1,2, \ldots, m \qquad (4.17)$$

or

$$\int_0^\beta N_i\left(\frac{\partial^6 w^{(e)}}{\partial \theta^6} + 2\frac{\partial^4 w^{(e)}}{\partial \theta^4} + X\frac{\partial^2 w^{(e)}}{\partial \theta^2} + C\left(\frac{E}{\alpha G}\left(\frac{I_1}{AR^2}\right)^2 C\frac{\partial^4}{\partial t^4}\left(\frac{\partial^2 w^{(e)}}{\partial \theta^2} - w^{(e)}\right) + \frac{\partial^2}{\partial t^2}\left(-\frac{I_1}{AR^2}\left(1+\frac{E}{\alpha G}\right)\frac{\partial^4 w^{(e)}}{\partial \theta^4} + \left(1-\frac{I_1}{AR^2}\left(2-\frac{E}{\alpha G}\right)\right)\frac{\partial^2 w^{(e)}}{\partial \theta^2} - \left(1+\frac{I_1}{AR^2}\right) w^{(e)}\right)\right) d\theta = 0, \quad i = 1,2, \ldots, m$$

Integration by parts results in

$$\left(N_i\left(\frac{\partial^5 w(e)}{\partial\theta^5} + 2\frac{\partial^3 w(e)}{\partial\theta^3} + X\frac{\partial w(e)}{\partial\theta} + C\left(\frac{E}{\alpha G}\left(\frac{I_1}{AR^2}\right)^2 C\frac{\partial \dddot{w}(e)}{\partial\theta} -\right.\right.\right.$$

$$\left.\left.\left.\frac{I_1}{AR^2}\left(1+\frac{E}{\alpha G}\right)\frac{\partial^3 \ddot{w}(e)}{\partial\theta^3} + \left(1-\frac{I_1}{AR^2}\left(2-\frac{E}{\alpha G}\right)\right)\frac{\partial \ddot{w}(e)}{\partial\theta}\right)\right)\right)\Bigg|_0^\beta -$$

$$\left(N_i'\left(\frac{\partial^4 w(e)}{\partial\theta^4} + 2\frac{\partial^2 w(e)}{\partial\theta^2} - C\frac{I_1}{AR^2}\left(1+\frac{E}{\alpha G}\right)\frac{\partial^2 \ddot{w}(e)}{\partial\theta^2}\right)\right)\Bigg|_0^\beta +$$

$$\left(N_i''\frac{\partial^3 w(e)}{\partial\theta^3}\right)\Bigg|_0^\beta - \int_0^\beta \left(N_i'''\frac{\partial^3 w(e)}{\partial\theta^3} - 2N_i''\frac{\partial^2 w(e)}{\partial\theta^2} + X N_i'\frac{\partial w(e)}{\partial\theta}\right)d\theta -$$

$$\frac{E}{\alpha G}\left(\frac{I_1}{AR^2}\right)^2 C^2 \int_0^\beta \left(N_i'\frac{\partial \dddot{w}(e)}{\partial\theta} + N_i \ddot{w}''(e)\right)d\theta -$$

$$C\int_0^\beta \left(\frac{I_1}{AR^2}\left(1+\frac{E}{\alpha G}\right)N_i''\frac{\partial^2 \ddot{w}(e)}{\partial\theta^2} + \left(1-\frac{I_1}{AR^2}\left(2-\frac{E}{\alpha G}\right)\right)N_i'\frac{\partial \ddot{w}(e)}{\partial\theta} +\right.$$

$$\left.\left(1+\frac{I_1}{AR^2}\right)N_i \ddot{w}(e)\right)d\theta = 0, \qquad i = 1,2,\ldots,m \qquad (4.18)$$

Substituting equation (4.10) and using vector notation in equation (4.18), we get

$$\left(\{N\}\left(\frac{\partial^5 w^{(e)}}{\partial\theta^5} + 2\frac{\partial^3 w^{(e)}}{\partial\theta^3} + X\frac{\partial w^{(e)}}{\partial\theta} + C\left(\frac{E}{\alpha G}\left(\frac{I_1}{AR^2}\right)^2 C\frac{\partial \dddot{w}^{(e)}}{\partial\theta} - \right.\right.\right.$$

$$\left.\left.\left.\frac{I_1}{AR^2}\left(1+\frac{E}{\alpha G}\right)\frac{\partial^3 \ddot{w}^{(e)}}{\partial\theta^3} + \left(1-\frac{I_1}{AR^2}\left(2-\frac{E}{\alpha G}\right)\right)\frac{\partial \ddot{w}^{(e)}}{\partial\theta}\right)\right)\right)\Big|_0^\beta -$$

$$\left(\{N'\}\left(\frac{\partial^4 w^{(e)}}{\partial\theta^4} + 2\frac{\partial^2 w^{(e)}}{\partial\theta^2} - C\frac{I_1}{AR^2}\left(1+\frac{E}{\alpha G}\right)\frac{\partial^2 \ddot{w}^{(e)}}{\partial\theta^2}\right)\right)\Big|_0^\beta +$$

$$\left(\{N''\}\frac{\partial^3 w^{(e)}}{\partial\theta^3}\right)\Big|_0^\beta - \int_0^\beta \left(\{N'''\}\lfloor N'''\rfloor - 2\{N''\}\lfloor N''\rfloor + \right.$$

$$\left.X\{N'\}\lfloor N'\rfloor\right)d\theta\{w\}^{(ne)} - \frac{E}{\alpha G}\left(\frac{I_1}{AR^2}\right)^2 C^2\int_0^\beta \left(\{N'\}\lfloor N'\rfloor + \right.$$

$$\left.\{N\}\lfloor N\rfloor\right)d\theta\{\dddot{w}\}^{(ne)} - C\int_0^\beta \left(\frac{I_1}{AR^2}\left(1+\frac{E}{\alpha G}\right)\{N''\}\lfloor N''\rfloor + \right.$$

$$\left(1-\frac{I_1}{AR^2}\left(2-\frac{E}{\alpha G}\right)\right)\{N'\}\lfloor N'\rfloor +$$

$$\left.\left(1+\frac{I_1}{AR^2}\right)\{N\}\lfloor N\rfloor\right)d\theta\{\ddot{w}\}^{(ne)} = 0 \qquad (4.19)$$

or

$$[M_2]^{(e)}\{\dddot{w}\}^{(ne)} + [M_1]^{(e)}\{\ddot{w}\}^{(ne)} + [K]^{(e)}\{w\}^{(ne)} = \{B_2\}^{(ne)} \qquad (4.20)$$

where

$$[M_2]^{(e)} = \frac{E}{\alpha G}\left(\frac{I_1}{AR^2}\right)^2 C^2([A_3] + [A_4])$$

$$[M_1]^{(e)} = C\left(\frac{I_1}{AR^2}\left(1+\frac{E}{\alpha G}\right)[A_2] + \left(1-\frac{I_1}{AR^2}\left(2-\frac{E}{\alpha G}\right)\right)[A_3] + \left(1+\frac{I_1}{AR^2}\right)[A_4]\right)$$

$$[K]^{(e)} = [A_1] - 2[A_2] + X[A_3]$$

and

$$\{B_2\}^{(ne)} = (\{N\}(\frac{\partial^5 w(e)}{\partial\theta^5} + 2\frac{\partial^3 w(e)}{\partial\theta^3} + X\frac{\partial w(e)}{\partial\theta} +$$

$$C(\frac{E}{\alpha G}(\frac{I_1}{AR^2})^2 C\frac{\partial\ddot{w}(e)}{\partial\theta} - \frac{I_1}{AR^2}(1+\frac{E}{\alpha G})\frac{\partial^3\ddot{w}(e)}{\partial\theta^3} +$$

$$(1-\frac{I_1}{AR^2}(2-\frac{E}{\alpha G}))\frac{\partial\ddot{w}(e)}{\partial\theta}))\Big|_0^\beta - (\{N'\}(\frac{\partial^4 w(e)}{\partial\theta^4} +$$

$$2\frac{\partial^2 w(e)}{\partial\theta^2} - C\frac{I_1}{AR^2}(1+\frac{E}{\alpha G})\frac{\partial^2\ddot{w}(e)}{\partial\theta^2}))\Big|_0^\beta + (\{N''\}\frac{\partial^3 w(e)}{\partial\theta^3})\Big|_0^\beta$$

$$= \{Y_4\} - \{Y_5\} + \{Y_3\}$$

4.3 SHAPE FUNCTIONS

The shape functions for analysis of thin rings and sector reported by various authors have been compared by Sabir and Ashwell [34]. The shape functions are

i) A two-dimensional (ring) form of Cantin and Clough's shape function for cylindrical shells [27] is

$$u = a_1 \sin\theta + a_2 \cos\theta + a_3 R \cos\tfrac{1}{2}\beta \sin\theta + a_5 y^2 + a_6 y^3 \qquad (4.21)$$

$$w = a_1 \cos\theta - a_2 \sin\theta - a_3 R(1-\cos\tfrac{1}{2}\beta \cos\theta) + a_4 y \qquad (4.22)$$

where $y = R\theta$ (4.23)

ii) A two-dimensional form of 48-nodal parameter shape function of Bogner et al [29] for cylindrical shells

$$u = a_1 + a_2y + a_3y^2 + a_4y^3 \qquad (4.24)$$

$$w = a_5 + a_6y + a_7y^2 + a_8y^3 \qquad (4.25)$$

has 8-nodal parameters, namely, w,w' - u/r, u and u' at each node.

iii) A reduced form of the above shape function, equations (4.24) and (4.25) is

$$u = a_1 + a_2y + a_3y^2 + a_4y^3 \qquad (4.26)$$

$$w = a_5 + a_6y \qquad (4.27)$$

having 6 nodal parameters.

and

iv) A constant circumferential strain, ε, and linear change of curvature is given by the model [33]

$$u = a_1 \cos\theta + a_2 \sin\theta + a_4 - a_6\theta \qquad (4.28)$$

$$w = -a_1\sin\theta + a_2 \cos\theta + a_3 + a_5\theta + \tfrac{1}{2}a_6\theta^2 \qquad (4.29)$$

It is obvious from equations (4.21) through (4.29) that none of the shape function (i) to (iv) satisfies the equation of inextensibility of the centre-line of the ring, equation (4.6). In fact, the number (iv) shape function is based on the assumption of linear circumferential strain.

Thus none of these shape functions represents the problem under consideration, which results in convergence problems, [34].

In the present work the shape functions are deduced considering the compatibility and completeness requirements [54] as governed by the equations (4.14) and (4.19). The highest order of the derivative appearing under the integral sign in both the equations (4.14) and (4.19) is three, thus, a compatibility of all derivatives of $w^{(e)}$ upto second order is required at the element interface. The completeness of all derivatives upto the fifth order, the highest order occurring in equations (4.14) and (4.19), is required. Since the requirements for the interpolation functions for the analysis of thin and thick rings is same, the functions must also be the same. A function satisfying these requirements is

$$w^{(e)} = a + b\theta + c\theta^2 + d\theta^3 + e\theta^4 + f\theta^5 \qquad (4.30)$$

Expressing in non-dimensional parameters, ξ_1 and ξ_2, and nodal parameters, the tangential displacement function becomes

$$w^{(e)} = \lfloor \xi_1^3(10-15\xi_1+6\xi_1^2) \quad \beta\xi_1^3\xi_2(1+3\xi_2) \quad \tfrac{1}{2}\beta^2\xi_1^3\xi_2^2 \quad \xi_2^3(10-15\xi_2+6\xi_2^2) \quad -\beta\xi_1\xi_2^3(1+3\xi_1) \quad \tfrac{1}{2}\beta^2\xi_1^2\xi_2^3 \rfloor \begin{Bmatrix} w_j \\ w_j' \\ w_j'' \\ w_k \\ w_k' \\ w_k'' \end{Bmatrix} \qquad (4.31)$$

where $\xi_1 = 1-\theta/\beta$ and $\xi_2 = \theta/\beta$.

The various matrices and natural boundary condition vectors, evaluated using the above shape function, equation (4.31), are given in Appendix B.

CHAPTER V

DISCS : FORMULATION AND SHAPE FUNCTIONS

The equation of motion for free vibrations of a rotating disc of thickness T, including Timoshenko effects is [58-60]

$$D\,\nabla^4 W-(\rho I+D\,\frac{\rho}{\alpha G})\,\nabla^2(\frac{\partial^2 W}{\partial t^2})+\rho I\,\frac{\rho}{\alpha G}\,\frac{\partial^4 W}{\partial t^4}+\rho T\,\frac{\partial^2 W}{\partial t^2}=$$

$$\frac{T}{R}\,\frac{\partial}{\partial R}(R\sigma_{RR}\,\frac{\partial W}{\partial R})-\frac{T\sigma_{\theta\theta}}{R^2}\,\frac{\partial^2 W}{\partial \theta^2} \qquad (5.1)$$

where

$D = EI/(1-\nu^2)$, the flexural rigidity

$W = W(R,\theta,t)$

$\sigma_{RR}, \sigma_{\theta\theta}$ are the stresses induced due to rotation.

All other symbols have the same meaning as in Chapter III.

Assuming a cosine function for the variation of displacement in the angular direction, we can write

$$W = w(R,t)\cos n\theta \qquad (5.2)$$

Substituting equation (5.2) in equation (5.1), we get

$$D\,\nabla^4 w-(\rho I+D\,\frac{\rho}{\alpha G})\,\nabla^2\ddot{w}+\rho I\,\frac{\rho}{\alpha G}\,\ddot{\ddot{w}}+\rho T\,\ddot{w}=\frac{T}{R}\,\frac{\partial}{\partial R}(R\sigma_{RR}\,\frac{\partial w}{\partial R})+$$

$$\frac{n^2 T\sigma_{\theta\theta}\,w}{R^2} \qquad (5.3)$$

as the one-dimensional equation to be solved for free vibrations of a disc.

5.1 FORMULATION

A typical annular element, e, of a disc is shown in Figure 5.1. The coordinate system is as shown. Transforming equation (5.3) in terms of the local variable, r, we get after suitable algebraic manipulations,

$$\frac{D}{R_j+r}\left(\frac{\partial^2}{\partial r^2}\left((R_j+r)\frac{\partial^2 w}{\partial r^2}\right)-(1+2n^2)\frac{\partial}{\partial r}\left(\frac{1}{R_j+r}\frac{\partial w}{\partial r}\right)+\frac{n^4-4n^2}{(R_j+r)^3}w\right)-$$

$$\left(\rho I+D\frac{\rho}{\alpha G}\right)\frac{1}{R_j+r}\left(\frac{\partial}{\partial r}\left((R_j+r)\frac{\partial \ddot{w}}{\partial r}\right)-\frac{n^2\ddot{w}}{R_j+r}\right)+\rho I\frac{\rho}{\alpha G}\ddot{\ddot{w}}+$$

$$\rho T\ddot{w}-\frac{T}{R_j+r}\frac{\partial}{\partial r}\left((R_j+r)\sigma_{rr}\frac{\partial w}{\partial r}\right)-\frac{n^2 T\sigma_{\theta\theta}w}{(R_j+r)^2}=0 \qquad (5.4)$$

Assuming a polynomial function for the displacement

$$w^{(e)} = \lfloor N \rfloor \{w\}^{(ne)} \qquad (5.5)$$

and substituting in equation (5.4) we get the residue as

$$Res^{(e)} = \frac{D}{R_j+r}\left(\frac{\partial^2}{\partial r^2}\left((R_j+r)\frac{\partial^2 w^{(e)}}{\partial r^2}\right)-(1+2n^2)\frac{\partial}{\partial r}\left(\frac{1}{R_j+r}\frac{\partial w^{(e)}}{\partial r}\right)+\right.$$

$$\left.\frac{n^4-4n^2}{(R_j+r)^3}w^{(e)}\right)-\left(\rho I+D\frac{\rho}{\alpha G}\right)\frac{1}{R_j+r}\left(\frac{\partial}{\partial r}\left((R_j+r)\frac{\partial \ddot{w}^{(e)}}{\partial r}-\frac{n^2\ddot{w}^{(e)}}{R_j+r}\right)+\right.$$

$$\left.\rho I\frac{\rho}{\alpha G}\ddot{\ddot{w}}^{(e)}+\rho T\ddot{w}^{(e)}-\frac{T}{R_j+r}\frac{\partial}{\partial r}\left((R_j+r)\sigma_{rr}\frac{\partial w^{(e)}}{\partial r}\right)-\right.$$

$$\frac{n^2 T\sigma_{\theta\theta}w^{(e)}}{(R_j+r)^2} \qquad (5.6)$$

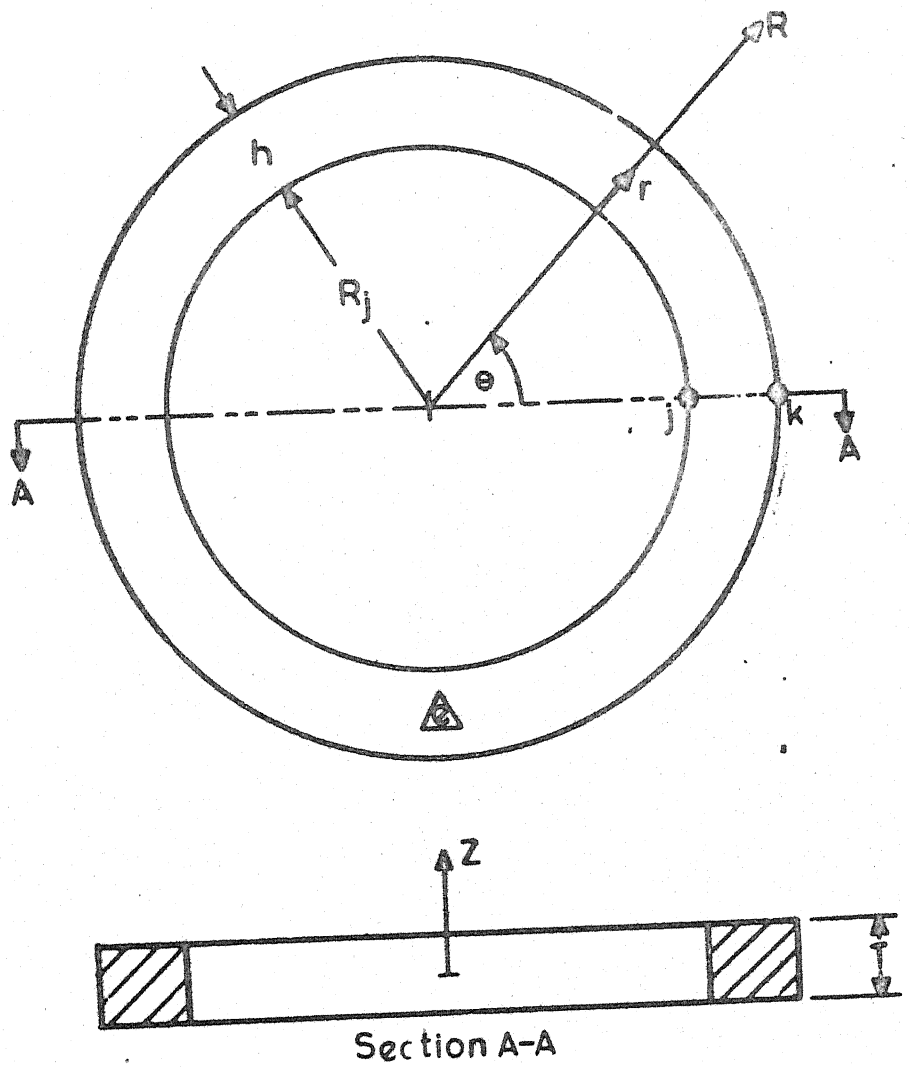

Figure 5.1. Typical annular finite element of a disc.

Applying the Galerkin method to minimize the residue of equation (5.6) over the domain of the element, we get

$$\int_0^h \int_0^{2\pi} N_i \, Res^{(e)} (R_j+r) d\Theta \, dr = 0 \qquad i = 1,2, \ldots, m \quad (5.7)$$

or

$$\int_0^h N_i (R_j+r) \, Res^{(e)} \, dr = 0 \qquad i = 1,2, \ldots, m \quad (5.8)$$

Substituting equation (5.6) in equation (5.8), we get

$$D \int_0^h N_i \left(\frac{\partial^2}{\partial r^2} \left((R_j+r) \frac{\partial^2 w^{(e)}}{\partial r^2} \right) - (1+2n^2) \frac{\partial}{\partial r} \left(\frac{1}{R_j+r} \frac{\partial w^{(e)}}{\partial r} \right) + \frac{n^4-4n^2}{(R_j+r)^3} w^{(e)} \right) dr - \left(\rho I + D \frac{\rho}{\alpha G} \right) \int_0^h N_i \left(\frac{\partial}{\partial r} \left((R_j+r) \frac{\partial \ddot{w}^{(e)}}{\partial r} \right) - \frac{n^2 \ddot{w}^{(e)}}{R_j+r} \right) dr + \rho I \frac{\rho}{\alpha G} \int_0^h (R_j+r) N_i \dddot{w}^{(e)} dr +$$

$$\rho T \int_0^h (R_j+r) N_i \ddot{w}^{(e)} dr - T \int_0^h N_i \frac{\partial}{\partial r} \left((R_j+r) \sigma_{rr} \frac{\partial w^{(e)}}{\partial r} \right) dr -$$

$$n^2 T \int_0^h \frac{\sigma_{\theta\theta}}{R_j+r} N_i w^{(e)} \, dr = 0 \qquad i = 1,2, \ldots, m \quad (5.9)$$

Integrating by parts and using equation (5.5) and vector notation, we get

such that

$$[A_1] = \int_o^h (R_j+r)\{N''\}\lfloor N''\rfloor \, dr$$

$$[A_2] = \int_o^h \frac{1}{R_j+r}\{N'\}\lfloor N'\rfloor \, dr$$

$$[A_3] = \int_o^h \frac{1}{(R_j+r)3}\{N\}\lfloor N\rfloor \, dr$$

$$[A_4] = \int_o^h \sigma_{rr}(R_j+r)\{N'\}\lfloor N'\rfloor \, dr$$

$$[A_5] = \int_o^h \frac{\sigma_{\theta\theta}}{R_j+r}\{N\}\lfloor N\rfloor \, dr$$

$$[A_6] = \int_o^h (R_j+r)\{N'\}\lfloor N'\rfloor \, dr$$

$$[A_7] = \int_o^h (R_j+r)\{N\}\lfloor N\rfloor \, dr$$

$$[A_8] = \int_o^h \frac{1}{R_j+r}\{N\}\lfloor N\rfloor \, dr$$

and

$$B^{(ne)} = -(\{N\}(D(\frac{\partial}{\partial r}((R_j+r)\frac{\partial^2 w^{(e)}}{\partial r^2})-(1+2n^2)\frac{1}{R_j+r}\frac{\partial w^{(e)}}{\partial r} -$$

$$T(R_j+r)\sigma_{rr}\frac{\partial w^{(e)}}{\partial r} - (\rho I+D\frac{\rho}{\alpha G})(R_j+r)\frac{\partial \ddot{w}^{(e)}}{\partial r}))\Big|_o^h +$$

$$(\{N'\}D(R_j+r)\frac{\partial^2 w^{(e)}}{\partial r^2})\Big|_o^h = -\{Y_1\} + \{Y_2\}$$

5.2 SHAPE FUNCTIONS

The simplest of the shape functions used by the various authors [43-49] to study the effects of rotation and pre-stress on free vibrations of thin circular discs, is, the transverse displacement, w, is approximated by

$$w(r,\theta) = (a_1+a_2r+a_3r^2+a_4r^3)\cos n\theta \qquad (5.12)$$

and the radial displacement function, u, is

$$u(r) = b_1+b_2r+b_3r^2+b_4r^3 \qquad (5.13)$$

Since cubic expressions are used for the radial and transverse displacement, a total of eight nodal parameters are required per element. There are other shape functions which require still higher number of nodal parameters per element.

The shape functions for the analysis of a thick disc, proposed by Wilson and Kirkhope [50] is

$$w(r,\theta) = (a_1+a_2r+a_3r^2+a_4r^3)\cos n\theta \qquad (5.14)$$

$$\gamma_r(r,\theta) = (a_5+a_6r)\cos n\theta \qquad (5.15)$$

and

$$\gamma_\theta(r,\theta) = (a_7+a_8r)\sin n\theta \qquad (5.16)$$

In the earlier works, reasons for selecting the nodal parameters or the shape functions are not given and in almost

every case the number of nodal parameters or the order of the functions is selected, unnecessarily, more than the required. In other words, the functions have been selected arbitrarily.

The compatibility and completeness requirements for the interpolating function [54] are governed by the equation (5.10). The highest order of derivative under the integral sign is two, so the compatibility of transverse displacement, w, and its first derivative is required. While the completeness of all derivatives upto third order, the highest order in equation (5.10), is required. These requirements are same as for the interpolation function for the beams, Chapter III. Hence, the function given by equation (3.22) is the required function, namely,

$$w^{(e)} = \lfloor \xi_1^2(3-2\xi_1) \quad \xi_1^2\xi_2 h \quad \xi_2^2(3-2\xi_2) \quad -\xi_1\xi_2^2 h \rfloor \begin{Bmatrix} w_j \\ w_j' \\ w_k \\ w_k' \end{Bmatrix} \qquad (5.17)$$

The elemental matrices $[A_1]$ to $[A_8]$ and the vectors $\{Y_1\}$ and $\{Y_2\}$ using this function are given in Appendix C.

The requirements for the interpolation function remain the same even if the Timoshenko effects are neglected. Hence, the function for both cases remains same.

CHAPTER VI

RESULTS AND DISCUSSION

Before discussing the numerical results, a brief discussion of the solution procedure is given.

6.1 SOLUTION PROCEDURE

An examination of the elemental equations (3.10), (3.20), (4.15), (4.20) and (5.11) reveals that the assembled system equations will essentially reduce to one of the following equations, after application of the boundary conditions.

6.1.1 Classical Equations

When the Timoshenko effects are not considered, the governing equations obtained are the simple second order equations of the type

$$[M] \{\ddot{w}\}^{(n)} + [K] \{w\}^{(n)} = \{0\} \tag{6.1}$$

The dynamical matrix for such equations is well established and is constructed as [55,62]

$$[D_1] = [K]^{-1} [M] \tag{6.2}$$

6.1.2 Equations with Timoshenko Effects

A fourth order governing equation of the type

$$[M_2] \{\ddot{\ddot{w}}\}^{(n)} + [M_1] \{\ddot{w}\}^{(n)} + [K] \{w\}^{(n)} = \{0\} \tag{6.3}$$

is obtained, when the Timoshenko effects are included in the analysis. The dynamical matrix for the fourth order equation (6.3) is constructed by the direct method, Przemeineicki [11], as

$$[D_2] = \begin{bmatrix} [K]^{-1}[M_1] & [K]^{-1}[M_2] \\ -[I] & [O] \end{bmatrix} \qquad (6.4)$$

In case of the structural components having rigid-body modes, a shift of origin, or the Shift, Bathe and Wilson [61], is applied to the stiffness matrix. The shift is applied to avoid the singularities while inverting the [K] matrix.

6.1.3 Solution Algorithm

The method of matrix iteration is applied to the dynamical matrix for finding the eigen values and eigen-vectors of the system of equations [55,62,63].

In this method, we assume a starting vector and multiply it with the dynamical matrix. Compare the new vector with the old vector for convergence. Drop the old vector and repeat the process with new vector till the two vectors become almost equal.

The solution procedure can be described by the following steps.

i) Get the assembled matrices from the elemental matrices and apply the appropriate boundary conditions.

ii) Apply the Shift, if required.

iii) Construct the dynamical matrix, [D], from the assembled matrices.

iv) Select an initial vector $\{X_o\}$ and set i = 0.

v) Construct a new vector as $\{X_{i+1}\} \leftarrow [D]\{X_i\}$,

vi) Compare $\{X_{i+1}\}$ with $\{X_i\}$, if $|X_{k,i+1} - X_{k,i}| \leq \varepsilon$ for all k, stop, otherwise, set i ← i+1 and repeat from step (v) onwards.

To save the computational efforts, the symmetry was exploited wherever possible. The free-ring results were obtained by analysis of a 180^o - sector. The constraints on radial displacement were applied from the symmetry considerations. This also avoided the problem of singular stiffness-matrix.

6.2 NUMERICAL RESULTS AND DISCUSSION

The various numerical results obtained are discussed in this section. The following non-dimensional parameters are used throughout the discussion to make the results more general.

$$\bar{\omega}_n^2 = \frac{\rho AL^4}{EI}\omega_n^2 \qquad (6.5)$$

$$re^2 = \frac{I}{AL^2} \qquad (6.6)$$

$$se^2 = \frac{EI}{\alpha AGL^2} \tag{6.7}$$

$$k_s = \frac{L^3}{EI} K_s \tag{6.8}$$

$$k_t = \frac{L^3}{EI} K_t \tag{6.9}$$

$$\bar{\Omega}^2 = \frac{\rho AL^4}{EI} \Omega^2 \tag{6.10}$$

The results of various authors have been reduced to these non-dimensional parameters for comparison. The results for many of the unattempted problems are also obtained.

6.2.1 Beams : Approach A

A number of problems have been solved and the comparison of results has been made with earlier results wherever possible.

Table 6.1 shows the results for the cantilever beam 1 analysed by Thomas et al [4]. The non-dimensional parameters for the beam are re = 0.002 and se = 0.007. It can be observed that the convergence rate is quite fast.

In Table 6.2 a comparison of % error in results has been made with Thomas et al [4], for the beam 1 [4]. Magnitude of % error in the results of Thomas et al [4] has been read from the graphs.

Table 6.1

Natural frequencies, $\overline{\omega}_n$, for cantilever beam 1 of Thomas et al [4]

Mode,n	Exact results [3]	Finite element results		
		2 elements	4 elements	6 elements
1	3.5155	3.5173	3.5157	3.5156
2	22.0155	22.2020	22.0412	22.0210
3	61.5712	74.9747	62.0465	61.6837
4	120.4468	216.2965	122.1886	121.2162

Table 6.2

Comparison of % error in results of Thomas et al[4] and present work

Mode,n	error in results of			
	reference[4] 9 nodal parameters	present work,8 nodal parameters	reference[4] 18 nodal parameters	present work 18 nodal parameters
1	0.01	0.006	~ 0.00	~ 0.000
2	0.30	0.100	0.05	0.006
3	1.25	0.800	0.20	0.040

A better rate of convergence is observed from the Table 6.2 for the present formulation as compared to the earlier formulation, element F, claimed as the best [4].

The results for the cantilever beam 2 of Thomas et al [4] are presented in Table 6.3, the non-dimensional parameters are re = 0.049 and se = 0.100. A good rate of convergence is observed even for the higher values of re and se.

Table 6.3

Natural frequencies, $\overline{\omega_n}$, of cantilever beam 2 of Thomas et al [4]

Mode,n	Exact results [3]	Finite element results		
		2 elements	4 elements	6 elements
1	3.4194	3.4204	3.4191	3.4190
2	18.6336	18.7693	18.6668	18.6545
3	44.6955	52.6259	45.1671	44.9597
4	74.6361	107.2538	76.8465	75.9180

A comparison of % error in results of the cantilever beam 2 of Thomas et al [4] with present work is made in Table 6.4.

The present formulation shows a better rate of convergence and a higher accuracy of results with fewer nodal parameters compared to the earlier formulations.

Table 6.4

Comparison of % error in results of reference [4] and present work

Mode, n	error in results of	
	reference [4] 9 nodal parameters	present work 8 nodal parameters
1	-	0.01
2	0.5	0.19
3	6.25	1.06

The % error in the results of Kapur [14] for cantilever and simply supported beams are compared with % error in results of present work in Table 6.5. The non-dimensional parameters are re = 0.080 and se = 0.160.

There seems to be some error in Kapur's results [14] for 4th mode of the simply-supported beam, because for the higher modes the error increases monotonically in all cases. The accuracy of the present formulation is in general higher than the earlier ones, though the error is slightly more in first two modes of the cantilever beam.

A comparison of the % error in results of present work and Davis et al [10] shows that there is a significant improvement in the accuracy. Results are presented in Table 6.6. In this case also the % error for the fourth mode of the simply-supported beam, as quoted by Davis et al [10] seems to be in error.

Table 6.5

Comparison of % error, in Kapur's results [14] and the present work, for 2 elements

Mode,n	% error in Cantilever beam results		% error in Simply-supported beam results	
	reference[14]	present work work	reference[14]	present work
1	0.03	0.0790	0.29	0.0266
2	0.57	0.8387	6.00	0.4060
3	7.88	3.0130	9.50	1.8950
4	14.90	7.3375	8.00	12.4750

The natural frequencies of simply-supported (S-S) and clamped-clamped (C-C) beams for low values of the non-dimensional parameters, re = 0.02 and se = 0.02, are obtained, and are given in Table 6.7 along with the exact results, using frequency equations of Huang [3]. A similar table, Table 6.8, for higher values of non-dimensional parameters, re = 0.10 and se = 0.10, is also obtained. An excellent trend of convergence, for both higher and lower values of re and se, is observed, except for an isolated case of a fourth mode of clamped-clamped beam for higher re and se. This may be due to the ill-conditioning of the equations.

Table 6.6

Comparison of % error in results of Davis et al [10] and the present work

No.of element	Mode,n	error in cantilever beam results		error in simply-supported beam results	
		reference[10]	present work	reference[10]	present work
2	1	0.25	0.027	1.79	0.394
	2	3.63	1.210	37.36	11.300
	3	50.86	18.610	56.69	24.958
	4	64.19	46.099	42.07	30.856
4	1	0.06	0.060	0.39	0.026
	2	1.23	0.665	3.99	0.406
	3	5.68	2.760	12.08	1.914
	4	10.78	7.088	32.23	12.799

Table 6.7

Natural frequencies $\overline{\omega_n}$, of simply-supported and clamped-clamped beams, re = 0.02 and se = 0.02

Mode n	Beam end condi-tions	Exact results[3]	Finite element results		
			2 elements	4 elements	6 elements
1	S-S	9.8298	9.8697	9.8335	9.8315
	C-C	22.1027	22.2943	22.2708	22.2667
2	S-S	38.8737	43.1393	39.0272	38.9054
	C-C	59.8611	61.1379	60.7023	60.6220
3	S-S	85.8765	106.2978	87.4384	86.2148
	C-C	114.6403	118.8134	117.3275	116.7771
4	S-S	149.0297	189.0053	165.3483	150.7824
	C-C	184.2068	218.6651	191.0595	189.0338

Table 6.8

Natural frequencies, $\overline{\omega_n}$, of simply-supported and clamped-clamped beams, re = 0.10 and se = 0.10

Mode, n	Beam end conditions	Exact results[3]	Finite element results		
			2 elements	4 elements	6 elements
1	S-S	.0505	9.0862	9.0529	9.0510
	C-C	17.7839	20.4035	20.3803	20.3763
2	S-S	30.2985	33.7447	30.4221	30.3241
	C-C	39.5839	47.6876	47.3032	47.2227
3	S-S	56.6895	71.4840	57.3058	56.9381
	C-C	64.5546	80.2149	80.3657	79.7297
4	S-S	85.2456	109.0813	97.1226	86.4388
	C-C	89.2407	107.4869	107.8482	108.1515

The versality of the formulation is proved by obtaining the natural frequencies of a few cases of non-simple boundary conditions, e.g., when different types of springs are attached to the free end of a cantilever beam. Figure 6.1 gives a plot of ω/ω^* versus k_s for the first three modes of a cantilever beam when a linear spring, k_s, is attached, where ω^* is the frequency for $k_s = 0$, the value of non-dimensional parameters are re = 0.02 and se = 0.02. The additional spring has maximum influence on the fundamental mode and almost negligible on higher modes. An identical trend can be observed for re = 0.07 and se = 0.10 values, as shown in Figure 6.2.

Figure 6.3 shows the variation of frequency when the same spring is attached to beams of different dimensions, such that se = 2 re. ω_o is the frequency for re = 0.0. The trend is same as for $k_s = 0$, except that for lower modes the rate of decrease of frequency is not so steep.

Figure 6.4 shows a similar graph when an additional torsional spring, k_t, is attached. In this case the rate of decrease of frequencies has been reduced for all modes compared to that for $k_t = 0$.

6.2.2 Beams : Approach B

The natural frequencies of uniform cantilever (C-F) and simply-supported beams are presented in Tables 6.9 and 6.10 for low and high values of non-dimensional parameters,

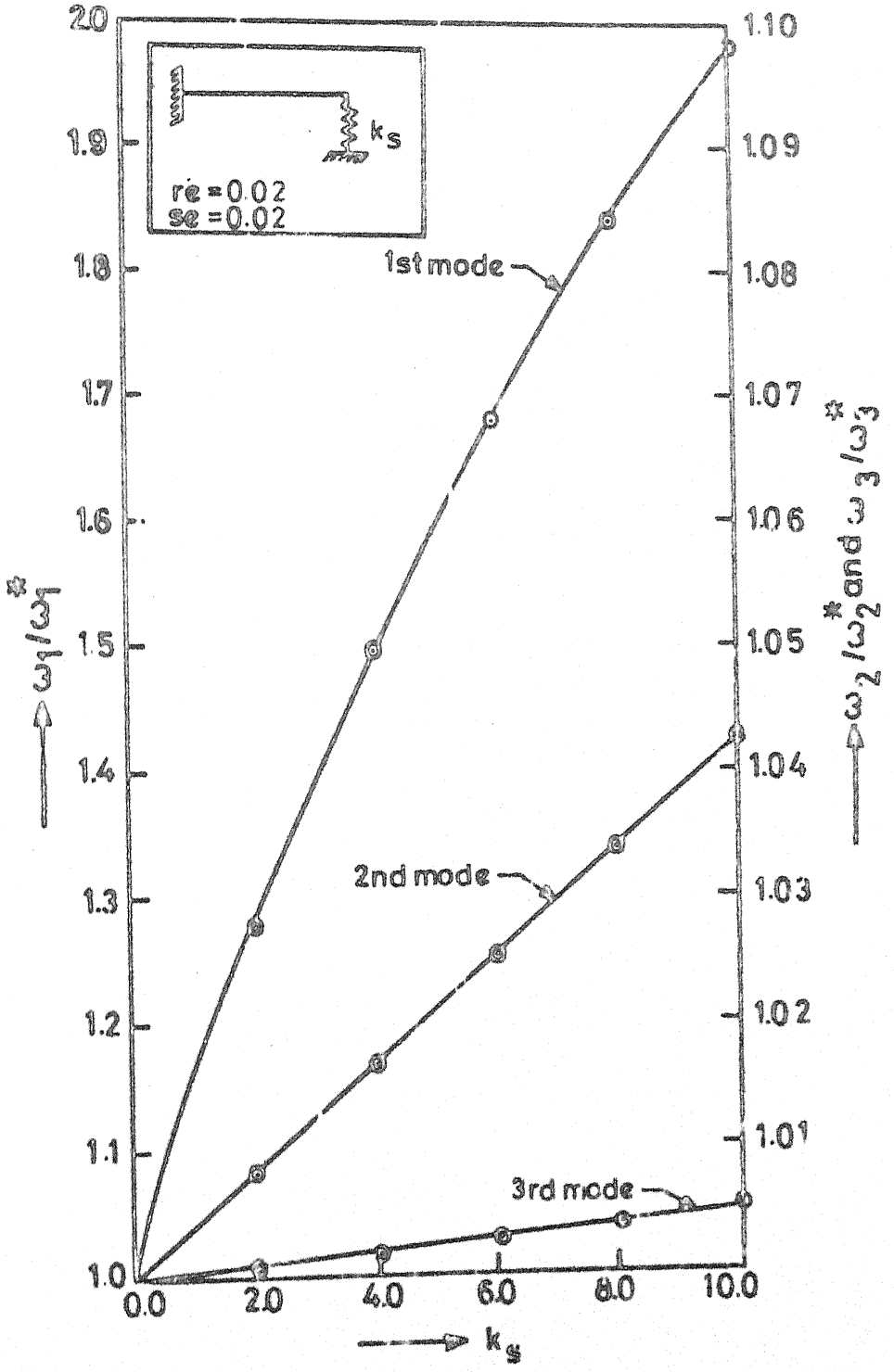

Figure 6.1. Variation of frequency with linear spring, k_s

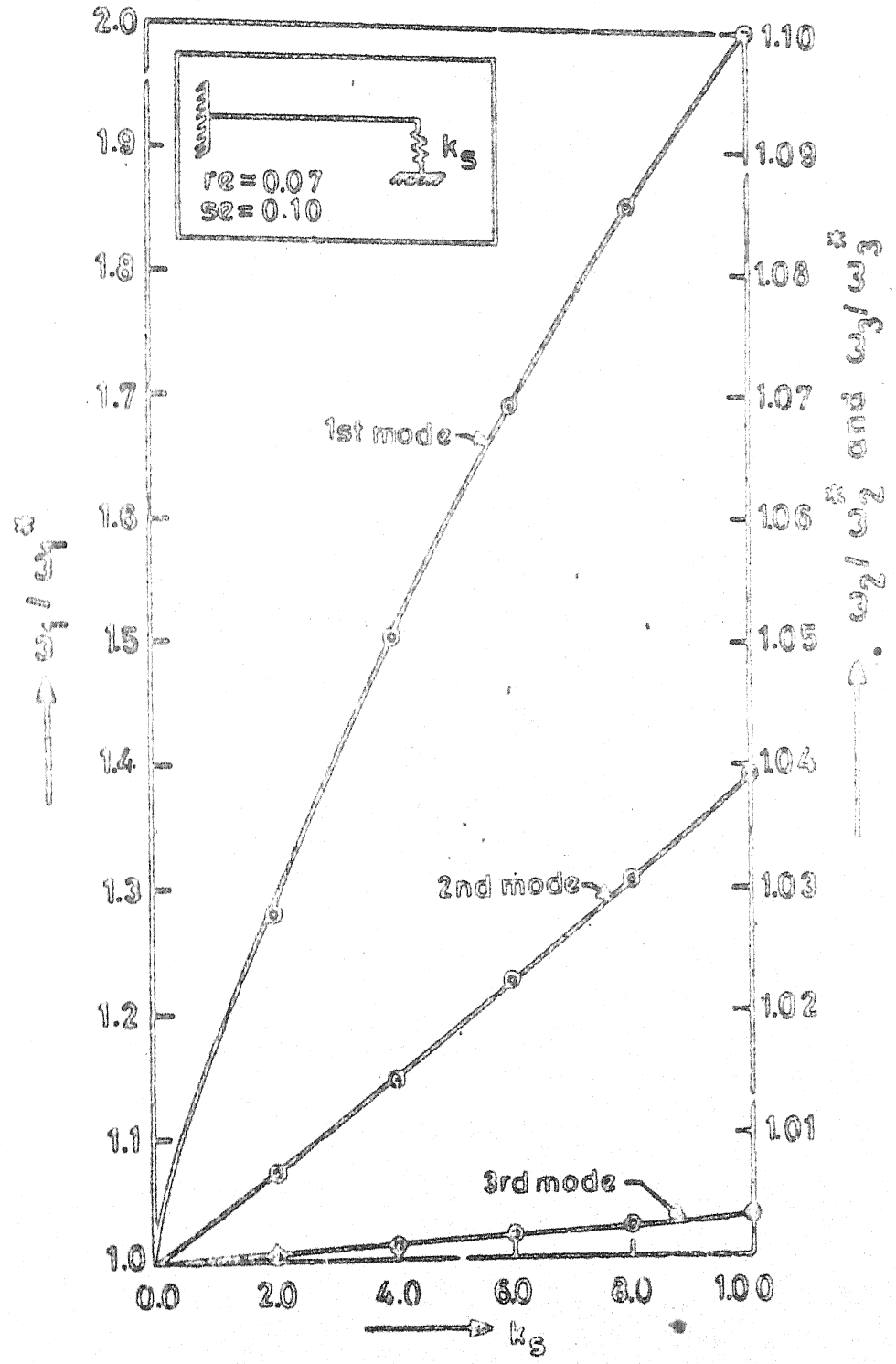

Figure 6.2. Variation of frequency with linear spring, k_s

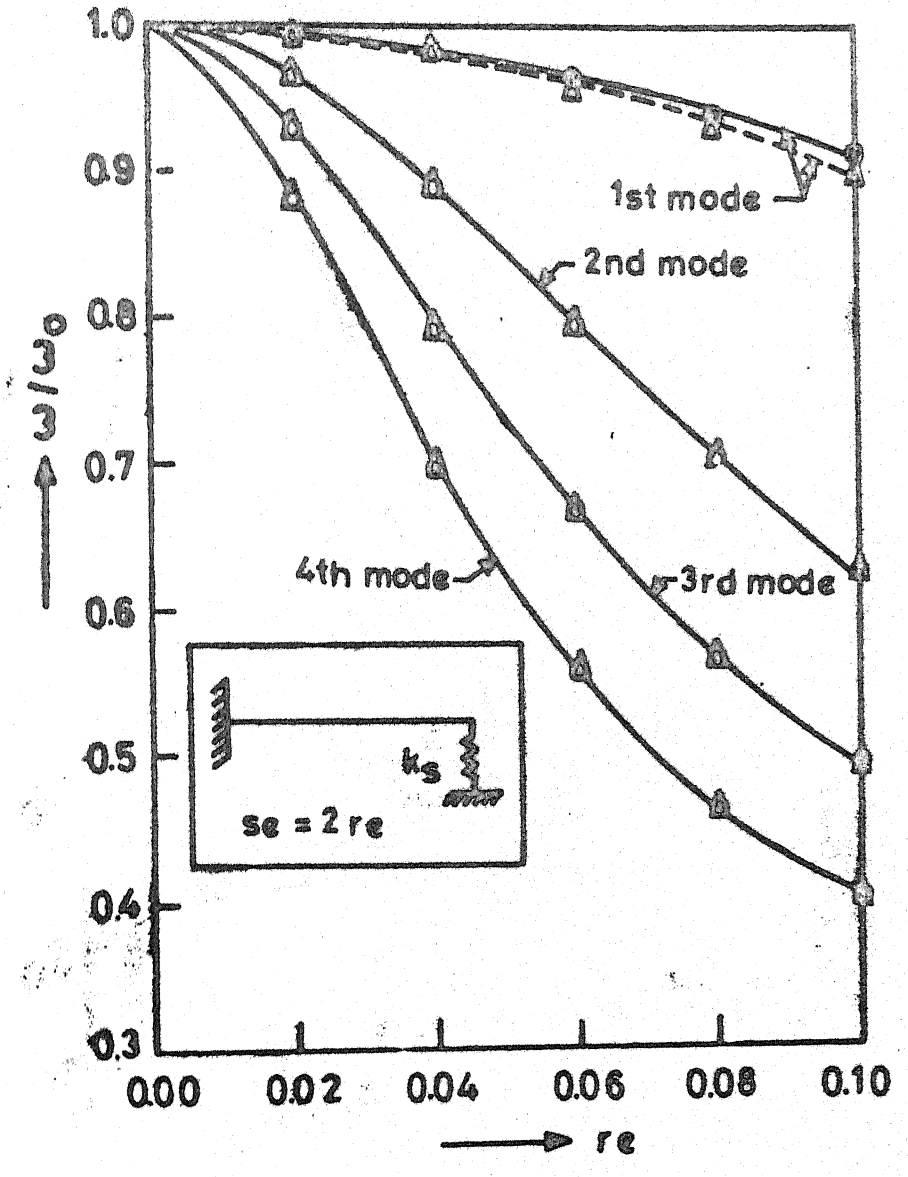

Figure 6.3. Variation of frequency with re, for given k_s=0.0, --Δ-- ; k_s=5.0, --○--

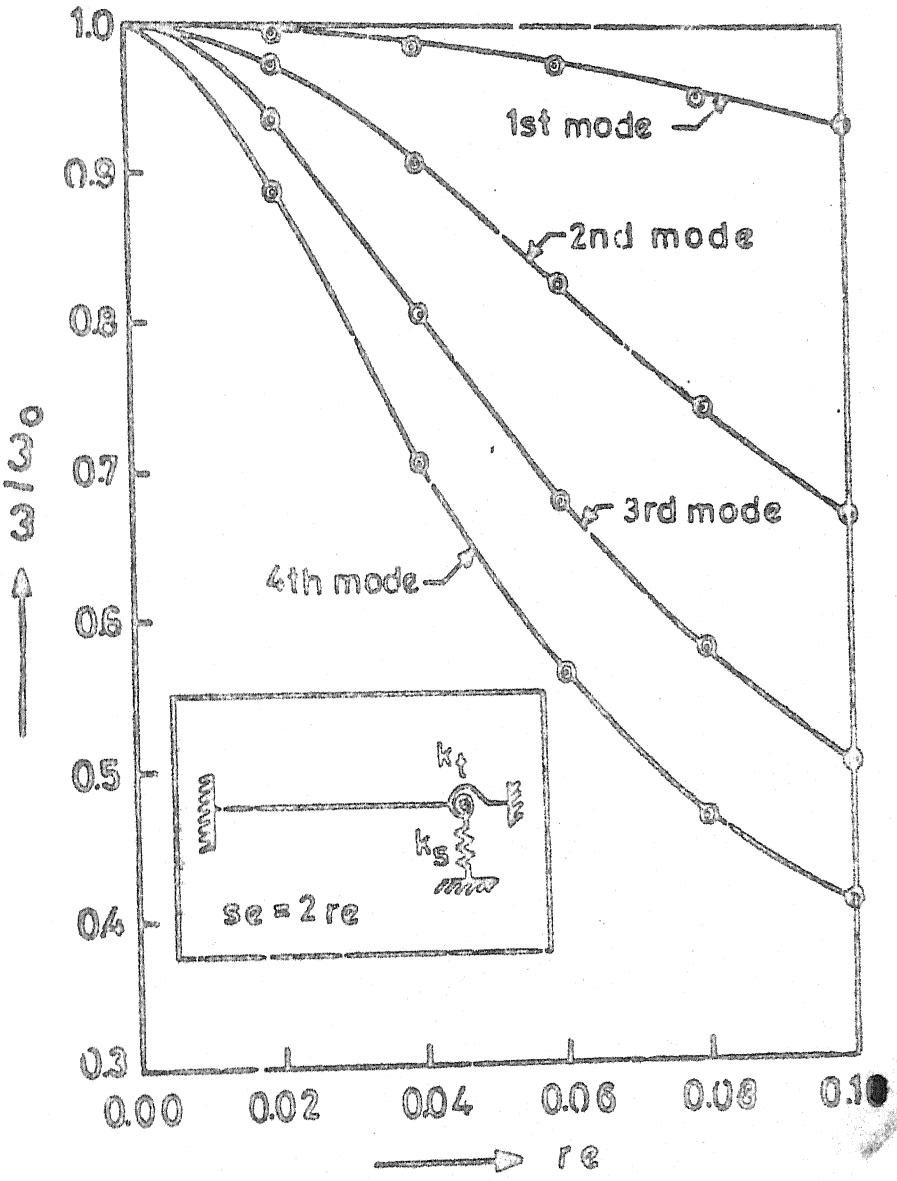

Figure 6.4. Variation of frequency with re, for given k_s 5.0 and k_t 50.

re and se. For low values of re and se the convergence rate is extremely poor, Table 6.9, whereas, the convergence rate is quite satisfactory for the higher values of re and se, Table 6.10. This poor rate of convergence is due to ill-conditioning or locking, as sometimes called in literature. Similar convergence problems were encountered in static analysis by various authors, Gallagher [64] and Hinton and Owen [65]. To avoid this ill-conditioning, the domain was divided into elements of unequal lengths to change the nature of the simultaneous equations to be solved. But there was no improvement. In static analysis the ill-conditioning was removed [65] by the reduced integration using 1-point Gauss-Legendre quadrature formula [61] for the shear stiffness matrix. The results using this technique for $[K_3]$ in equation (3.20) are also given in Tables 6.9 and 6.10, and the marked improvement in convergence rate can be observed. Still the effects of the ill-conditioning can be observed for the fourth mode of the simply-supported beam, re = 0.10 and se = 0.15, where the frequency has converged to a value less than the exact value.

The natural frequencies, $\overline{\omega}_n$, of tapered cantilever beams are given in Table 6.11. The taper ratio, T_p, as shown in Figure 6.5, is 0.90 and 0.70, re = 0.10, and se = 0.15. As expected the frequency increases compared to the uniform beam. A good rate of convergence is observed.

Table 6.9

Natural frequencies, $\overline{\omega_n}$, of the uniform cantilever and simply-supported beams, re = 0.02 and se = 0.02

Mode, n	Beam end conti-ons	Exact results [3]	K-exact integration results for, elements			K-reduced integration results for, elements		
			2	4	6	2	4	6
1	C-F	3.5095	24.9385	13.0767	9.1241	3.5850	3.5343	3.5211
	S-S	9.8298	87.0656	38.7362	26.2007	13.7688	10.6330	10.1753
2	C-F	21.7547	173.2017	86.3078	58.3158	39.2212	25.2893	23.2648
	S-S	38.8767	2498.7421	176.8049	110.7537	346.4102	54.0750	44.6945
3	C-F	59.8895	2507.8337	264.1590	171.1343	1498.2243	93.1311	72.5300
	S-S	85.8765	2511.7028	459.3491	271.4173	2178.4899	192.1184	118.2493
4	C-F	114.6379	2520.2310	532.3260	357.3499	2440.7932	307.2841	168.4112
	S-S	149.0297	2523.8994	2498.5452	529.8627	2550.0035	692.8206	265.5702

Table 6.10

Natural frequencies, $\overline{\omega}_n$, of the uniform cantilever and simply-supported beams, re = 0.10 and se = 0.15

Mode, n	Beam end condi-tions	Exact results [3]	K-exact integration results for, elements			K-reduced integration results for, elements		
			2	4	6	2	4	6
1	C-F	3.2822	4.4683	3.6293	3.4418	3.3500	3.3040	3.2923
	S-S	8.6431	14.3672	10.0520	9.2687	11.3856	9.2375	8.9005
2	C-F	15.4357	24.2218	18.0309	16.6091	21.4931	16.9877	16.1193
	S-S	27.1303	66.6667	35.2767	30.6371	66.6667	33.4585	29.7792
3	C-F	34.2048	73.6107	43.4892	38.4812	68.3712	41.6698	37.5902
	S-S	48.4716	77.2746	66.6667	58.6865	70.2640	66.6660	57.6221
4	C-F	53.1105	88.4085	68.8178	61.9543	74.2891	67.9074	61.1145
	S-S	70.5300	96.1486	70.2519	66.6667	69.2820	68.8009	66.6667

Table 6.11

Natural frequencies, $\overline{\omega}_n$, of a tapered cantilever beam, re = 0.10 and se = 0.15

Taper ratio, T_p	Mode, n	Exact results for uniform beam[3]	Finite element results for tapered beam		
			2 element	4 element	6 element
0.90	1	3.2822	3.5605	3.4311	3.4056
	2	15.4357	21.8877	17.2148	16.3135
	3	34.2048	68.4379	41.8637	37.7497
	4	53.1105	74.5818	68.0111	61.2571
0.70	1	Same	4.0455	3.7423	3.6845
	2	as	22.8502	17.7625	16.7784
	3	above	68.5763	42.3534	38.1455
	4		75.4504	68.2938	61.6321

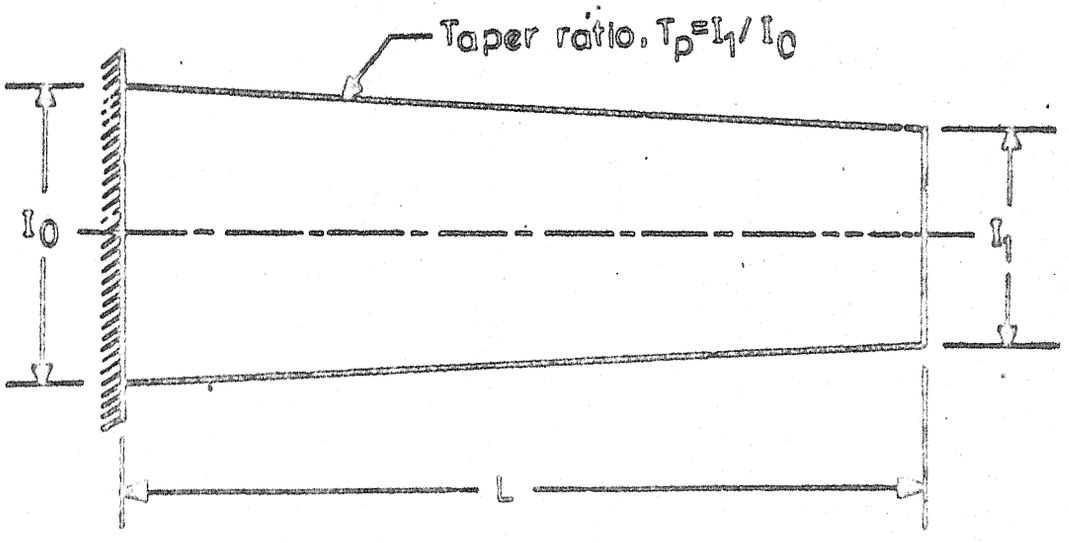

Figure 6.5. A tapered beam.

6.2.3 Thin Rings

Non-dimensional natural frequencies, $\overline{\omega}_n$, are obtained for various configurations of rings and sectors. Natural frequencies of a free ring are compared with exact results of Hoppe [16] and finite difference results of Ball [19] and finite element results of Sabir and Ashwell [34] in Table 6.12. An 180°-sector with radial displacement zero at the ends was used to find the frequencies of a free-ring, from symmetry considerations.

The results from the present study converge monotonically from the higher side to exact values. The accuracy is considerably higher even for 4 elements 180°-sector (13 nodal parameters) results than seven elements 90°-sector (19 nodal parameters) results of Sabir and Ashwell[34]. It is interesting to note that this improvement in accuracy is achieved despite the fact that the actual element size in the present study is almost four times of that used by Sabir and Ashwell [34]. When the element size is about double the size of the element of Sabir and Ashwell [34], i.e., for six elements, the results converge to almost exact values. The finite difference results [19] are less than the exact values.

Natural frequencies, $\overline{\omega_n}$, of different sectors with free-, hinged-, and clamped- end conditions, as shown in Figure 6.6 are given in Table 6.13.

Table 6.12

Natural frequencies, $\overline{\omega_n}$, of a free-ring

Mode,n	Exact results[16]	Finite difference results[19]	Finite element results[34] 90°-sector, 7 element	Finite element results for 180°-sector		
				2 elements	4 elements	6 elements
1	0.0	0.0	0.0	0.0	0.0	0.0
2	2.6833	2.5544	2.6671	2.6846	2.6836	2.6833
3	7.5901	-	-	7.8827	7.5965	7.5901
4	14.5521	11.3071	14.5753	18.9407	14.5590	14.5583
5	23.5339	-	--	33.8620	23.8501	23.5677
6	34.5238	20.7359	34.5975	35.6696	34.5507	34.5261

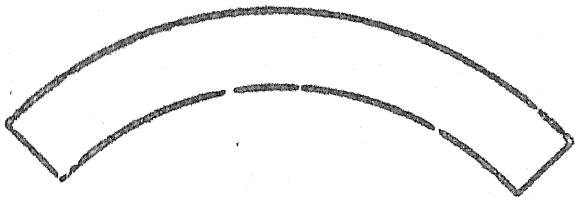

(a) Free-free sector

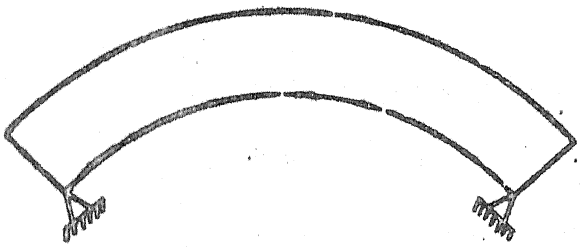

(b) Hinged-hinged sector

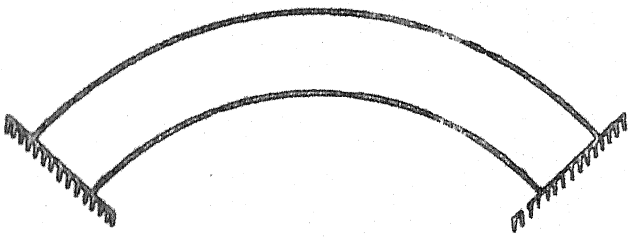

(c) Fixed-fixed sector

Figure 6.6. Sectors on various end conditions.

Table 6.13

Natural frequencies, $\overline{\omega}_n$, of different sectors with free-, hinged-, fixed-ends

Sector Angle	End conditions	Mode, n	Natural frequency, $\overline{\omega}_n$, for		
			2 elements	4 elements	6 elements
90°	F-F	1,2,3	0.0	0.0	0.0
		4	8.4107	8.3914	8.3910
		5	24.1399	23.9376	23.9267
		6	49.0616	47.9738	47.8124
	S-S	1	13.7678	13.7646	13.7638
		2	33.5448	32.4232	32.4055
		3	78.6954	61.6909	61.6952
		4	134.7429	97.6988	96.5655
		5	210.5188	146.2239	141.7034
		6	-	205.2581	194.1875
	C-C	1	22.6650	22.6300	22.6255
		2	45.2531	43.3313	43.2614
		3	119.2643	78.3515	78.2903
		4	-	117.0949	115.7615
		5	-	172.3631	166.3525
		6	-	231.8083	221.4385
180°	F-F	1,2,3	0.0	0.0	0.0
		4	1.8455	1.8373	1.8372
		5	5.3682	5.3118	5.3089
		6	11.4418	11.1610	11.1182

contd...

Sector Angle	End conditions	Mode, n	Natural frequency, $\bar{\omega}_n$, for		
			2 elements	4 elements	6 elements
	S-S	1	2.2679	2.2669	2.2667
		2	7.2115	6.9280	6.9238
		3	18.0850	13.9824	13.9828
		4	32.1272	23.1352	22.8484
		5	50.7828	35.0758	33.9399
		6	-	50.0236	47.2303
	C-C	1	4.3934	4.3857	4.3845
		2	10.1419	9.6708	9.6533
		3	28.0947	17.9433	17.9348
		4	-	27.9365	27.6035
		5	-	41.3444	39.8456
		6	-	56.6120	53.9585
270°	F-F	1,2,3	0.0	0.0	0.0
		4	0.7699	0.7601	0.7600
		5	2.0374	2.0021	2.0006
		6	4.5613	4.4294	4.4082
	S-S	1	0.4749	0.4744	0.4743
		2	2.4972	2.3680	2.3660
		3	7.1354	5.3512	5.3510
		4	13.2730	9.4099	9.2798
		5	21.4941	14.6522	14.1440
		6	-	21.3304	20.0730
	C-C	1	1.4030	1.3957	1.3950
		2	3.7908	3.5946	3.5859
		3	11.4990	7.0499	7.0471
		4	-	11.5209	11.3729
		5	-	17.3509	16.6853
		6	-	24.2311	23.0185

contd ...

Sector Angle	End conditions	Mode, n	Natural frequency, $\overline{\omega}_n$, for		
			2 elements	4 elements	6 elements
359°	F-F	1,2,3	0.0	0.0	0.0
		4	0.4525	0.4399	0.4398
		5	0.9995	0.9604	0.9592
		6	2.2502	2.1697	2.1551
	S-S	1	0.0118	0.0065	0.0032
		2	0.9900	0.9120	0.9107
		3	3.4809	2.4650	2.4529
		4	6.8363	4.7018	4.5685
		5	11.4796	7.6295	8.0841
		6	-	11.3680	9.9833
	C-C	1	0.5832	0.5720	0.5714
		2	1.7137	1.6157	1.6092
		3	5.8855	3.4155	3.4136
		4	-	5.8981	5.8142
		5	-	9.1324	8.7564
		6	-	13.0313	12.3304

Table 6.13 shows that convergence is equally efficient for all sector angles contrary to the problems encountered and mentioned by Sabir and Ashwell [34], namely, the number of elements required for large angle sectors is more than that for the small angle sectors for the same accuracy. Thus the present formulation is simple and more efficient as compared to the earlier models.

Natural frequencies, $\bar{\omega}_n$, for a full ring on different number of equi-spaced radial supports, Figure 6.7, are presented in Table 6.14. The results are compared with the exact values given by Mallik and Mead [24]. The accuracy of the exact results [24] is limited by the accuracy with which the graph can be read.

Table 6.14

Natural frequencies, $\bar{\omega}_n$, of a ring on different number of equi-spaced radial supports

No.of supports	Mode, n	Exact results [24]	Finite element results, elements in each bay		
			2	4	6
2	1	2.26	2.2679	2.2669	2.2667
	2	4.38	4.3933	4.3857	4.3845
	3	6.92	7.2115	6.9280	6.9238
	4	9.64	10.1419	9.6709	9.6538
	5	-	18.0850	13.9824	13.9828
	6	-	28.0947	17.9434	17.9348
3	1	6.92	6.9291	6.9272	6.9268
	2	10.44	10.4291	10.4102	10.4086
	3	10.44	10.4291	10.4102	10.4087
	4	19.10	19.8289	19.0907	19.0768
	5	19.10	19.8289	19.0907	19.0768
	6	23.70	24.7323	23.6548	23.6155

contd...

No.of supports	Mode, n	Exact results [24]	Finite element results, elements in each bay		
			2	4	6
4	1	13.76	13.7678	13.7646	12.3595
	2	17.90	17.8948	17.8724	17.3260
	3	17.90	17.8948	17.8724	17.8699
	4	22.62	22.6650	22.6300	22.6256
	5	32.28	33.5448	32.4233	33.4557
	6	37.70	39.2632	37.7295	37.6961

A good consistent agreement between the finite element results and the exact results [24] is observed. The usual convergence from the higher side to the exact values is obtained.

The natural frequencies, $\bar{\omega}_n$, of a rotating ring, shown in Figure 6.8, for different speeds, $\bar{\Omega}^2$, are given in Table 6.15.

The natural frequencies increase with increase in rotational speed, $\bar{\Omega}$. The effect of speed is felt more on ring with fewer number of supports and on lower modes. With increase in number of supports or for higher modes the increase in frequency due to rotational speed is marginal. This is because as the number of supports increase or it vibrates in higher modes the ring becomes more and more stiff and, hence, the relative contribution of the rotational speed decreases. The inclusion of the rotational speed

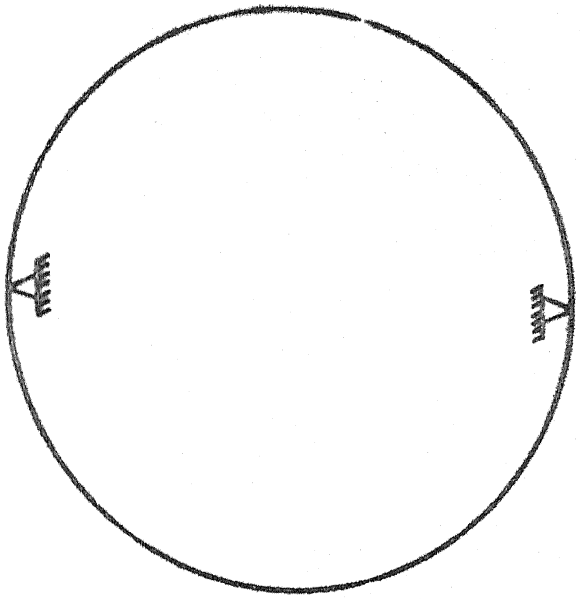

(a) Ring on two supports

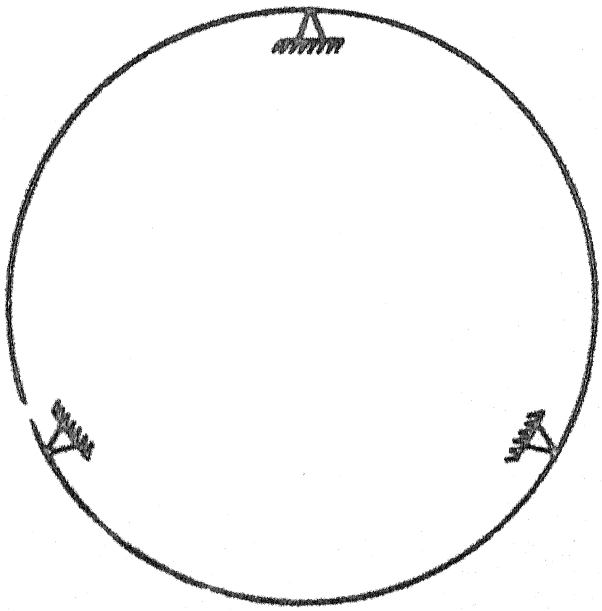

(b) Ring on three supports

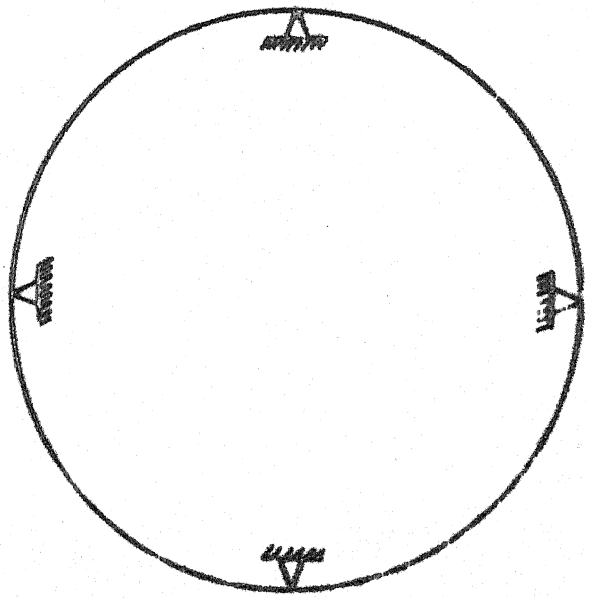

(c) Ring on four supports

Figure 6.7. Rings on different number of equi-spaced radial supports.

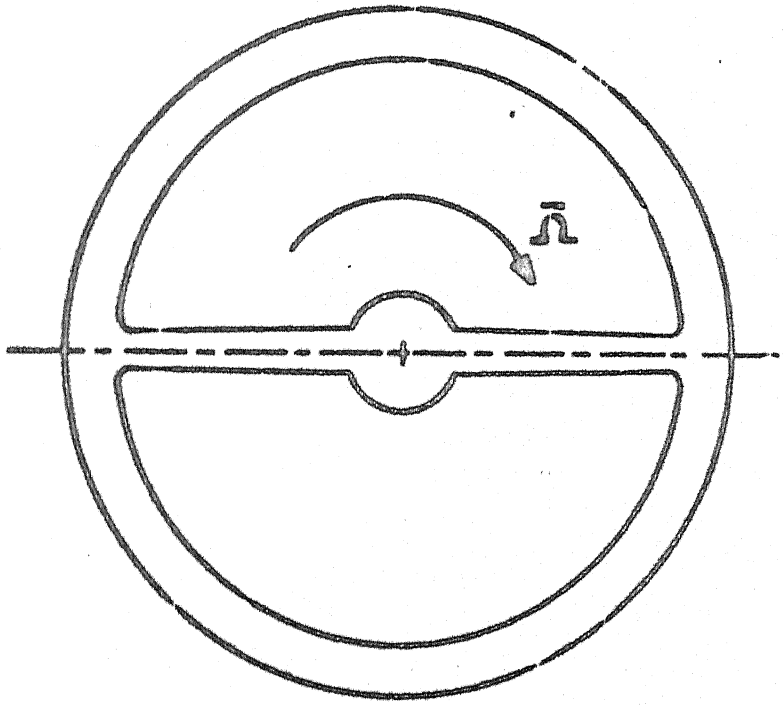

Figure 6.8. Rotating ring on two radial supports.

Table 6.15

Natural frequencies, $\bar{\omega}_n$, of a rotating ring for different rotational speeds, $\bar{\Omega}$

No.of supports	Rotational speed, $\bar{\Omega}^2$	Mode, n	Finite element results for			
			2 elements	4 elements	6 elements	Zero speed 6 elements
2	5.0	1	2.8275	2.8265	2.8264	2.2667
		2	4.7343	4.7284	4.7274	4.3845
		3	7.4952	7.2221	7.2181	6.9238
		4	10.3519	9.8892	9.8721	9.6533
		5	18.2060	14.1400	14.1403	13.9828
		6	28.1750	18.0649	18.0566	17.9348
	10.0	1	3.2932	3.2920	3.2919	Same as
		2	5.0521	5.0476	5.0467	above
		3	7.7686	7.5047	7.5008	
		4	10.5576	10.1028	10.0862	
		5	18.3264	14.2960	14.2962	
		6	28.2552	18.1859	18.1778	
3	5.0	1	7.1944	7.1926	7.1921	6.9268
		2	10.6146	10.5963	10.5948	10.4086
		3	10.6146	10.5963	10.5948	10.4087
		4	19.9446	19.2107	19.1969	19.0768
		5	19.9446	19.2107	19.1969	19.0768
		6	24.8264	23.7528	23.7138	23.6155
	10.0	1	7.4503	7.4484	7.4481	Same
		2	10.7969	10.7792	10.7777	as above
		3	10.7969	10.7792	10.7777	
		4	20.0597	19.3300	19.3162	
		5	20.0597	19.3300	19.3162	
		6	24.9201	23.8504	23.8116	

contd ...

No.of supports	Rotational speed, $\bar{\Omega}^2$	Mode, n	Finite element results for			
			2 elements	4 elements	6 elements	Zero speed 6 elements
4	5.0	1	13.9198	13.9166	12.5281	12.3595
		2	18.0141	17.9919	17.4489	17.3260
		3	18.0141	17.9919	17.4489	17.8699
		4	22.7605	22.7258	22.7214	22.6256
		5	33.6158	32.4966	33.5268	33.4557
		6	39.3242	37.7927	37.7594	37.6961
	10.0	1	14.0702	14.0670	12.6946	Same as
		2	18.1326	18.1107	17.5710	above
		3	18.1326	18.1107	18.1081	
		4	22.8557	22.8213	22.8169	
		5	33.6866	32.5697	33.5977	
		6	39.3849	37.8557	37.8226	

does not pose any additional difficulty and the efficiency of the formulation remains uneffected.

The versatility of the formulation is further illustrated by obtaining the natural frequencies, $\bar{\omega}_n$, of an 180°-sector with three radial supports, placed at unsymmetric positions, as shown in Figure 6.9. The results are given in Table 6.16. The middle support is placed at varying angles from one end. All results are for six-elements in each bay.

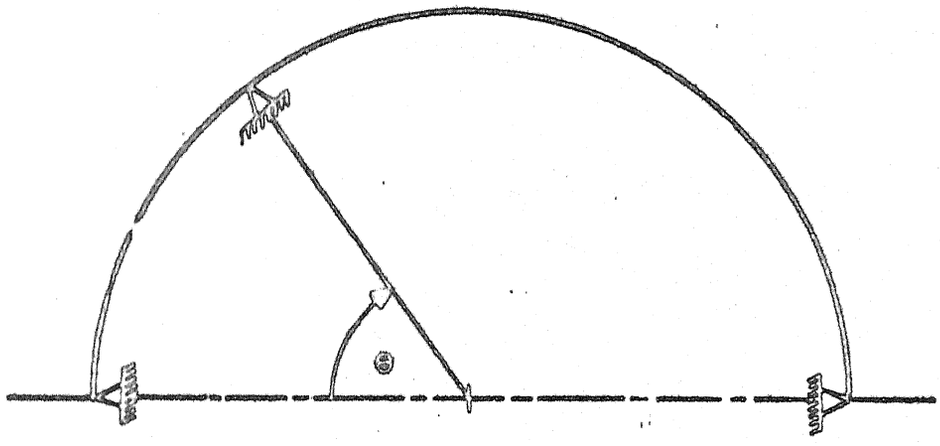

Figure 6.9. 180° sector on three radial supports with unequal bays.

Table 6.16

Natural frequencies, $\bar{\omega}_n$, of an 180^o-sector on 3-supports with unequal bays

Mode, n	Angle Θ						
	0^o	15^o	30^o	45^o	60^o	75^o	90^o
1	2.2667	4.0121	5.0194	6.3908	8.3085	11.0282	13.7638
2	6.9238	9.8697	12.0082	14.8978	18.8429	22.0896	17.8705
3	13.9828	18.8553	22.7949	28.0826	33.7344	27.0225	32.4055
4	22.8484	29.6849	35.6965	43.5798	40.3728	45.7707	37.6956

It can be observed that the fundamental frequency increases monotonically as the middle support moves from one end towards the symmetric position. This gives a significant conclusion that the fundamental frequency can be adjusted, by moving the middle support position, anywhere between the minimum and maximum values for that configuration. The same analysis can be extended to rings and sectors on any number of supports.

6.2.4 Thick Rings

The natural frequencies, $\bar{\omega}_n$, of the free-ring, re = 0.10 and se = 0.1704, are given in Table 6.17 and compared with the analytical values of Kirkhope [36] and experimental results of Lincoln and Volterra [18].

Table 6.17

Natural frequencies, $\overline{\omega}_n$, of a free-ring, re = 0.10 and se = 0.1704

Nodal diameters, n	Classical results [16]	Equation (1.1) [36]	Experimental results [18]	Finite element results for		
				2 elements	4 elements	6 elements
1	0.0	0.0	0.0	0.0	0.0	0.0
2	2.6833	2.5208	2.5861	2.5209	2.5199	2.5196
3	7.5901	6.6265	6.8098	6.8386	6.5985	6.5908
4	14.5521	11.6705	12.0129	14.8130	11.5193	11.5203
5	23.5339	17.2838	17.7873	23.5409	17.0776	16.8876

A good rate of convergence of the finite element results can be observed from Table 6.17. As expected, the frequency decreases by considering Timoshenko effects in this case also. The finite element results are close to the analytical results [36], and are on the lower side. Since the finite element results are always higher than the exact, the error in Kirkhope's results [36] is more than the finite element results.

A second comparison of finite element results is made with the experimental values of Kuhl [35] and analytical results obtained by Kirkhope [36] in Table 6.18. The non-dimensional parameters for this ring are re = 0.1378 and se = 0.2015.

Table 6.18

Natural frequencies, $\bar{\omega}_n$, of a free ring, re = 0.1378 and se = 0.2425

Nodal diameters, n	Classical results [16]	Equation (1.1) [36]	Experimental results [35]	Finite element results for		
				2 elements	4 elements	6 elements
1	0.0	0.0	0.0	0.0	0.0	0.0
2	2.6833	2.4581	2.4821	2.4544	2.4535	2.4532
3	7.5436	6.2948	6.1964	6.4549	6.2310	6.2259
4	14.5521	10.8148	10.4519	13.5379	10.5620	10.5630
5	23.5339	15.7857	14.9708	20.9261	15.2752	15.1078

Consistent with the trend, the frequency decreases further with increase in re and se values, the rate of convergence is unaffected by this increase. An excellent agreement with the experimental values of Kuhl [25] is observed. The analytical results of Kirkhope [36] deviate more from experimental values compared to the finite element results.

The ring on radial supports, with Timoshenko effects, is analysed and results for the parameters, re = 0.05 and se = 0.0866 are given in Table 6.19. The results are compared with those given by Rao and Sundrarajan [22]. The classical results, i.e., the results without Timoshenko effects, are the finite element results for six elements from Tables 6.12 and 6.14.

Table 6.19

Natural frequencies, $\overline{\omega}_n$, of a ring on radial supports, re = 0.05 and se = 0.0866

No.of supports	Mode, n	Classical results, 6 elements	Rao and Sundrarajan [22]	Finite element results for		
				2 elements	4 elements	6 elements
0	1	0.0	0.0	0.0	0.0	0.0
	2	2.6833	2.631	2.6395	2.6385	2.6382
	3	7.5901	7.292	7.5699	7.2979	7.2918
	4	14.5583	13.570	17.5646	13.5562	13.5575
1	1	0.0	-	-	0.0	0.0
	2	1.5957	2.948	-	1.5892	1.5828
	3	2.4479	7.740	-	2.4127	2.4126
	4	5.7745	14.570	-	5.7025	5.6220
2	1	2.2667	-	2.2397	2.2388	2.2386
	2	4.3845	3.000	4.3266	4.3181	4.3169
	3	6.9238	7.990	6.9661	6.6955	6.6913
	4	9.6533	15.240	9.7311	9.3009	9.2828

The results for a free ring match very well with those given by Rao and Sundrarajan [22]. All the results are less than the classical values, as expected. The results for thick rings on radial supports reported by Rao and Sundrarajan [22] are inaccurate, because the values are more than the corresponding classical values. The finite element results show the desired trend and a good rate of convergence.

The natural frequencies, $\overline{\omega}_n$, of various sectors, with the parameters re = 0.05 and se = 0.0866, both ends hinged, are given in Table 6.20. The classical results are the finite element results for six elements from Table 6.13.

Table 6.20

Natural frequencies, $\overline{\omega}_n$, of various sectors on hinged ends, re = 0.05 and se = 0.0866

Sector angle	Mode, n	Classical results, 6 elements	Finite element results for		
			2 elements	4 elements	6 elements
90°	1	13.7638	60.3622	12.9076	12.9069
	2	32.4055	90.6235	28.2802	28.2643
	3	61.6952	108.8558	48.5269	48.5306
	4	96.5655	190.3344	69.8358	69.0849
180°	1	2.2667	16.5207	2.2388	2.2386
	2	6.9238	24.1192	6.6955	6.6913
	3	13.9828	35.1093	13.0842	13.0847
	4	22.8484	70.7622	20.8589	20.6074
270°	1	0.4743	6.5675	0.4722	0.4721
	2	2.3660	9.6990	2.3360	2.3340
	3	5.3510	16.0474	5.2037	5.2036
	4	9.2798	34.9962	8.9853	8.8626

The finite element results show a good rate of convergence and the appropriate trend. The influence of Timoshenko effects is felt more on small sectors and higher modes, this also confirms to the logic.

A similar set of results for sector with clamped-clamped ends is given in Table 6.21. The classical results are again finite elements results for six elements from Table 6.13. The non-dimensional parameters are re= 0.05 and se = 0.0866.

These results follow the same pattern as the results for hinged-hinged sectors and exactly the same conclusions can be drawn.

The rings on radial supports spinning at constant speed are analysed and results are presented in Table 6.22. The non-dimensional parameters are re = 0.05 and se = 0.0866. The rotational speeds are $\bar{\Omega}^2$ = 5.0 and 10.0. The six element results for a non-rotating ring are also given, from Table 6.19, for comparison.

The trend of the effect of rotational speed on a thick ring is same as that on a thin ring. Hence, the conclusions from Table 6.22 are same as those from Table 6.15, namely, the frequency increases with speed and the increase is more for a ring on fewer number of radial supports. Here also the convergence rate is not affected by the inclusion of rotational speed.

Table 6.21

Natural frequencies, $\bar{\omega}_n$, of various fixed-fixed sectors, re = 0.05 and se = 0.0866

Sector angle	Mode, n	Classical results 6 elements	Finite element results for 2 elements	4 elements	6 elements
90°	1	22.6255	21.0221	20.9687	20.9634
	2	43.2614	38.5719	37.2035	37.1269
	3	78.2903	87.6019	60.7020	60.5692
	4	115.7615	-	82.3650	81.4379
180°	1	4.3845	4.3266	4.3181	4.3169
	2	9.6533	9.7311	9.3009	9.2828
	3	17.9348	25.6310	16.6959	16.6826
	4	27.6035	-	25.0164	24.7265
270°	1	1.3950	1.3952	1.3878	1.3871
	2	3.5859	3.7276	3.5382	3.5294
	3	7.0471	11.0481	6.8366	6.8331
	4	11.3729	-	10.9630	10.8245

6.2.5 Thin Discs

The natural frequencies, $\bar{\omega}_n$, for a centrally clamped, outer-edge free disc, for various values of Ratio = a/b, the ratio of inner to outer diameter, are obtained and compared with the exact values given by Southwell [41] wherever possible.

Table 6.22

Natural frequencies, $\bar{\omega}_n$, of rotating rings on radial supports, re = 0.05 and se = 0.0866

No.of supports	Rotational speed, $\bar{\Omega}^2$	Mode, n	Finite element results for			
			2 elements	4 elements	6 elements	Zero speed
2	5.0	1	2.7924	2.7915	2.7914	2.2386
		2	4.6623	4.6556	4.6546	4.3169
		3	7.2402	6.9797	6.9758	6.6913
		4	9.9326	9.5109	9.4933	9.2828
	10.0	1	3.2523	3.2511	3.2510	Same
		2	4.9754	4.9701	4.9692	as
		3	7.5042	7.2528	7.2490	above
		4	10.1300	9.7164	9.6992	
3	5.0	1	6.9552	6.9535	6.9531	6.6965
		2	10.2040	10.1829	10.1812	10.0022
		3	10.2040	10.1829	10.1812	10.0022
		4	18.3661	17.7129	17.6993	17.6887
	10.0	1	7.2026	7.2009	7.2005	Same
		2	10.3793	10.3587	10.3571	as
		3	10.3793	10.3587	10.3571	above
		4	18.4720	17.8228	17.8093	

The results are given in Tables 6.23 and 6.24. The value of the Poisson's ratio, ν, has been used as 0.3. In case of a disc vibrating in n-nodal diameter mode, the natural boundary conditions at free end are [60]

$$\frac{d}{dR}\left(R\frac{d^2w}{dR^2}\right) - \frac{1+2n^2}{R}\frac{dw}{dR} + \frac{\nu n^2}{R}\frac{dw}{dR} + \frac{(3-\nu)n^2w}{R^2} = 0 \qquad (6.11)$$

$$R\frac{d^2w}{dR^2} + \nu\frac{dw}{dR} - \frac{\nu n^2 w}{R} = 0 \qquad (6.12)$$

After assembly of equations (5.11), the terms at the free-end node in the vector $\{B\}^{(n)}$ are

$$B_{ND-1} = \left(\frac{d}{dr}\left((R_j+r)\frac{d^2w}{dr^2}\right) - \frac{1+2n^2}{R_j+r}\frac{dw}{dr}\right)_{R=b} \qquad (6.13)$$

$$B_{ND} = \left((R_j+r)\frac{d^2w}{dr^2}\right)_{R=b} \qquad (6.14)$$

where ND, is the total number of nodal parameters.

Using the boundary conditions, equations (6.11) and (6.12), the terms of equations (6.13) and (6.14) reduce to

$$B_{ND-1} = -\frac{(3-\nu)n^2 w_b}{b^2} - \frac{\nu n^2}{b}\left(\frac{dw}{dr}\right)_{R=b} \qquad (6.15)$$

$$B_{ND} = \frac{\nu n^2}{b} w_b - \nu\left(\frac{dw}{dr}\right)_{R=b} \qquad (6.16)$$

where, subscript, b, means evaluated at radius b.

These terms must be transferred to the left hand side and added at the appropriate places in the stiffness matrix to

satisfy the natural boundary conditions. To illustrate the influence of these terms on convergence the results with improper boundary conditions for Ratio = 0.276 are also given in Table 6.23.

Since the results of Southwell [41] were obtained by evaluating the determinant and then plotting a graph to find the root, the decimal accuracy cannot be expected i.e., the accuracy may be limited to the first decimal place. A fairly good agreement between the exact and finite element results is observed. As can be seen from the Table 6.23, the results with improper boundary conditions are not reliable, because the values converge sometimes to higher values sometimes to lower values, and the trend with increasing nodal diameters is not correct. The values increase continuously, instead of decreasing for one nodal diameter and then increasing. The rate of convergence of results with proper boundary conditions is quite fast.

It can be observed that within the accuracy of Southewell's results [41], the finite element results match very well. The results converge rapidly for lower as well as higher values of Ratio, and for lower and higher nodal diameter vibration modes.

Table 6.23

Natural frequencies, $\overline{\omega}_n$, of a centrally clamped disc, Ratio = 0.276

Nodal diameters	Nodal circles	Southwell [41]	Finite element results, with					
			Proper boundary conditions			Improper boundary conditions		
			2 elements	4 elements	6 elements	2 elements	4 elements	6 elements
0	0	6.55	6.5453	6.5115	6.5085	6.1582	6.0997	6.0906
	1	-	42.9630	41.7353	41.6409	45.0487	41.0948	40.7165
	2		152.7190	122.1858	121.1163	200.1460	126.8883	121.4056
	3	-	464.6880	244.7047	240.9288	863.6039	290.9880	247.8420
1	0	-	6.3711	6.3216	6.3166	7.7475	7.6620	7.6435
	1	-	45.0880	43.9047	43.8055	47.6703	43.8170	43.4420
	2	-	154.8113	124.7455	123.6200	202.1485	129.5305	124.2210
	3	-	466.2176	247.4704	243.7922	865.4269	293.3765	250.6618

contd...

Nodal diameters	Nodal circles	Southwell [41]	Finite element results, with					
			Proper boundary conditions			Improper boundary conditions		
			2 elements	4 elements	6 elements	2 elements	4 elements	6 elements
2	0	-	7.8658	7.8017	7.7922	12.3797	12.2838	12.2599
	1	-	51.7559	50.7667	50.6592	55.4230	51.9809	51.6444
	2	-	161.1836	132.7504	131.7073	208.1945	137.5974	132.8494
	3	-	470.8418	255.8987	252.5486	870.9989	300.6236	259.2300
3	0	-	13.6308	13.5928	13.5847	20.2134	20.1731	20.1553
	1	-	63.5283	62.9196	62.8122	68.0676	65.4936	65.2548
	2	-	172.4035	146.6897	145.7106	218.3778	151.4206	147.6677
	3	-	478.6610	270.4068	267.5644	880.2692	312.9584	273.8497

Table 6.24

Natural frequencies, $\overline{\omega}_n$, of a centrally clamped disc vibrating in zero-nodal circle mode for various values of ratio

Ratio	Nodal diameters	Southwell [41]	Finite elements results for		
			2 elements	4 elements	6 elements
0.642	0	26.21	26.9426	26.9174	26.9162
0.397	1	9.43	9.4128	9.3794	9.3769
0.603	1	22.18	22.2221	22.1955	22.1939
0.186	2	6.55	6.6246	6.5644	6.5514
0.349	2	9.43	9.4125	9.3538	9.3473
0.430	3	16.77	16.4413	16.3779	16.3709
0.590	3	26.21	26.0301	25.9718	25.9675

The results for a centrally clamped disc, Ratio = 0.3, are given in Table 6.25. A comparison with the results given by Leissa [66] and Mota Soares et al [53] is also made.

It can be observed that the current results match very well with the earlier reported results. A good rate of convergence is there. In the current analysis the number of nodal parameters for six elements is twleve, which is far less than those reported by Mota Soares et al [53]. The accuracy remains of the same order. So the use of complicated higher order interpolation functions, as in [53], is unnecessary for the problem under consideration.

Table 6.25

Natural frequencies, $\bar{\omega}_n$, of a centrally clamped disc, Ratio = 0.300

Nodal diameters	Nodal circles	Mote [42]	Leissa [66]	Mota Soares et al [53] 4 elements (24 nodal parameters)	Finite element results		
					2 elements	4 elements	6 elements (12 nodal parameters)
0	0	6.9826	6.98	6.98	7.0202	6.9563	6.9455
	1	-	44.66	44.66	49.4702	45.1519	44.7636
	2	-	-	130.20	215.6412	136.7424	130.9310
	3	-	-	258.82	931.4672	312.2573	266.0356
1	0	6.8712	6.64	6.87	6.9153	6.8305	6.8138
	1	-	46.75	46.75	51.4346	47.2640	46.8807
	2	-	-	132.61	217.2644	139.0288	133.3869
	3	-	-	261.44	932.7850	314.3753	268.5675

contd ...

Nodal diameters	Nodal circles	Mote [42]	Leissa [66]	Mota Soares et al [53] 4 elements (24 nodal parameters)	Finite element results		
					2 elements	4 elements	6 elements (12 nodal parameters)
2	0	8.3774	8.34	8.34	8.3751	8.2791	8.2537
	1	-	53.36	53.36	57.5026	53.8522	53.5039
	2	-	-	140.16	222.1950	146.0474	140.9400
	3	-	-	269.62	936.6944	320.8089	276.2523
3	0	13.9676	13.91	13.91	13.8888	13.8416	13.8253
	1	-	65.10	65.10	68.0723	65.3913	65.1317
	2	-	-	153.36	230.6054	158.1971	154.0204
	3	-	-	183.46	943.2535	331.7842	289.3750

Tables 6.23 and 6.25 show that the frequency for zero-nodal circle modes of disc is less for one-nodal diameter compared to the zero-nodal diameter mode of vibration. For higher nodal circle modes the frequencies increase monotonically with increase of nodal diameters. To study this effect in detail, the natural frequencies, $\overline{\omega}_n$, for various values of Ratio, of a centially clamped disc vibrating in zero-nodal circle and 0-, 1-, and 2-nodal diameter modes are calculated. The results are presented in Table 6.26.

Table 6.26

Natural frequencies, $\overline{\omega}_n$, of a centrally clamped disc vibrating in zero-nodal circle modes, for various values of Ratio

Ratio	Nodal diameters	Finite elements results for		
		2 elements	4 elements	6 elements
.050	0	4.2358	4.1600	4.1380
	1	3.3079	3.1348	3.0659
	2	5.7160	5.7058	5.7006
.100	0	4.5580	4.4763	4.4538
	1	3.8708	3.7291	3.6838
	2	5.9537	5.9200	5.9032

contd ...

Ratio	Nodal diameters	Finite elements results for		
		2 elements	4 elements	6 elements
.150	0	4.9776	4.8973	4.8789
	1	4.4749	4.3530	4.3197
	2	6.3194	6.2622	6.2383
.200	0	5.5092	5.4333	5.4170
	1	5.1583	5.0511	5.0259
	2	6.8266	6.7505	6.7233
.250	0	6.1778	6.1079	6.0955
	1	5.9574	5.8626	5.8412
	2	7.4999	7.4107	7.3850
.300	0	7.0202	6.9563	6.9455
	1	6.9153	6.8305	6.8138
	2	8.3751	8.2791	8.2537
.350	0	8.0892	8.0310	8.0234
	1	8.0890	8.0125	8.0004
	2	9.5039	9.4059	9.3860
.355	0	8.2113	8.1536	8.1467
	1	8.2211	8.1460	8.1310
	2	9.6334	9.5351	9.5129
.358	0	8.2860	8.2285	8.2195
	1	8.3017	8.2275	8.2154
	2	9.7127	9.6147	9.5922

contd ...

Ratio	Nodal diameters	Finite elements results for		
		2 elements	4 elements	6 elements
.359	0	8.3112	8.2539	8.2466
	1	8.3288	8.2542	8.2459
	2	9.7394	9.6412	9.6199
.360	0	8.3364	8.2793	8.2705
	1	8.3561	8.2817	8.2675
	2	9.7662	9.6679	9.6477
.361	0	8.3619	8.3049	8.2961
	1	8.3835	8.3092	8.2981
	2	9.7932	9.6948	9.6736
.362	0	8.3874	8.3305	8.3234
	1	8.4110	8.3373	8.3263
	2	9.8203	9.7222	9.7019
.363	0	8.4131	8.3563	8.3482
	1	8.4387	8.3647	8.3484
	2	9.8476	9.7493	9.7286
.364	0	8.4389	8.3822	8.3746
	1	8.4664	8.3929	8.3815
	2	9.8749	9.7768	9.7545
.365	0	8.4648	8.4082	8.4007
	1	8.4943	8.4206	8.4065
	2	9.9025	9.8045	9.7850

contd...

Ratio	Nodal diameters	Finite elements results for		
		2 elements	4 elements	6 elements
.400	0	9.4619	9.4086	9.4017
	1	9.5581	9.4895	9.4800
	2	10.9616	10.8650	10.8473
.450	0	11.2526	11.2040	11.1969
	1	11.4387	11.3776	11.3790
	2	12.8607	12.7678	12.7492

From Table 6.26 the change in response of the disc with change of the Ratio can be noted very clearly. When the Ratio is less than or equal to 0.360, the frequencies for 1-nodal diameter and zero-nodal circle are less than those for zero-nodal diameter. As the Ratio attains a value more than 0.360, the values start increasing monotonically. This indicates that for discs having Ratio $\leq$ 0.360, the critical frequency is for zero-nodal circle, 1-nodal diameter mode instead of the so-called fundamental mode of zero-nodal circle and zero-nodal diameter. This Ratio of 0.360 is termed as the critical Ratio.

The effects of rotational speed on the natural frequencies of a centrally clamped disc are studied, the results are presented in Table 6.27. The results for zero rotational speed are the 6-element results from Table 6.23.

Table 6.27

Natural frequencies, ω_n, of a centrally clamped rotating disc, Ratio = 0.276

Rotational speed, $\bar{\Omega}^2$	Nodal diameters	Nodal circles	Finite element results for			
			2 elements	4 elements	6 elements	Zero speed
5.0	0	0	10.3874	10.2554	10.2280	6.5085
		1	51.0739	47.3103	46.9055	41.6409
		2	205.2642	133.1301	127.8337	121.1163
		3	873.9979	296.8883	254.4215	240.9288
	1	0	9.4947	9.3156	9.2739	6.3166
		1	52.6242	48.9223	48.5146	43.8055
		2	206.8256	135.2674	130.1232	123.6200
		3	875.3087	298.9886	256.9289	243.7922
	2	0	8.1182	7.8444	7.7744	7.7922
		1	57.6444	54.2812	53.8992	50.6592
		2	211.5950	141.9196	137.2789	131.7073
		3	879.2324	305.3953	264.5980	252.5486

Rotational speed, $\frac{\Omega}{\omega}^2$	Nodal diameters	Nodal circles	Finite element results for			
			2 elements	4 elements	6 elements	Zero speed
	3	0	10.8927	10.7290	10.6790	13.5847
		1	66.9865	64.4778	64.1950	62.8122
		2	219.8090	153.6978	149.9825	145.7106
		3	885.7871	316.4111	277.8351	267.5644
10.0	0	0	13.0964	12.9017	12.8558	Same as
		1	55.4287	51.9525	51.5327	above
		2	208.4822	138.1023	133.0512	
		3	875.4669	301.4565	259.8600	
	1	0	11.7328	11.4669	11.4026	Same as
		1	56.6207	53.1338	52.7033	above
		2	209.9613	140.0314	135.0959	
		3	876.7676	303.4668	262.2397	

contd ...

Rotational speed, $\bar{\Omega}^2$	Nodal diameters	Nodal circles	Finite element results for			
			2 elements	4 elements	6 elements	Zero Speed
	2	0	8.1216	7.5966	7.4613	Same as
		1	60.6340	57.2900	56.8633	above
		2	214.4905	146.0868	141.5567	
		3	880.6650	309.6084	269.5241	
	3	0	6.6601	6.0603	5.8871	Same as
		1	68.5384	65.8299	65.4864	above
		2	222.3238	156.9581	153.2243	
		3	887.1873	320.1978	282.1528	

A study of the Table 6.27 reveals some interesting and important trends. The same trends are confirmed for various values of the Ratio and rotational speeds in Figures 6.10 to 6.12. As expected the so-called fundamental frequency increases monotonically with increase in rotational speed. The frequency of all other modes, except the zero-nodal circle modes, also increases monotonically, though the increase is marginal for higher modes. The critical trend is for the frequencies of zero-nodal circles. As the rotational speed increases the decrease of frequency continues even for nodal diameters more than one. The number of nodal diameters for which the frequency decreases, increases with increase in rotational speed. At higher speeds the lowest frequency can be less than the lowest frequency of the non-rotating disc, thus, rendering a critical frequency value to a higher mode, instead of the so-called fundamental mode. Hence, from the design safety point-of-view, the lowest frequency must be evaluated. The reason for this decrease is the dominating effect of the tangential stress, $\sigma_{\theta\theta}$, in the 2-D state of stress induced in the disc by the rotation. The contribution to stiffness by $\sigma_{\theta\theta}$ is negative, equation (5.10).

A tapered disc has been idealized by constant thickness elements, as shown in Figure 6.13. The results for taper ratio, T = 0.90 and 0.70 are given in Table 6.28, for a

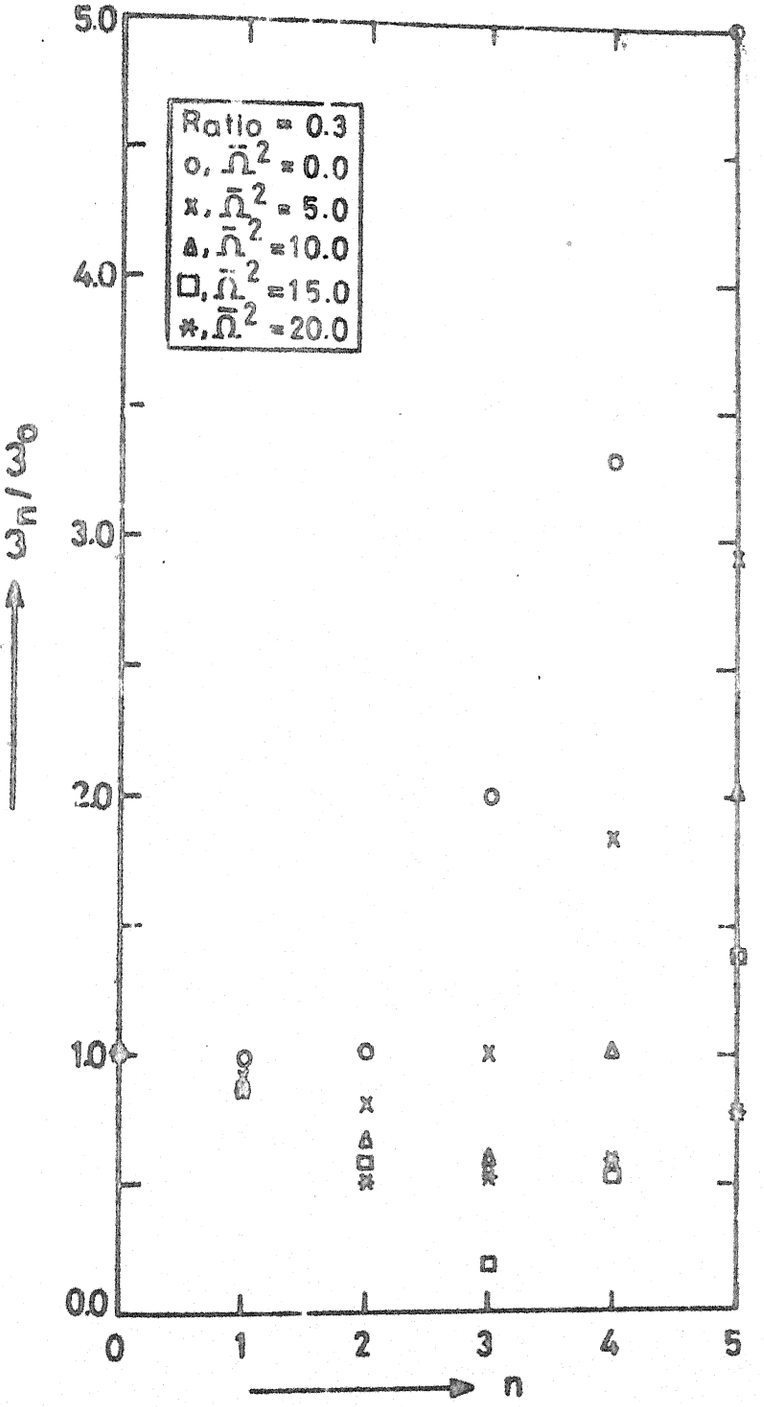

Figure 6.10. Variation of frequency with nodal diameters, n, for various rotational speeds, $\bar{\Omega}$.

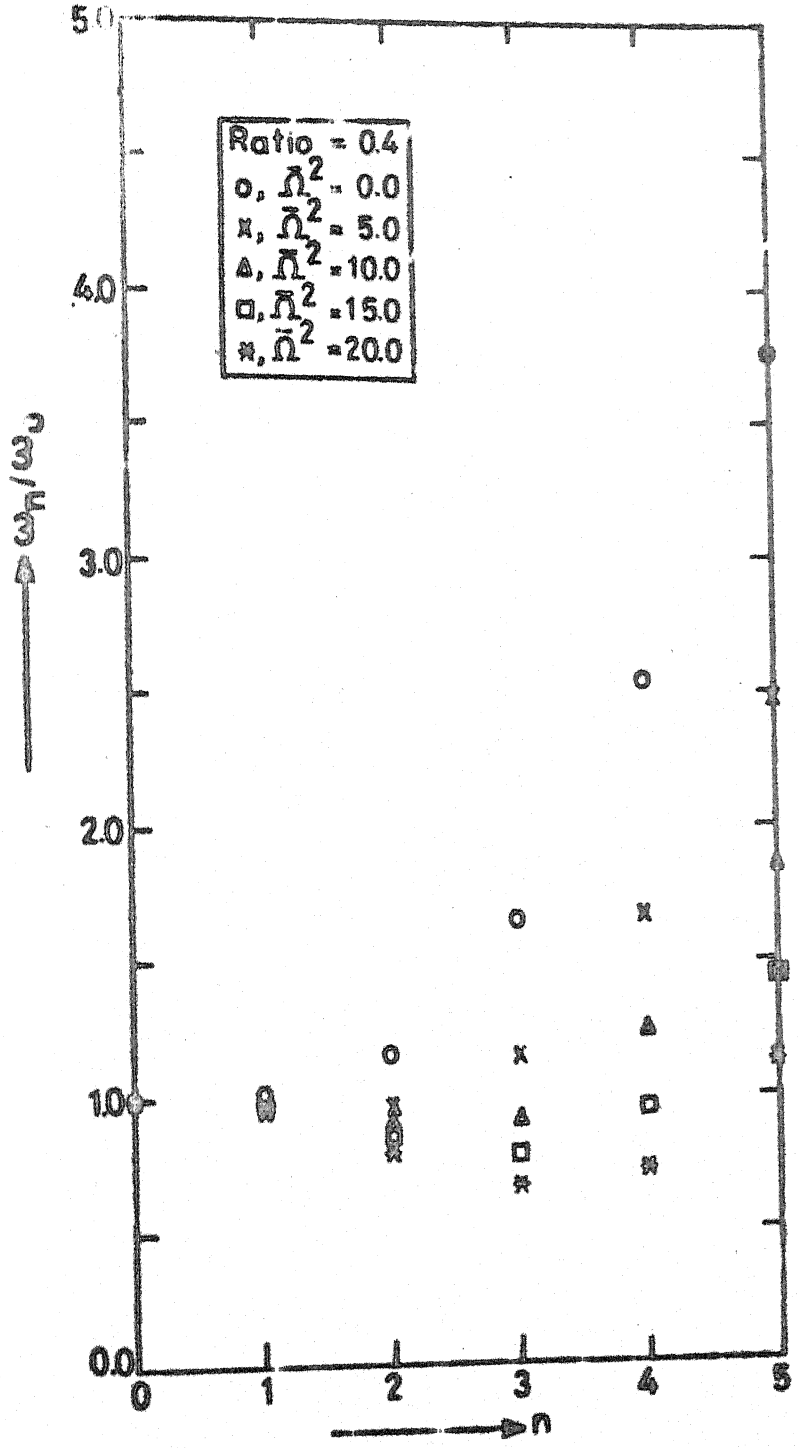

Figure 6.11. Variation of frequency with nodal diameters, n, for various rotational speeds, $\bar{\Omega}$.

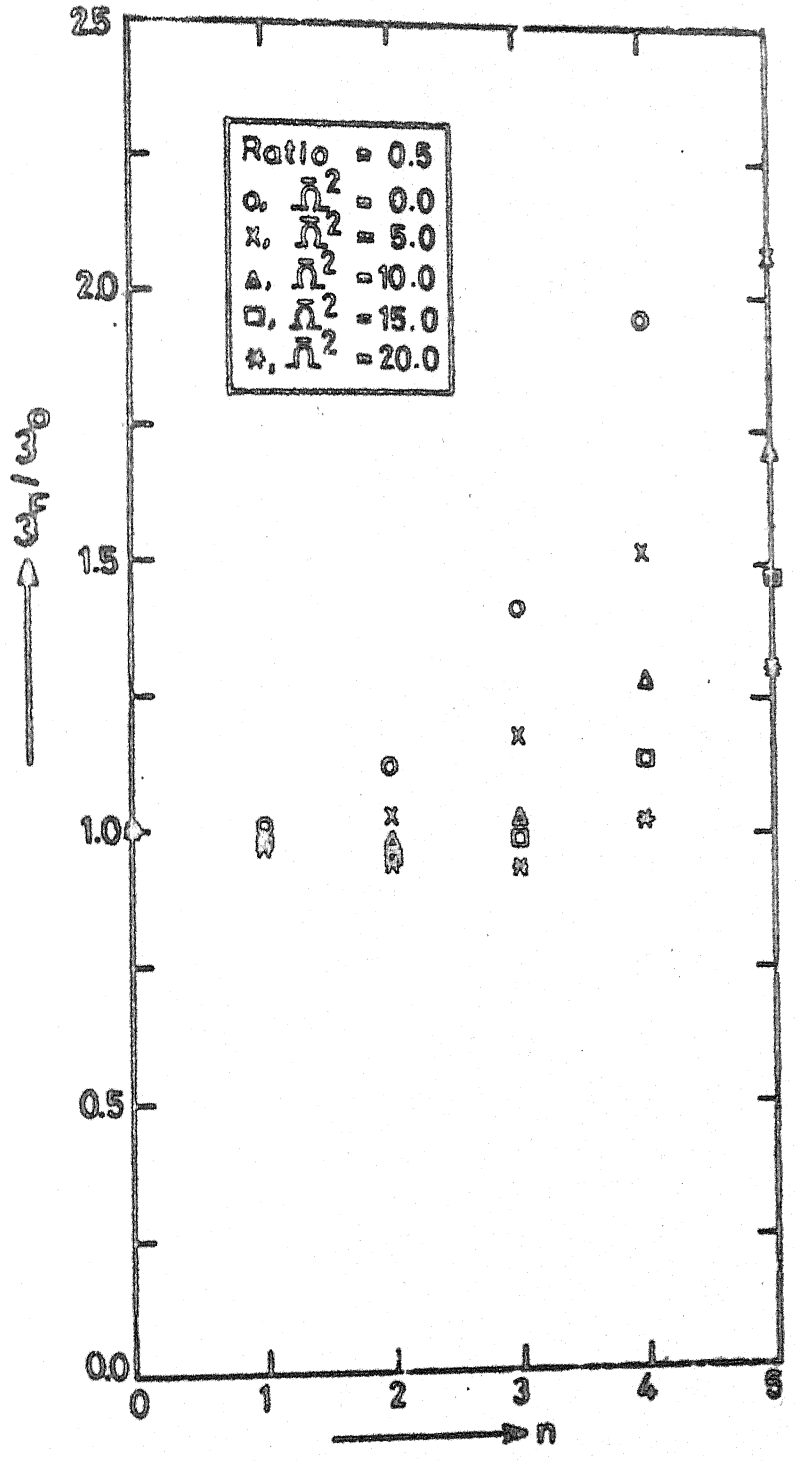

Figure 6.12. Variation of frequency with nodal diameters, n, for various rotational speeds, Ω.

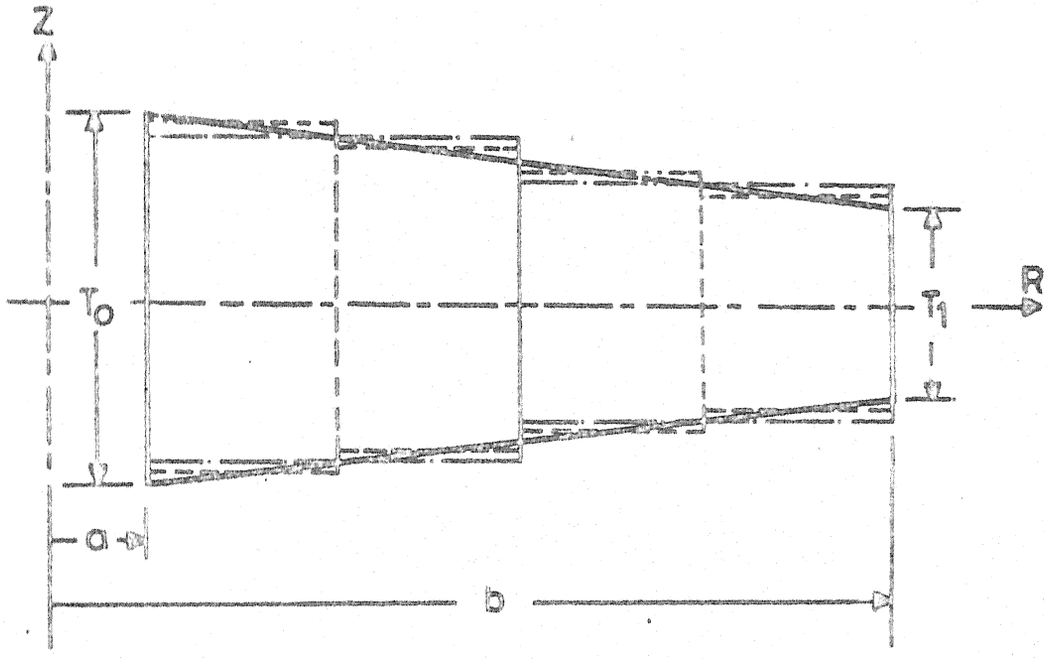

Figure 6.13. Constant thickness element idealization of a tapered disc, 2-element — —, 4-element — — —.

Table 6.28

Natural frequencies, $\overline{\omega}_n$, of a centrally clamped tapered disc, Ratio = 0.276

Taper, T_p	Nodal diameters	Nodal circles	Finite element results for			
			2 elements	4 elements	6 elements	uniform disc
0.90	0	0	6.4256	6.4490	6.4557	6.5085
		1	40.3026	40.1630	40.1621	41.6409
		2	151.2875	115.9497	115.4617	121.1163
		3	324.2126	255.9254	229.5504	240.9288
	1	0	6.3421	6.4400	6.4774	6.3166
		1	42.4330	42.1809	42.1839	43.8055
		2	153.4561	118.4328	117.8940	123.6200
		3	326.3139	258.6527	232.3156	243.7922
	2	0	7.8343	8.0800	8.1861	7.7922
		1	49.1408	48.5845	48.5984	50.6592
		2	160.2713	126.1524	125.4412	131.7073
		3	332.7780	267.0084	240.7809	252.5486

contd...

Taper, T_p	Nodal diameter	Nodal circles	Finite element results for			
			2 elements	4 elements	6 elements	uniform disc
	3	0	13.1496	13.4390	13.5839	13.5847
		1	60.9737	59.9640	59.9923	62.8122
		2	172.5059	139.7378	138.6832	145.7106
		3	344.0918	281.4513	255.3711	267.5644
0.70	0	0	6.1414	6.2924	6.3256	
		1	36.2427	36.6945	36.9217	
		2	138.7009	103.1160	103.1568	
		3	289.3547	233.0701	204.2137	
	1	0	6.2015	6.5551	6.6661	Same as
		1	38.2835	38.4287	38.6599	above
		2	140.5302	105.3988	105.2984	
		3	291.3309	235.4929	206.7444	

contd ...

Taper, T_p	Nodal diameter	Nodal circles	Finite element results for			
			2 elements	4 elements	6 elements	uniform disc
	2	0	7.6136	8.3660	8.6486	
		1	44.6155	43.9520	44.1917	
		2	146.3315	112.4949	111.9559	
		3	297.4452	242.9152	214.4735	
	3	0	12.0070	12.9071	13.3187	
		1	555.5505	53.7917	54.0316	
		2	156.8910	124.9793	123.6416	
		3	308.2632	255.7720	227.8558	

centrally clamped disc. The results for uniform disc are six element results from Table 6.23.

For a tapered disc the convergence trends are not as expected, Table 6.28. The reason for this unexpected trend is that, by changing number of elements we are changing the physical system being analysed, as is clear from Figure 6.13. Under such conditions the convergence may or may not have a definite trend. Hence, for all such cases the element matrices must be evaluated by considering the thickness variations to have more reliable results.

6.2.6 Thick Discs

The numerical results are obtained for a centrally clamped, outer-edge free, rotating and non-rotating disc including Timoshenko effects, to illustrate the applicability of the same finite element model for thick discs also. The boundary conditions at free-end are satisfied in the same fashion as in case of a thin disc, the boundary conditions are given in Appendix C.

The natural frequencies, $\bar{\omega}_n$, of a centrally clamped disc with Ratio = 0.276, and re = 0.02, se = 0.02 are given in Table 6.29. The classical results are the six element results from Table 6.23.

Table 6.29

Natural frequencies, $\bar{\omega}_n$, of a centrally clamped disc, Ratio = 0.276, re = 0.02 and se = 0.02

Nodal diameters	Nodal circles	Classical results, 6 elements	Finite element results for		
			2 elements	4 elements	6 elements
0	0	6.5085	6.5733	6.5072	6.4968
	1	41.6409	44.9508	41.0976	40.7332
	2	121.1163	183.0038	120.1680	115.4480
	3	240.9288	619.3625	258.9909	223.8489
1	0	6.3166	6.4108	6.3224	6.3013
	1	43.8055	46.8494	43.1641	42.8077
	2	123.6200	184.3757	122.2675	117.7245
	3	243.7922	620.1070	260.7212	226.0236
2	0	7.7922	7.8847	7.7922	7.7684
	1	50.6592	52.7491	49.6522	49.3448
	2	131.7073	188.5624	128.7435	124.7605
	3	252.5486	622.3426	265.9945	232.6268
3	0	13.5847	13.5314	13.4961	13.4788
	1	62.8122	63.0767	61.0304	60.8269
	2	145.7106	195.7560	140.0171	136.9882
	3	267.5644	626.0807	275.0220	243.9486

As expected the frequencies decrease with the Timoshenko effects, the effect of re and se is more on higher modes. A good rate of convergence is observed even with Timoshenko effects included.

The natural frequencies, ω_n, of a centrally clamped disc with Ratio = 0.276 and re = 0.08, se = 0.08 are given in Table 6.30. The classical results are the six element results from Table 6.23.

Table 6.30

Natural frequencies, $\bar{\omega}_n$, of a centrally clamped disc, Ratio = 0.276, re = 0.08 and se = 0.08

Nodal diameters	Nodal circles	Classical results, 6 elements	Finite elements results for		
			2 elements	4 elements	6 elements
0	0	6.5085	6.3226	6.2664	6.2577
	1	41.6409	33.2700	31.4267	31.2565
	2	121.1163	105.5068	76.8795	75.4227
	3	240.9288	159.7074	142.6501	127.2207
1	0	6.3166	6.1121	6.0348	6.0159
	1	43.8055	34.4758	32.7532	32.5878
	2	123.6200	105.7663	77.7201	76.3193
	3	243.7922	161.4257	142.9210	127.8302
2	0	7.7922	7.3259	7.2458	7.2248
	1	50.6592	38.1984	36.8723	36.7353
	2	131.7073	106.7731	80.4683	79.2612
	3	252.5486	166.2195	144.0323	129.9035

contd...

Nodal diameters	Nodal circles	Classical results, 6 elements	Finite elements results for		
			2 elements	4 elements	6 elements
3	0	13.5847	12.0849	12.0564	12.0499
	1	62.8122	44.5675	43.8599	43.7779
	2	145.7106	108.9957	85.5436	84.6819
	3	267.5644	173.3067	146.4855	133.8605

Consistent with the trend the frequencies decrease further with increase in values of re and se. Table 6.30 shows a good rate of convergence even for higher values of re and se. This proves the applicability of the present formulation for the analysis of discs including Timoshenko effects.

To study the influence of rotational speed, $\bar{\Omega}$, on the natural frequencies, a centrally clamped disc with Ratio = 0.276, re = 0.02 and se = 0.02 is analysed for rotational speed, $\bar{\Omega}^2$ = 5.0 and 10.0. The results are presented in Table 6.31, the zero speed results are six element results from Table 6.29.

The trend of the results in Table 6.31 is exactly same as in Table 6.27 for thin discs. The only difference is that the values in Table 6.31 are lower than the corresponding value in Table 6.27, which is as per the expectations. Hence, for thick disc also the rotational speed has exactly the same effect as on a thin disc, and

Table 6.31

Natural frequencies, $\bar{\omega}_n$, of a centrally clamped rotating disc, Ratio = 0.276, re = 0.02 and se = 0.02

Rotational speed, $\bar{\Omega}^2$	Nodal diameters	Nodal circles	Finite element results for 2 elements	4 elements	6 elements	Zero speed
5.0	0	0	10.3607	10.2303	10.2032	6.4968
		1	49.5560	46.1021	45.7292	40.7332
		2	185.9770	125.0171	120.5761	115.4480
		3	620.5471	263.1034	228.8881	223.8489
	1	0	9.4644	9.2870	9.2456	6.3013
		1	51.0212	47.6286	47.2532	42.8077
		2	187.2666	126.8943	122.5885	117.7245
		3	621.2715	264.7450	230.9235	226.0236
	2	0	8.0768	7.8052	7.7356	7.7684
		1	55.7588	52.6977	52.3469	49.3448
		2	191.2148	132.7407	128.8828	124.7605
		3	623.4758	269.7568	237.1433	232.6288
	3	0	10.8020	10.6400	10.5905	13.4788
		1	64.5425	62.2994	62.0424	60.8269
		2	198.0335	143.0786	140.0364	136.9882
		3	627.1676	278.3696	247.8678	243.9486

contd...

Rotational speed, $\frac{\rho}{\Omega^2}$	Nodal diameters	Nodal circles	Finite element results for			
			2 elements	4 elements	6 elements	Zero speed
10.0	0	0	13.0641	12.8717	12.8263	
		1	53.7715	50.6083	50.2235	
		2	188.9033	129.6675	125.4605	
		3	621.7218	267.1426	233.8097	
	1	0	11.6969	11.4333	11.3695	Same as
		1	54.8849	51.7122	51.3170	above
		2	190.1133	131.3409	127.2344	
		3	622.4418	268.6986	235.7195	
	2	0	8.0816	7.5599	7.4255	
		1	58.6385	55.6045	55.2125	
		2	193.8299	136.6070	132.8537	
		3	624.6108	273.4569	241.5722	
	3	0	6.6061	6.0114	5.8397	
		1	66.0247	63.5953	63.2814	
		2	200.2841	146.0698	143.0113	
		3	628.2533	281.6684	251.7189	

same conclusions can be drawn. A good rate of convergence can be observed from Table 6.31.

6.3 SUMMARY

The finite element formulations for the beams, the rings, the sectors, and the discs including Timoshenko effectshave been proposed in a systematic and logical fashion. The models proposed are the simplest requiring minimum number of nodal parameters per element. The formulations proposed are capable of analysing the effects of rotational speed or prestressing. The efficiency and accuracy of the formulations is illustrated.

The effects of ratio of inner diameter to outer diameter and rotational speed on vibration modes of a disc are studied very critically. Two important conclusions have been drawn in case of the discs.

CHAPTER VII

CONCLUSIONS

The following conclusions are drawn from the present study :

1. Systematically and logically developed finite element formulations for the structural components, beams, rings, sectors and discs, including Timoshenko effects, are simple and efficient compared to all the earlier proposed formulations. The efficiency of the formulations is illustrated by many numerical examples. The accuracy is proved by comparison of the results with exact/experimental/approximate results wherever possible.

2. The inclusion of the Timoshenko effects, rotational speed, pre-stress, etc., in the analysis of the structural components does not necessitate the change of interpolating function i.e., the interpolation polynomial remains same irrespective of the fact that whether these effects are included in the analysis or not.

3. In case of an 180°-sector on two supports, if a third support is added at varying angles from one support, the fundamental frequency increases monotonically with

increase in the angle till the symmetric position is attained. A similar trend can be expected for other configurations.

4. In a non-rotating centrally clamped disc with inner to outer diameter ratio less than or equal to 0.360, the minimum frequency occurs for zero-nodal circle, one-nodal diameter mode instead of the zero-nodal circle, zero-nodal diameter mode. As the inner to outer diameter ratio becomes more than 0.360 the minimum frequency is for the zero-nodal circle, zero-nodal diameter mode.

5. Depending upon the rotational speed, the lowest frequency in a centrally clamped disc may occur for any mode with zero-nodal circle and any nodal diameter, irrespective of the value of the inner to outer diameter ratio.

REFERENCES

1. J.S. Archer 1963 Proceedings of the American Society of Civil Engineers, 89, ST4, 161-178, Consistent mass matrix for distributed mass systems.

2. S.P. Timoshenko, D.H. Young, and W. Weaver, Jr. 1974, Vibration Problems in Engineering. John Wiley, Fourth Edition.

3. T.C. Huang 1961 Journal of Applied Mechanics 28, 579-584, The effect of rotatory inertia and of shear deformation on the frequency and normal mode equations of uniform beams with simple end conditions.

4. D.L. Thomas, J.M. Wilson and R.R. Wilson 1973 Journal of Sound and Vibration 31, 315-330. Timoshenko beam finite elements.

5. R.B. McCalley 1963 General Electric Knolls Atomic Power Laboratory, Schenectady, New York, Report DIG/SA 63-68. Mass lumping for beams.

6. R.B. McCalley 1963 General Electric Knolls Atomic Power Laboratory, Schenectady, New York, Report DIG/SA 69-73. Rotary inertia correction for mass matrices.

7. J.S. Archer 1965 American Institute of Aeronautics and Astronautics Journal 3, 1910-1918. Consistent mass formulations for structural analysis using finite-element techniques.

8. R. Ali, J.L. Hedges and B. Mills 1971 Proceedings of the Institution of Mechanical Engineers, Automobile Division 185, 665-674. Static analysis of an automobile chassis frame.

9. R. Ali, J.L. Hedges and B. Mills 1971 Proceedings of the Institution of Mechanical Engineers, Automobile Division 185, 683-690. Dynamic analysis of an automobile chassis frame.

10. R. Davis, R.D. Henshell and G.B. Warburton 1972 Journal of Sound and Vibration 22, 475-487. A Timoshenko beam element.

11. J.S. Przemieniecki 1968 Theory of Matrix Structural Analysis. McGraw-Hill.

12. R.T. Severn 1970 Journal of Strain Analysis 5, 239-241. Inclusion of shear deformation in the stiffness matrix for a beam element.

13. R.E. Nickell and G.A. Secor 1972 International Journal for Numerical Methods in Engineering 5, 243-253. Convergence of consistently derived Timoshenko beam finite elements.

14. K.K. Kapur 1966 Journal of Acoustical Society of America 40, 1058-1063. Vibrations of a Timoshenko beam, using finite element approach.

15. W. Carnegie, J. Thomas and E. Documaki 1969 The Aeronautical Quarterly 20, 321-332. An improved method of matrix displacement analysis in vibration problems.

16. R. Hoppe 1871 Crelle Journal of Mathematics 73, 158-170. The bending vibrations of a circular ring.

17. Lord Rayleigh 1877 The Theory of Sound (two volumes). Dover Publications, second Edition.

18. J.W. Lincoln and E. Volterra 1967 Experimental Mechanics 24, 211-217. Experimental and theoretical determination of frequencies of elastic toroids.

19. R.E. Ball 1967 Journal of Engineering Mechanics Division, American Society of Civil Engineers 93, 1-10. Dynamic analysis of rings by finite-differences.

20. A.E.H. Love 1934 Treatise on the Mathematical Theory of Elasticity. Cambridge University Press.

21. L.L. Philipson 1956 American Society of Mechanical Engineers, Journal of Applied Mechanics 23, 364-366. On the role of extension in the flexural vibrations of ring.

22. S.S. Rao and V. Sundrarajan 1969 American Society of Mechanical Engineers, Journal of Applied Mechanics 91, 620-625. In-plane flexural vibrations of circular rings.

23. V.R. Murthy and N.C. Nigam 1975 Journal of Sound and Vibration 39, 237-245. Dynamic characteristics of stiffened rings by transfer matrix technique.

24. A.K. Mallik and D.J. Mead 1977 Journal of Sound and Vibration 54, 13-27. Free vibrations of thin circular rings on periodic radial supports.

25. K.B. Sahay and V. Sundrarajan 1972 Journal of Sound and Vibration 22, 467-473. Vibration of a stiffened ring considered as a cyclic structure.

26. T.J. McDaniel 1971 Journal of Aircrafts 8, 143-149. Dynamics of circular periodic structures.

27. G. Cantin and R. Clough 1968 American Institute of Aeronautics and Astronautics Journal 6, 1057-1062. A curved cyclindrical shell, finite element.

28. R.H. Gallagher 1966 Ph.D. Thesis, State University of New York. The development and evaluation of matrix methods for thin shell structural analysis.

29. F.K. Bogner, R.L. Fox and L.A. Schmit 1967 American Institute of Aeronautics and Astronautics Journal 5, 745-750. A cylindrical shell discrete element.

30. A.B. Sabir and D.G. Ashwell 1969 International Journal of Mechanical Sciences 11, 269-279. A stiffness matrix for shallow shell finite elements.

31. A.B. Sabir 1970 International Journal of Mechanical Sciences 12, 287-292. An extension of the shallow to the non-shallow stiffness matrix for cylindrical shell finite elements.

32. D.G. Ashwell and A.B. Sabir 1971 International Journal of Mechanical Sciences 13, 133-139. Limitations of certain curved finite elements when applied to arches.

33. D.G. Ashwell, A.B. Sabir and T.M. Roberts 1971 International Journal of Mechanical Sciences 13, 507-517. Further studies in the application of curved finite elements to circular arches.

34. A.B. Sabir and D.G. Ashwell 1971 Journal of Sound and Vibration 18, 555-563. A comparison of curved beam finite elements when used in vibration problems.

35. W. Kuhl 1942 Akhustiche Zietschrift 7, 10-26. Measurements to the theories of resonant vibrations of circular rings of arbitrary wall thickness.

36. J. Kirkhope 1976 Journal of the Acoustical Society of America 59, 86-89. Simple frequency expression for in-plane vibration of thick circular rings.

37. K. Federhofer 1935 S.B. Akad. Wiss. Wien, Series IIa, 144, 561-576. Two dimension theory of bending vibrations of a circular ring of rectangular cross-section.

38. B.S. Seidel and E.A. Erdelyi 1964 Journal of Engineering for Industry, Trans., ASME 86, 240-244. On the vibrations of a thick ring in its own plane.

39. G. Kirchhoff 1850 Journal fur die reine und angewandte Mathematik 40, 51-88. Uber das gleichgewicht und die bewegungeiner elastischen Scheibe.

40. H. Lamb and R.V. Southwell 1921 Proceedings of the Royal Society of London 99, 272-280. The vibrations of a spinning disk.

41. R.V. Southwell 1922 Proceedings of the Royal Society of London 101, 133-153. On the free transverse vibrations of a uniform circular disc clamped at its centre; and on the effects of rotation.

42. C.D. Mote 1965 Journal of Engineering for Industry, Trans., ASME 87, 258-264. Free vibration of initially stressed circular disks.

43. J. Kirkhope and G.J. Wilson 1972 International Journal for Numerical Methods in Engineering 4, 181-193. Vibration of circular and annular plates using finite elements.

44. J. Kirkhope and G.J. Wilson 1976 Journal of Sound and Vibration 44, 461-474. Vibration and stress analysis of thin rotating discs using annular finite elements.

45. W. Kennedy and D. Gorman 1977 Journal of Sound and Vibration 53, 81-101. Vibration analysis of variable thickness discs subjected to centrifugal and thermal stresses.

46. G.C. Pardoen 1973 Computers and Structures 3, 355-375. Static, vibrations and buckling analysis of axisymmetric circular plates using finite elements.

47. G.C. Pardoen 1975 Computers and Structures 5, 197-202. Asymmetric bending of circular plates using the finite element method.

48. G. Nerli 1975 Computers and Structures 5, 233-239. The study of umbrella oscillations of turbine discs of arbitrary profile by the finite element method.

49. C.A. Mota Soares, M. Petyt and A.M. Salama 1976 Structural Dynamic Aspects of Bladed Disk Assemblies (edited by A.V. Srinivasan). ASME Publication. Finite element analysis of bladed discs.

50. G.J. Wilson and J. Kirkhope 1976 Journal of Engineering for Industry 98, 1008-1013. Vibration analysis of axial flow turbine discs using finite elements.

51. E. Hinton 1976 Journal of Sound and Vibration 46, 465-472. The dynamic transient analysis of axisymmetric circular plates by the finite element method.

52. K. Kanaka Raju and G. Venkateswara Rao 1976 Journal of Sound and Vibration 47, 179-184. Axisymmetric vibrations of circular plates including the effect of geometric non-linearity, shear deformation and rotary inertia.

53. C.A. Mota Soares and M. Petyt 1978 Journal of Sound and Vibration 61, 547-560. Finite element dynamic analysis of practical discs.

54. K.H. Huebner 1975 The Finite Element Method for Engineers. John Wiley and Sons.

55. L.R. Meirovitch 1967 Analytical Methods in Vibrations. Macmillan.

56. C.S. Desai and J.F. Abel 1972 Introduction to the Finite Element Method. Litton Educational Publishing, Inc.

57. T.E. Lang 1962 Jet Propulsion Laboratory Technical Report No. 32-261. Vibration of thin circular rings.

58. J. Prescott 1924 Applied Elasticity. Dover Publications, first edition.

59. C.L. Dym and I.H. Shames. 1973 Solid Mechanics: A Variational Approach. McGraw-Hill, Inc.

60. E. Volterra and E.C. Zachmanoglou 1965 Dynamics of Vibrations. Charles E. Merrill Books, Inc.

61. K.J. Bathe and E.L. Wilson 1976 Numerical Methods in Finite Element Analysis. Prentice Hall, Inc.

62. W.C. Hurty and M.F. Rubinstein 1964 Dynamics of Structures. Prentice Hall, Inc.

63. A. Ralston and P. Rabinowitz 1978 A First Course in Numerical Analysis. McGraw-Hill Kogakusha, Ltd., second edition.

64. R.H. Gallagher 1975 Finite Element Analysis. Prentice Hall, Inc.

65. E. Hinton and D.R.J. Owen 1979 An Introduction to Finite Element Computations. Pineridge Press Ltd.

66. A.W. Leissa 1969 NASA SP-160. Vibration of plate.

APPENDIX A

BOUNDARY CONDITIONS AND ELEMENT MATRICES FOR BEAMS

A.1 BOUNDARY CONDITIONS

The boundary conditions for the Timoshenko beams are [3,55] :

i) Hinged end

$$w = o \tag{A.1}$$

$$\psi' = o \text{ (at extreme boundaries only)} \tag{A.2}$$

ii) Clamped end

$$w = o \tag{A.3}$$

$$\psi = o \tag{A.4}$$

iii) Free end

$$\psi' = o \tag{A.5}$$

$$\frac{1}{L} w' - \psi = o \tag{A.6}$$

where L is the length of the beam.

A.2 ELEMENT MATRICES

The various constitutive matrices for the elemental stiffness and mass matrices are given below.

A.2.1 Approach A

$$[A_1] = \int_0^h \{N''\}[N'']\,dx = \frac{1}{h^3}\begin{bmatrix} 12 & & \text{symmetric} & \\ 6h & 4h^2 & & \\ -12 & -6h & 12 & \\ 6h & 2h^2 & -6h & 4h^2 \end{bmatrix}$$

$$[A_2] = \int_0^h \{N'\}[N']\,dx = \frac{1}{h}\begin{bmatrix} 6/5 & & & \\ h/10 & 2h^2/15 & \text{symmetric} & \\ -6/5 & -h/10 & 6/5 & \\ h/10 & -h^2/30 & -h/10 & 2h^2/15 \end{bmatrix}$$

$$[A_3] = \int_0^h \{N\}[N]\,dx = \frac{h}{420}\begin{bmatrix} 156 & & & \\ 22h & 4h^2 & \text{symmetric} & \\ 54 & 13h & 156 & \\ -13h & -3h^2 & -22h & 4h^2 \end{bmatrix}$$

$$\{Y_1\} = \begin{Bmatrix} \left(EI\frac{\partial^3 w(e)}{\partial x^3} - \left(\rho I + EI\frac{\rho}{\alpha G}\right)\frac{\partial^3 w(e)}{\partial x \partial t^2}\right)\Big|_j \\ 0 \\ -\left(EI\frac{\partial^3 w(e)}{\partial x^3} - \left(\rho I + EI\frac{\rho}{\alpha G}\right)\frac{\partial^3 w(e)}{\partial x \partial t^2}\right)\Big|_k \\ 0 \end{Bmatrix}$$

$$\{Y_2\} = \begin{Bmatrix} 0 \\ -EI\left.\frac{\partial^2 w(e)}{\partial x^2}\right|_j \\ 0 \\ EI\left.\frac{\partial^2 w(e)}{\partial x^2}\right|_k \end{Bmatrix}$$

where subscripts j and k means the evaluation at jth and kth nodes respectively.

A.2.2 Approach B

The linear variation of the cross-sectional properties can be expressed as

$$I^{(e)} = \lfloor \xi_1 \quad \xi_2 \rfloor \begin{Bmatrix} I_j \\ I_k \end{Bmatrix}$$

and

$$A^{(e)} = \lfloor \xi_1 \quad \xi_2 \rfloor \begin{Bmatrix} A_j \\ A_k \end{Bmatrix}$$

The constitutive matrices for this variation are :

$$[K_1] = \int_0^h \alpha AG \{N'\} \lfloor N' \rfloor dx = \frac{\alpha G(A_j+A_k)}{2h} \begin{bmatrix} 1 & -1 \\ -1 & 1 \end{bmatrix}$$

$$[K_2] = -\int_0^h \alpha AG \{N'\} \lfloor N \rfloor dx = \frac{\alpha G}{6} \begin{bmatrix} 2A_j+A_k & A_j+2A_k \\ -(2A_j+A_k) & -(A_j+2A_k) \end{bmatrix}$$

$$[K_3] = \int_0^h (EI \{N'\} \lfloor N' \rfloor + \alpha AG \{N\} \lfloor N \rfloor) dx =$$

$$\frac{E(I_j+I_k)}{2h} \begin{bmatrix} 1 & -1 \\ -1 & 1 \end{bmatrix} + \frac{\alpha Gh}{12} \begin{bmatrix} 3A_j+A_k & A_j+A_k \\ A_j+A_k & A_j+3A_k \end{bmatrix}$$

$$[M_1] = \int_0^h \rho A \{N\} \lfloor N \rfloor dx = \frac{\rho h}{12} \begin{bmatrix} 3A_j+A_k & A_j+A_k \\ A_j+A_k & A_j+3A_k \end{bmatrix}$$

$$[M_2] = \int_0^h \rho I \{N\}[N]\, dx = \frac{\rho h}{12} \begin{bmatrix} 3I_j+I_k & I_j+I_k \\ I_j+I_k & I_j+3I_k \end{bmatrix}$$

$$\{B_2\}^{(ne)} = \begin{Bmatrix} -(\alpha AG(\frac{\partial w^{(e)}}{\partial x} - \psi^{(e)}))\Big|_j \\ (\alpha AG(\frac{\partial w^{(e)}}{\partial x} - \psi^{(e)}))\Big|_k \\ -(EI \frac{\partial \psi^{(e)}}{\partial x})\Big|_j \\ (EI \frac{\partial \psi^{(e)}}{\partial x})\Big|_k \end{Bmatrix}$$

such that the elemental vector of nodal parameters is

$$\{w\}^{(e)} = \begin{Bmatrix} w_j \\ w_k \\ \psi_j \\ \psi_k \end{Bmatrix}$$

$[K_3]$ matrix using 1-point Gauss-Legendre integration formula is

$$[K_3] = \frac{E(I_j+I_k)}{2h} \begin{bmatrix} 1 & -1 \\ -1 & 1 \end{bmatrix} + \frac{\alpha G(A_j+A_k)h}{8} \begin{bmatrix} 1 & 1 \\ 1 & 1 \end{bmatrix}$$

APPENDIX B

BOUNDARY CONDITIONS AND ELEMENT MATRICES FOR RINGS

B.1 BOUNDARY CONDITIONS

The boundary conditions for rings are [57] :

i) Pinned end

$$w = 0 \tag{B.1}$$

$$\frac{\partial w}{\partial \theta} = 0 \tag{B.2}$$

$$\frac{\partial^3 w}{\partial \theta^3} = 0 \tag{B.3}$$

ii) Clamped end

$$w = 0 \tag{B.4}$$

$$\frac{\partial w}{\partial \theta} = 0 \tag{B.5}$$

$$\frac{\partial^2 w}{\partial \theta^2} = 0 \tag{B.6}$$

iii) Free end

$$\frac{\partial w}{\partial \theta} + \frac{\partial^3 w}{\partial \theta^3} = 0 \tag{B.7}$$

$$\frac{\partial^2 w}{\partial \theta^2} + \frac{\partial^4 w}{\partial \theta^4} = 0 \qquad \text{(B.8)}$$

$$\frac{\partial w}{\partial \theta} - C\ \frac{\partial \ddot{w}}{\partial \theta} - \frac{\partial^5 w}{\partial \theta^5} = 0 \qquad \text{(B.9)}$$

B.2 ELEMENT MATRICES

The various constitutive matrices for the elemental stiffness and mass matrices are :

$$[A_1] = \int_0^\beta \{N'''\}\lfloor N'''\rfloor d\theta = \frac{3}{\beta}\begin{bmatrix} 240 & & & & & \text{symmetric} \\ 120\beta & 64\beta^2 & & & & \\ 20\beta^2 & 12\beta^3 & 3\beta^4 & & & \\ -240 & -120\beta & -20\beta^2 & 240 & & \\ 120\beta & 56\beta^2 & 8\beta^3 & -120\beta & 64\beta^2 & \\ -20\beta^2 & -8\beta^3 & -\beta^4 & 20\beta^2 & -12\beta^3 & 3\beta^4 \end{bmatrix}$$

$$[A_2] = \int_0^\beta \{N''\}\lfloor N''\rfloor d\theta = \frac{1}{35\beta^3}\begin{bmatrix} 600 & & & & & \text{symmetric} \\ 300\beta & 192\beta^2 & & & & \\ 15\beta^2 & 11\beta^3 & 3\beta^4 & & & \\ -600 & -300\beta & -15\beta^2 & 600 & & \\ 300\beta & 108\beta^2 & 4\beta^3 & -300\beta & 192\beta^2 & \\ -15\beta^2 & 4\beta^3 & \beta^4/2 & 15\beta^2 & -11\beta^3 & 3\beta^4 \end{bmatrix}$$

$$[A_3] = \int_0^{\beta} \{N'\}\ [N']\,d\theta = \frac{1}{105\beta}$$

$$\begin{bmatrix}
150 & & & & & \\
\frac{45}{2}\beta & 24\beta^2 & & \text{symmetric} & & \\
\frac{5}{4}\beta^2 & \frac{7}{4}\beta^3 & \frac{\beta^4}{6} & & & \\
-150 & -\frac{45}{2}\beta & -\frac{5}{4}\beta^2 & 150 & & \\
\frac{45}{2}\beta & -\frac{3}{2}\beta^2 & -\frac{\beta^3}{2} & -\frac{45}{2}\beta & 24\beta^2 & \\
-\frac{5}{4}\beta^2 & \frac{\beta^3}{2} & \frac{\beta^4}{12} & \frac{5}{4}\beta^2 & -\frac{7}{4}\beta^3 & \frac{\beta^4}{6}
\end{bmatrix}$$

$$[A_4] = \int_0^{\beta} \{N\}\,[N]\,d\theta = \frac{\beta}{462}$$

$$\begin{bmatrix}
181 & & & & & \\
\frac{311}{10}\beta & \frac{104}{15}\beta^2 & & \text{symmetric} & & \\
\frac{281}{120}\beta^2 & \frac{23}{40}\beta^3 & \frac{\beta^4}{20} & & & \\
50 & \frac{151}{10}\beta & \frac{181}{120}\beta^2 & 181 & & \\
-\frac{151}{10}\beta & \frac{133}{30}\beta^2 & -\frac{13}{30}\beta^3 & -\frac{311}{10}\beta & \frac{104}{15}\beta^2 & \\
\frac{181}{120}\beta^2 & \frac{13}{30}\beta^3 & \frac{\beta^4}{24} & \frac{218}{120}\beta^2 & -\frac{23}{40}\beta^3 & \frac{\beta^4}{20}
\end{bmatrix}$$

$$\text{Temp}_1 = \frac{\partial^5 w(e)}{\partial \theta^5} + 2\,\frac{\partial^3 w(e)}{\partial \theta^3} + X\,\frac{\partial w(e)}{\partial \theta} + C\,\frac{\partial \ddot{w}(e)}{\partial \theta}$$

$$\{Y_1\} = \begin{Bmatrix}
-\text{Temp}_1\big|_j \\
0 \\
0 \\
\text{Temp}_1\big|_k \\
0 \\
0
\end{Bmatrix}$$

$$\{Y_2\}= \begin{Bmatrix} 0 \\ -\left(\frac{\partial^4 w(e)}{\partial\theta^4} + 2\frac{\partial^2 w(e)}{\partial\theta^2}\right)\Big|_j \\ 0 \\ 0 \\ \left(\frac{\partial^4 w(e)}{\partial\theta^4} + 2\frac{\partial^2 w(e)}{\partial\theta^2}\right)\Big|_k \end{Bmatrix} \quad \{Y_3\}= \begin{Bmatrix} 0 \\ 0 \\ -\left(\frac{\partial^3 w(e)}{\partial\theta^3}\right)\Big|_j \\ 0 \\ \left(\frac{\partial^3 w(e)}{\partial\theta^3}\right)\Big|_k \end{Bmatrix}$$

$$\text{Temp}_2 = \frac{\partial^5 w(e)}{\partial\theta^5} + 2\frac{\partial^3 w(e)}{\partial\theta^3} + X\frac{\partial w(e)}{\partial\theta} + \frac{I_1}{AR^2}\frac{EI_1}{\alpha AGR^2}C^2\frac{\partial\dddot{w}(e)}{\partial\theta} -$$

$$C\left(\frac{I_1}{AR^2} + \frac{EI_1}{\alpha AGR^2}\right)\frac{\partial^3\ddot{w}(e)}{\partial\theta^3} + C\left(1-2\frac{I_1}{AR^2} + \frac{EI_1}{\alpha AGR^2}\right)\frac{\partial\ddot{w}(e)}{\partial\theta}$$

$$\{Y_4\}= \begin{Bmatrix} -\text{Temp}_2\big|_j \\ 0 \\ 0 \\ \text{Temp}_2\big|_k \\ 0 \\ 0 \end{Bmatrix}$$

$$\text{Temp}_3 = \frac{\partial^4 w(e)}{\partial\theta^4} + 2\frac{\partial^2 w(e)}{\partial\theta^2} - C\left(\frac{I_1}{AR^2} + \frac{EI_1}{\alpha AGR^2}\right)\frac{\partial^2\ddot{w}(e)}{\partial\theta^2}$$

$$\{Y_5\}= \begin{Bmatrix} 0 \\ -\text{Temp}_3\big|_j \\ 0 \\ 0 \\ \text{Temp}_3\big|_k \\ 0 \end{Bmatrix}$$

APPENDIX C

BOUNDARY CONDITIONS AND ELEMENT MATRICES FOR DISCS

C.1 BOUNDARY CONDITIONS

The boundary conditions for a thick disc, vibrating in n-nodal diameter mode, are [59] :

i) Hinged end

$$w = 0 \tag{C.1}$$

$$R\frac{\partial^2 w}{\partial R^2} + \nu\frac{\partial w}{\partial R} - \nu n^2 \frac{w}{R} = 0 \tag{C.2}$$

ii) Clamped end

$$w = 0 \tag{C.3}$$

$$w' = 0 \tag{C.4}$$

iii) Free end

$$D\left(\frac{\partial}{\partial R}\left(R\frac{\partial^2 w}{\partial R^2}\right) - (1+2n^2)\frac{1}{R}\frac{\partial w}{\partial R} + \nu n^2 \frac{1}{R}\frac{\partial w}{\partial R} + (3-\nu)n^2 \frac{w}{R^2}\right) - \left(\rho I + D\frac{\rho}{\alpha G}\right)R\frac{\partial \ddot{w}}{\partial R} = 0 \tag{C.5}$$

$$R\frac{\partial^2 w}{\partial R^2} + \nu\frac{\partial w}{\partial R} - \nu n^2 \frac{w}{R} = 0 \tag{C.6}$$

C.2 ELEMENT MATRICES

The stresses induced due to rotation are given by [58]

$$\sigma_{RR} = C_1 - \frac{C_2}{R^2} - C_3 R^2 \qquad (C.7)$$

$$\sigma_{\theta\theta} = C_1 + \frac{C_2}{R^2} - C_4 R^2 \qquad (C.8)$$

where

$$C_1 = \frac{C_2}{b^2} + C_3 b^2 \qquad (C.9)$$

$$C_2 = \frac{1}{8}\rho\,\Omega^2 a^2 b^2 \frac{(1-\nu^2)a^3-(3-2\nu-\nu^2)b^2}{(1-\nu)\,a^2+(1+\nu)b^2} \qquad (C.10)$$

$$C_3 = \frac{1}{8}(3+\nu)\,\rho\,\Omega^2 \qquad (C.11)$$

$$C_4 = \frac{1}{8}(1+3\nu)\,\rho\,\Omega^2 \qquad (C.12)$$

The various constitutive matrices for the elemental stiffness and mass matrices are given below.

$$[A_1] = \int_o^h (R_j+r)\,\{N''\}\,[N'']dr =$$

$$\frac{R_j}{h^3}\begin{bmatrix} 12 & & & \\ 6h & 4h^2 & \text{symmetric} & \\ -12 & -6h & 12 & \\ 6h & 2h^2 & -6h & 4h^2 \end{bmatrix} + \frac{1}{h^2}\begin{bmatrix} 6 & & & \\ 2h & h^2 & \text{symmetric} & \\ -6 & -2h & 6 & \\ 4h & h^2 & -4h & 3h^2 \end{bmatrix}$$

$$[A_2] = \int_0^h \frac{1}{R_j+r} \{N'\}[N']dr =$$

$$\frac{1}{h^2}\begin{bmatrix} 36(F_2-2F_3+F_4) & & & \\ -6h(F_1-5F_2+7F_3-3F_4) & h^2(F_o-8F_1+22F_2-24F_3+9F_4) & \text{symmetric} & \\ -36(F_2-2F_3+F_4) & 6h(F_1-5F_2+7F_3-3F_4) & 36(F_2-2F_3+F_4) & \\ 6h(2F_2-5F_3+3F_4) & -h^2(2F_1-11F_2+18F_3-9F_4) & -6h(2F_2-5F_3+3F_4) & h^2(4F_2-12F_3+9F_4) \end{bmatrix}$$

where $F_o = \ln(1+h/R_j)$ (C.13)

$$F_i = \frac{1}{i} - \frac{R_j}{h} F_{i-1}, \quad i = 1,2, \ldots, 6 \qquad \text{(C.14)}$$

$$[A_3] = \int_o^h \frac{1}{(R_j+r)^3} \{N\}[N]dr =$$

$$h\begin{bmatrix} Z_o-6Z_2+4Z_3+9Z_4-12Z_5+4Z_6 & & & \\ h(Z_1-2Z_2-2Z_3+8Z_4-7Z_5+2Z_6) & h^2(Z_2-4Z_3+6Z_4-4Z_5+Z_6) & \text{symmetric} & \\ 3Z_2-2Z_3-9Z_4+12Z_5-4Z_6 & h(3Z_3-8Z_4+7Z_5-2Z_6) & 9Z_4-12Z_5+4Z_6 & \\ -h(Z_2-Z_3-3Z_4+5Z_5-2Z_6) & -h^2(Z_3-3Z_4+3Z_5-Z_6) & -h(3Z_4-5Z_5+2Z_6) & h^2(Z_4-2Z_5+Z_6) \end{bmatrix}$$

where

$$Z_o = \frac{h(R_j+R_k)}{2R_j^2 R_k^2} \qquad \text{(C.15)}$$

$$Z_1 = \frac{1}{R_j R_k} - \frac{(R_j+R_k)}{2R_j R_k^2} \qquad (C.16)$$

$$Z_2 = \frac{1}{h^2}\ln(R_k/R_j) - \frac{2}{hR_k} + \frac{R_j + R_k}{2h\,R_k} \qquad (C.17)$$

$$Z_3 = \frac{1}{h^2} - \frac{3R_j}{h^3}\ln(R_k/R_j) + \frac{3R_j}{h^2 R_k} - \frac{R_j(R_j+R_k)}{2h^2 R_k^2} \qquad (C.18)$$

$$Z_4 = \frac{1}{2h^3}(R_j+R_k) - \frac{4R_j}{h^3} + \frac{6R_j^2}{h^4}\ln(R_k/R_j) - \frac{4R_j^2}{h^3 R_k} + \frac{R_j^2(R_j+R_k)}{2h^3 R_k^2} \qquad (C.19)$$

$$Z_5 = \frac{R_k^3-R_j^3}{h^5} - \frac{5R_j}{2h^4}(R_j+R_k) + \frac{10R_j^2}{h^4} - \frac{10R_j^3}{h^5}\ln(R_k/R_j) + \frac{5R_j^3}{h^4 R_k} - \frac{R_j^3(R_j+R_k)}{2h^4 R_k^2} \qquad (C.20)$$

$$Z_6 = \frac{R_k^4-R_j^4}{h^6} - \frac{6R_j(R_k^3-R_j^3)}{h^6} + \frac{15R_j^2}{2h^5}(R_j+R_k) - \frac{20R_j^3}{h^5} + \frac{15R_j}{h^6}\ln(R_k/R_j) - \frac{6R_j^4}{h^5 R_k} + \frac{R_j^4(R_j+R_k)}{2h^5 R_k^2} \qquad (C.21)$$

$$[A_4] = \int_0^h \sigma_{rr}(R_j+r)\,\{N'\}[N']\,dr$$

$$= (C_1 - R_j^2 C_3)[A_6] - C_2[A_2] -$$

$$C_3\Big(2\begin{bmatrix} 3/5 & & & \\ h/10 & h^2/30 & \text{symmetric} & \\ -3/5 & -h/10 & 3/5 & \\ 0 & -h^2/60 & 0 & h^2/10 \end{bmatrix} + 3R_j h \begin{bmatrix} 12/35 & \text{symmetric} & & \\ h/14 & 2h^2/105 & & \\ -12/35 & -h/14 & \frac{12}{35} & \\ -h/35 & -h^2/70 & \frac{h}{35} & \frac{3h^2}{35} \end{bmatrix}$$

$$+h^2 \begin{bmatrix} 3/14 & & & \\ h/20 & 11h^2/840 & \text{symmetric} & \\ -3/14 & -h/20 & 3/14 & \\ -h/28 & -11h^2/840 & h/28 & 13h^2/168 \end{bmatrix})$$

$$[A_5] = \int_o^h \frac{\sigma_{\theta\theta}}{R_j+r} \{N\}[N]dr = C_1[A_8] + C_2[A_3] - C_4[A_7]$$

$$[A_6] = \int_o^h (R_j+r) \{N\}[N']dr =$$

$$\frac{R_j}{h} \begin{bmatrix} 6/5 & & & \\ h/10 & 2h^2/15 & \text{symmetric} & \\ -6/5 & -h/10 & 6/5 & \\ h/10 & -h^2/30 & -h/10 & 2h^2/15 \end{bmatrix} + \begin{bmatrix} 3/5 & & & \\ h/10 & h^2/30 & \text{symmetric} & \\ -3/5 & -h/10 & 3/5 & \\ 0 & -h^2/60 & 0 & h^2/10 \end{bmatrix}$$

$$[A_7] = \int_o^h (R_j+r) \{N\}[N]dr =$$

$$\frac{hR_j}{420} \begin{bmatrix} 156 & & & \\ 22h & 4h^2 & \text{symmetric} & \\ 54 & 13h & 156 & \\ -13h & -h^2/30 & -22h & 4h^2 \end{bmatrix} + \mathbf{h^2} \begin{bmatrix} 3/35 & & & \\ h/60 & h^2/280 & \text{symmetric} & \\ 9/140 & h/60 & 2/7 & \\ -h/10 & -h^2/280 & -h/28 & h^2/168 \end{bmatrix}$$

$$[A_8] = \int_o^h \frac{1}{R_j+r} \{N\} [N] dr =$$

$$h \begin{bmatrix} F_o-6F_2+4F_3+ & & & \\ 9F_4-12F_5+4F_6 & \text{symmetric} & & \\ h(F_1-2F_2-2F_3+ & h^2(F_2-4F_3+ & & \\ 8F_4-7F_5+2F_6) & 6F_4-4F_5+F_6) & & \\ 3F_2-2F_3-9F_4+ & h(3F_3-8F_4+ & 9F_4-12F_5+4F_6 & \\ 12F_5-4F_6 & 7F_5-2F_6) & & \\ -h(F_2-F_3-3F_4+ & -h^2(F_3-3F_4+ & -h(3F_4-5F_5+2F_6) & h^2(F_4-2F_5+ \\ 5F_5-2F_6) & 3F_5-F_6) & & F_6) \end{bmatrix}$$

$$\text{Temp} = D \frac{\partial}{\partial r} \left(R \frac{\partial^2 w^{(e)}}{\partial r^2}\right) - (1+2n^2) D \frac{1}{R} \frac{\partial w^{(e)}}{\partial r} -$$

$$\left(\rho I + D \frac{\rho}{\alpha G}\right) R \frac{\partial \ddot{w}^{(e)}}{\partial r} - TR \sigma_{rr} \frac{\partial w^{(e)}}{\partial r}$$

$$\{Y_1\} = \begin{Bmatrix} -\text{Temp}|_j \\ 0 \\ \text{Temp}|_k \\ 0 \end{Bmatrix}$$

$$\{Y_2\} = \begin{Bmatrix} 0 \\ -D\left(R \frac{\partial^2 w^{(e)}}{\partial r^2}\right)_j \Big|_j \\ 0 \\ D\left(R \frac{\partial^2 w^{(e)}}{\partial r^2}\right) \Big|_k \end{Bmatrix}$$